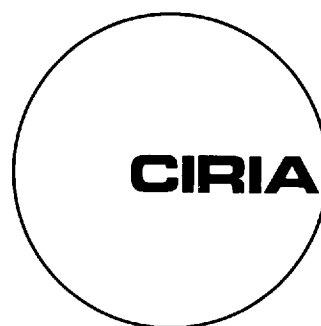
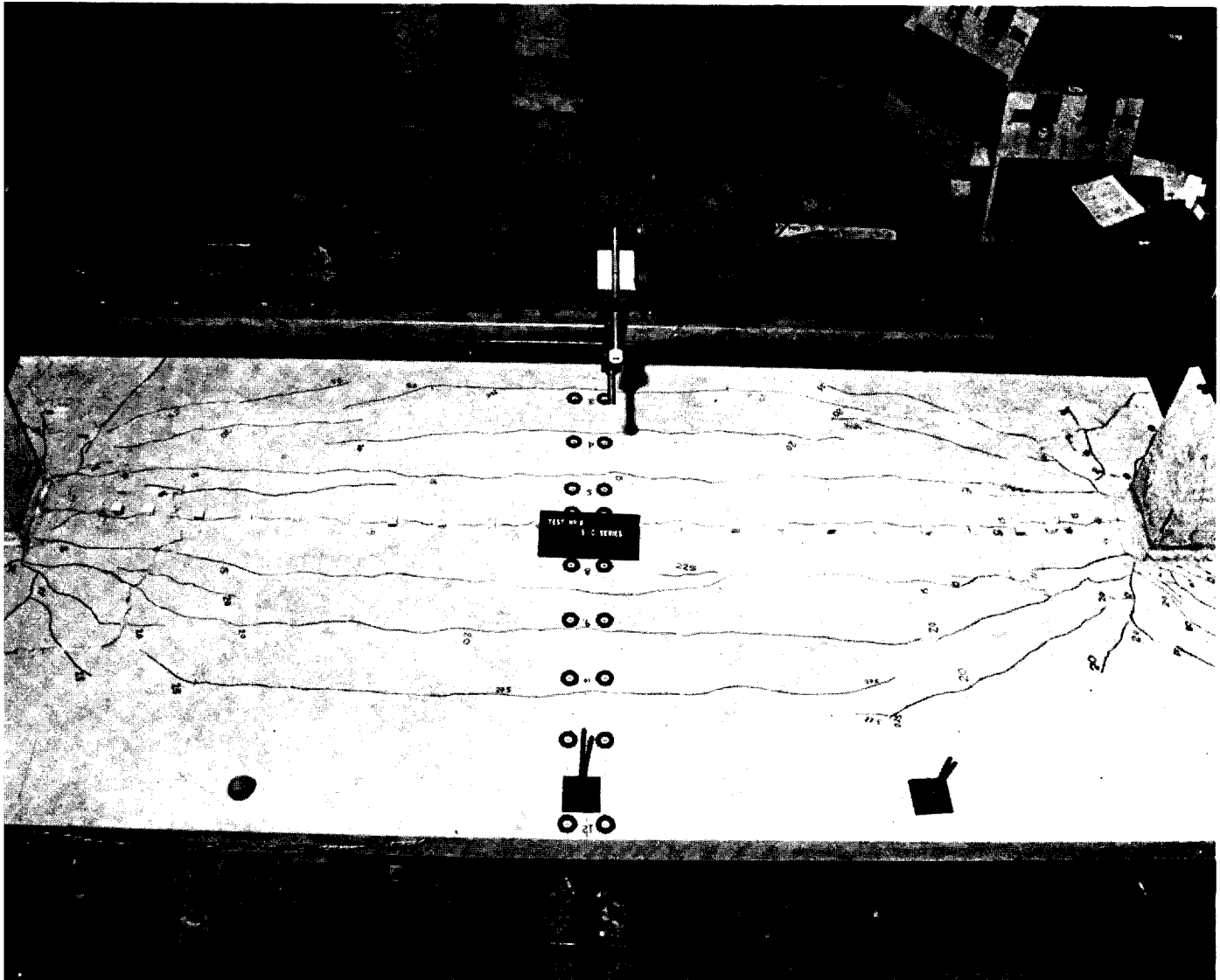


Behaviour of reinforced concrete flat slabs

P. E. REGAN



CIRIA REPORT 89

How CIRIA operates

The Construction Industry Research and Information Association (CIRIA) is an industrial co-operative research association set up and operated by the British construction industry with the support of the UK Government. Its main role is to organise co-operation within the industry and between it and Government for identifying, financing and managing research, other investigations, and the collection and dissemination of information. CIRIA also has a separately-financed group—UEG—which acts as the research and information group for the underwater and offshore engineering industries.

Membership is open to all firms, companies, corporations and other organisations in Britain and in other countries that are concerned in any way with construction or offshore engineering.

CIRIA is financed by subscriptions from its members and grants and other funds from the Department of the Environment. CIRIA's research projects are financed principally from special contributions made by industry and government.

An unusual feature of CIRIA is that it has no laboratory and implements its projects by placing fixed-price contracts with those best able to do the work required. These 'contractors' may be other research organisations, companies, professional firms or universities. This system not only makes available the best knowledge, skills and experience in many fields, but is also economical, flexible and allows the Association to adjust its programme to the needs of its members without the constraints of long-term commitments in specialised staff and laboratory facilities.

With this flexibility it is possible for CIRIA to provide its members with freedom in selecting its programme of projects that is rare among industrial research organisations, and to employ effectively the knowledge and experience of its members in jointly producing and implementing what is in effect their own programme to meet their own needs. This is achieved by a group of six Sectional Committees, which advise the main Research Committee, and by the UEG Committee, all assisted by steering groups set up to consider specialised subjects. The Research Committee and the UEG Committee report direct to the Council.

A total of over 400 experts serve on all these committees, and together they make up what is probably the most representative organised cross-section of knowledge and industrial experience applied to research in Britain in the fields of construction and offshore engineering.

The Association undertakes projects of many kinds which cover a wide range of subjects. The type of work done includes research, the experimental determination of data, state-of-the-art reviews, guides to good practice and the collection of information, while the subjects covered include safety, health, properties of materials, design, construction processes, standardisation, rationalisation, management and similar topics.

The full-time staff of 45 comprises a group of research managers supported by specialised administrative, accounting, information and secretarial staff. The research managers serve the committees and with them identify and define the needs of the industry for research and information and agree priorities. They then specify the projects required to meet the needs, negotiate with possible 'contractors', raise any special funds which may be required, manage the projects (with the help of steering groups of members), ensure that publications are in a suitable form for use by the members, and assist in the exploitation of results, sometimes by holding seminars.

The main publications include Reports, interim or specialised Technical Notes, guides to practice, and the proceedings of seminars. Short non-confidential profiles (summaries) of all Reports are available to non-members, as is the annual report.

The Association provides an information service for its members which is particularly useful in establishing direct contacts with the appropriate prime source of knowledge, identified by the staff as a result of their many contacts in both the industrial and research fields.

MEMBERSHIP SUBSCRIPTION RATES, 1981. VAT at the standard rate to be added:

CIRIA membership

Professional offices	£5.10 a year per person employed on activities in construction (excluding those working on sites). Minimum subscription £170
Contractors	88p a year per operative employed on construction. Minimum subscription £170
Local authorities	£2.55 per 4000 population. Minimum subscription £170 a year
Universities and educational bodies	£170 a year
All other members	By negotiation subject to a minimum of £170 a year
Associate members (Head Office outside UK)	Same subscription as that paid by an ordinary member in an equivalent category, subject to a minimum annual subscription of £250

UEG membership

From £280 minimum to £5650 a year, depending on degree of involvement and scale of operation in offshore engineering.

Enquiries about membership and any other requests for information should be sent to the Secretary, CIRIA, 6 Storey's Gate, London SW1P 3AU.

Summary

REGAN, P. E.

Behaviour of reinforced concrete flat slabs

Construction Industry Research and Information Association

Report 89, February 1981

The design of reinforced concrete flat slabs is studied with regard to flexure, punching shear, and deflection. The basis of the project was a comprehensive experimental programme of slab tests to failure. Design expressions are developed to take account of the equivalent beam behaviour of the slab, and the reduction in effective slab width close to exterior columns. Detailing procedures are presented which reflect the distribution of slab moments and torsion local to the columns. Additional aspects considered include use of shear reinforcement, avoidance of progressive collapse, and design of waffle and drop head slabs.

Keywords (from *Construction Industry Thesaurus*)

Columns; Failure; Joints; Laboratory testing; Loading properties;
Reinforced concrete; Statically indeterminate; Structural design;
Two-direction spanning floors

Reader Interest

Concrete Designers

Behaviour of reinforced concrete flat slabs

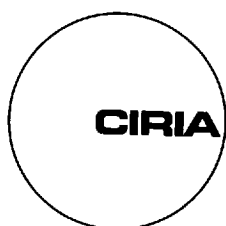
P. E. Regan PhD BSc DIC SVR

Price: £40 (£8 CIRIA Members)

ISBN: 0 86017 150 7

ISSN: 0305-408X

©CIRIA 1981



CONSTRUCTION INDUSTRY RESEARCH AND INFORMATION ASSOCIATION
6 STOREY'S GATE, LONDON, SW1P 3AU
Telephone 01-222 8891

The research was carried out under contract to CIRIA at the Polytechnic of Central London, where Dr Regan is Reader in the Civil Engineering Department. The research was guided throughout by the CIRIA Project Steering Group:

J. A. Waller BSc DIC CEng FICE FIStructE ACGI (Chairman)	Oscar Faber & Partners
A. W. Beeby PhD BSc CEng MICE MIStructE	Cement and Concrete Association (from April 1978)
F. K. Garas PhD BSc CEng MICE MIStructE	Taylor Woodrow Construction Limited
A. E. Long PhD BSc CEng MICE MIStructE	Queen's University Belfast
P. Sims BSc	Building Research Establishment (from November 1978)
A. Stamenkovic PhD BSc DIC DipIng CEng MICE MIStructE	Kingston Polytechnic
H. P. J. Taylor PhD BSc CEng MICE MIStructE	Dow Mac Concrete Ltd* (until April 1978)
R. T. Whittle MA CEng MICE	Ove Arup & Partners
R. H. Wood DSc PhD CEng MIStructE MICE	Building Research Establishment (until November 1978)
J. S. Armitage BSc CEng MICE MIStructE	CIRIA (until May 1979)
R. M. Lawson PhD BSc CEng MICE MIStructE ACGI	CIRIA (from May 1979)

*Formerly Cement and Concrete Association

Contents

LIST OF ILLUSTRATIONS	4
LIST OF TABLES	6
NOTATION	7
SUMMARY	8
1. INTRODUCTION	8
2. TWO-WAY SLAB SYSTEMS	11
2.1 Overall equilibrium	11
2.2 Distribution of moment	11
2.3 Deflection	12
2.4 Shear	13
2.5 Frame action	14
3. THE BACKGROUND OF FLAT SLAB DESIGN	14
3.1 Overall distribution of moment	14
3.2 Resistance to punching shear	16
3.3 Local flexural strength	18
3.4 Serviceability	19
4. FLEXURAL DESIGN	20
4.1 Determination of gross frame moment	20
4.2 Distribution of moment across frame	35
4.3 Local flexure at slab-column connections	38
4.4 Detailing	42
4.5 Serviceability	45
5. PUNCHING SHEAR	48
5.1 Punching in the absence of unbalanced moment	48
5.2 Punching in the presence of unbalanced moment	59
5.3 Progressive collapse	67
6. FLAT SLAB VARIANTS	69
6.1 Slabs with column capitals	69
6.2 Slabs with drop panels	69
6.3 Waffle or coffered slabs	71
6.4 Post-tensioned slabs	74
7. DESIGN CONCLUSIONS	75
7.1 Overall flexural design	75
7.2 Distribution of moment across frame width	76
7.3 Punching shear	77
7.4 Precaution against progressive collapse	81
7.5 Control of deflection	82
8. PROPOSALS FOR FUTURE RESEARCH	83
REFERENCES	83
ACKNOWLEDGEMENTS	89

List of illustrations

- Figure 1** *Slab specimens in test programme*
- Figure 2** *Series SC slab, showing local flexural cracking at corner columns*
- Figure 3** *Series SI slab, showing punching failure resulting from combined shear and moment transferred to column*
- Figure 4** *Moment diagram for beam-slab system under uniform loading*
- Figure 5** *Distribution of moment in continuous two-way slab*
- Figure 6** *Behaviour of elongated panels of continuous slabs*
- Figure 7** *Influence of edge beam stiffness on central deflection of square panel simply supported at its corners*
- Figure 8** *Deflection of square slabs on corner columns with and without edge beams*
- Figure 9** *Deformation at edge of an elastic plate near a column*
- Figure 10** *Model of slab behaviour in Kinnunen and Nylander's treatment of punching*
- Figure 11** *Deflections of an interior panel*
- Figure 12** *Positive moments at midspan for an edge panel and an interior panel*
- Figure 13** *Deformations of slab-columns and beam-column structures*
- Figure 14** *Models of structures with deformable joints*
- Figure 15** *Compatibility of slab and column rotations*
- Figure 16** *American Concrete Institute equivalent frame method*
- Figure 17** *Rotations at edges of a simply supported slab strip*
- Figure 18** *Proposed approach—addition of torsion strip to slab contacting column at inner face only*
- Figure 19** *Joint stiffness— K_j*
- Figure 20** *Comparison between various equivalent frame methods, for moment attracted to columns*
- Figure 21** *Comparison between methods, for moment attracted to perimeter columns*
- Figure 22** *Proposed treatment of horizontal loading expressed in terms of equivalent slab breadths*
- Figure 23** *Actual and predicted column moments for test series SC*
- Figure 24** *Actual and predicted column moments for test series SE 12 to 15*
- Figure 25** *Slab and column rotations for test SC 6*
- Figure 26** *Rotation along edge of slab at perimeter column*
- Figure 27** *Compressive membrane effects*
- Figure 28** *Bands for detailing of reinforcement*
- Figure 29** *Distribution of radial and tangential moments in an elastic-plastic flat plate*
- Figure 30** *Combination of basic and additional mid span moments*
- Figure 31** *Reinforcement arrangements and steel strains—rectangular slab SC 11*

- Figure 32** *Reinforcement strains near an edge column for slab SE 9*
- Figure 33** *Final crack patterns in a test of a 4-panel flat plate*
- Figure 34** *Local ring and fan mechanisms*
- Figure 35** *Local yield line patterns and slab deformations at internal columns with eccentric loading*
- Figure 36** *Local conditions at edge column—slab connection*
- Figure 37** *Failure mechanism at edge column—slab connection subject to bending*
- Figure 38** *Local yield lines at corner columns*
- Figure 39** *Arrangements of top reinforcement at edge and corner columns*
- Figure 40** *Local yield lines at roof level, which may reduce flexural capacity*
- Figure 41** *Reduction of maximum moments for design to take account of finite column sizes*
- Figure 42** *Comparison of actual and predicted deflections for tests of slabs on corner columns*
- Figure 43** *Comparison of actual and predicted deflections for tests by Ingvarsson*
- Figure 44** *Comparison of actual and predicted deflections for tests by Kinnunen*
- Figure 45** *Load-deflection relationships for slabs with and without shear reinforcement*
- Figure 46** *Use of fracture surface approach to deal with various punching situations*
- Figure 47** *Fracture surface used in calculation of punching resistance*
- Figure 48** *Influence of concrete strength on punching resistance*
- Figure 49** *Influence of ratio of column size to slab depth on punching resistance*
- Figure 50** *Punching test failure cone*
- Figure 51** *Influence of column shape on punching resistance for a constant perimeter length*
- Figure 52** *Influence of slab depth on punching resistance*
- Figure 53** *Influence of ratio of flexural reinforcement on punching resistance*
- Figure 54** *Punching shear test results for internal slab-column connections under concentric load*
- Figure 55** *Possible modes of shear failure for slabs with shear reinforcement*
- Figure 56** *Distribution of stresses on fracture surface due to unbalanced column moment loading*
- Figure 57** *Test results for internal slab-column connections under eccentric loading*
- Figure 58** *Results for edge column-slab connection with moments parallel to slab edge*
- Figure 59** *Interaction mode for edge column contacting slab at one face only*
- Figure 60** *Typical punching failure at an edge column*
- Figure 61** *Limiting conditions for shear-moment interaction at edge columns*
- Figure 62** *Comparison of test and calculated resistance of edge column-slab connections for moments perpendicular to the slab edge*

- Figure 63** *Shear-moment interaction at edge column-slab connection for slab overhang*
- Figure 64** *Comparison of test data for edge and corner column-slab connections with simplified Equation (61)*
- Figure 65** *Limiting conditions for shear-moment interaction at corner columns*
- Figure 66** *Behaviour of slabs after punching*
- Figure 67** *Surfaces used in shear calculations for slabs with column capitals and drop panels*
- Figure 68** *Negative moment in slabs with drop panels*
- Figure 69** *Comparison of moment distribution in waffle and solid slabs*
- Figure 70** *Distribution of negative moment in waffle slabs*
- Figure 71** *Distribution of positive moment in waffle slabs*
- Figure 72** *Critical design moment for rib concrete*
- Figure 73** *Shear or suspension reinforcement at edge of solid slab*
- Figure 74** *Widths of loading for equivalent frames*
- Figure 75** *Reinforcement layout for typical slab*
- Figure 76** *Concrete areas used in punching calculations*
- Figure 77** *Representation of central slab deflection*

List of tables

- Table 1** *Comparison of experimental column moment with values predicted by proposed method and by CP 110*
- Table 2** *Distribution of positive moment at midspan*
- Table 3** *Distribution of negative moment at column lines*
- Table 4** *Creep coefficients*
- Table 5** *Proportions of negative moment*
- Table 6** *Proportions of positive moment*

Notation

A_c	area of concrete in fracture surface at a punching failure
A_s	area of reinforcement
A'_{st}	area of top reinforcement parallel to a slab edge and passing through an edge column (acts as torsional reinforcement)
A_{sw}	area of one leg of stirrup
A_{sx}, A_{sy}	area of tension reinforcement in x and y slab directions
b	width of slab (in an equivalent frame, b = total width contributing load)
b_e	equivalent width of an equivalent frame (i.e. width determining stiffness)
b_{eq}	equivalent width of slab for horizontal loading
$c; \sum c$	column dimension; column perimeter
c_1, c_2	column dimensions parallel and perpendicular to span under consideration
c_x, c_y	column dimensions in x and y directions
D	flexural rigidity of slab per unit width
D_g, D_{cr}	flexural rigidity of uncracked and cracked slab
d	effective depth of slab
E_c	modulus of elasticity of concrete
e	eccentricity of load at a slab/column joint
e_x, e_y	eccentricity of load (\bar{M}/V) in the x and y direction
f_{cu}	cube compressive strength of concrete
f_r	flexural tensile strength of concrete ($\approx 0.45\sqrt{f_{cu}}$ in N/mm ²)
f_y	yield or 0.2% proof stress of reinforcement
f_{yd}	design ultimate stress for reinforcement ($= 0.87f_y$)
g	dead load per unit area of slab
h	overall thickness of slab
K_a	coefficient expressing influence of aggregate type on punching resistance
K_c	column stiffness, moment transferred from slab per unit rotation of column at level of slab (for fixed-ended columns $K_c = \sum 4EI/l$ for the columns above and below the slab)
K_{ce}	effective column stiffness
K_j	joint stiffness (i.e. moment per unit rotation of slab/column joint)
K_{sc}	shape factor of column influencing punching resistance
K_{se}	effective slab stiffness of two spans meeting at a joint for horizontal loading
K_{sl}, K_{s2}	slab stiffness based on widths b_e
l	span of slab frame under consideration
l_x, l_y	span in x and y directions
M, M'	positive and negative moments (i.e. moments in span and support moments, respectively)
M'_1, M'_2	negative moments at the supports
M_f	moment directly resisted by face of column
M_s	part of \bar{M} resisted because of action of reinforcement
M_t	moment of resistance provided by torsion at side face of a column
\bar{M}	unbalanced moment transferred from slab to column
m	bending moment per unit width
m, m'	positive and negative moments per unit width
m_{cr}	flexural cracking resistance per unit width
m_y	positive moment per unit width at mid span in the y direction
p	live load per unit area of slab
Q	total load on a panel or span of an equivalent frame
q	load per unit area of slab

r	slab width at side of column within which top reinforcement contributes to M_t
s	spacing of bars
V	shear force
V_c	punching strength of slab without shear reinforcement
V_{Rd}	design ultimate resistance to punching
V_u	ultimate shear force at punching failure
V_{ud}	design shear force for the ultimate limit state
V_{ue}	ultimate shear load under combination of shear and moment
V_{uo}	ultimate shear load resistance under concentric load
v	punching shear stress
z	internal lever arm
α	proportion of unbalanced moment at a slab/column connection transferred by unevenly distributed shear
δ	deflection of slab
θ	angle between fracture surface and plane of slab
θ_b	rotation derived from CP110 frame analysis
θ_c	rotation of column at slab level
θ_j	effective joint rotation between slab and column
θ_s	rotation of slab at column according to elastic plate theory
ξ_s	depth factor = $\sqrt[3]{300/d}$ (for d in mm)
σ_{vu}	nominal ultimate stress (V_u/A_c) on punching surface
ϕ	bar diameter
ν	creep coefficient

Summary

The design of reinforced concrete flat slabs is studied with regard to flexure, punching shear, and deflection. The basis of the project was a comprehensive experimental programme of slab tests to failure.

Design expressions are developed to take account of the equivalent beam behaviour of the slab, and the reduction in effective slab width close to exterior columns. Detailing procedures are presented which reflect the distribution of slab moments and torsion local to the columns. Additional aspects considered include use of shear reinforcement, avoidance of progressive collapse, and design of waffle and drop head slabs.

1. Introduction

The impetus for this research arose from criticisms about the treatment of flat slabs in the British Standard Code of Practice for structural use of concrete (CP 110 : 1972). The methods of determining moment transfer to the columns from the slab, and the influence on the slab punching shear capacity resulting from this moment and shear interaction, were considered to be the main subjects requiring investigation.

There appear to have been few instances of the collapse of flat slabs, but there are examples of unsatisfactory behaviour at service loads. Where collapses occurred (generally during construction), they were serious and spread far beyond the local failures which initiated them.

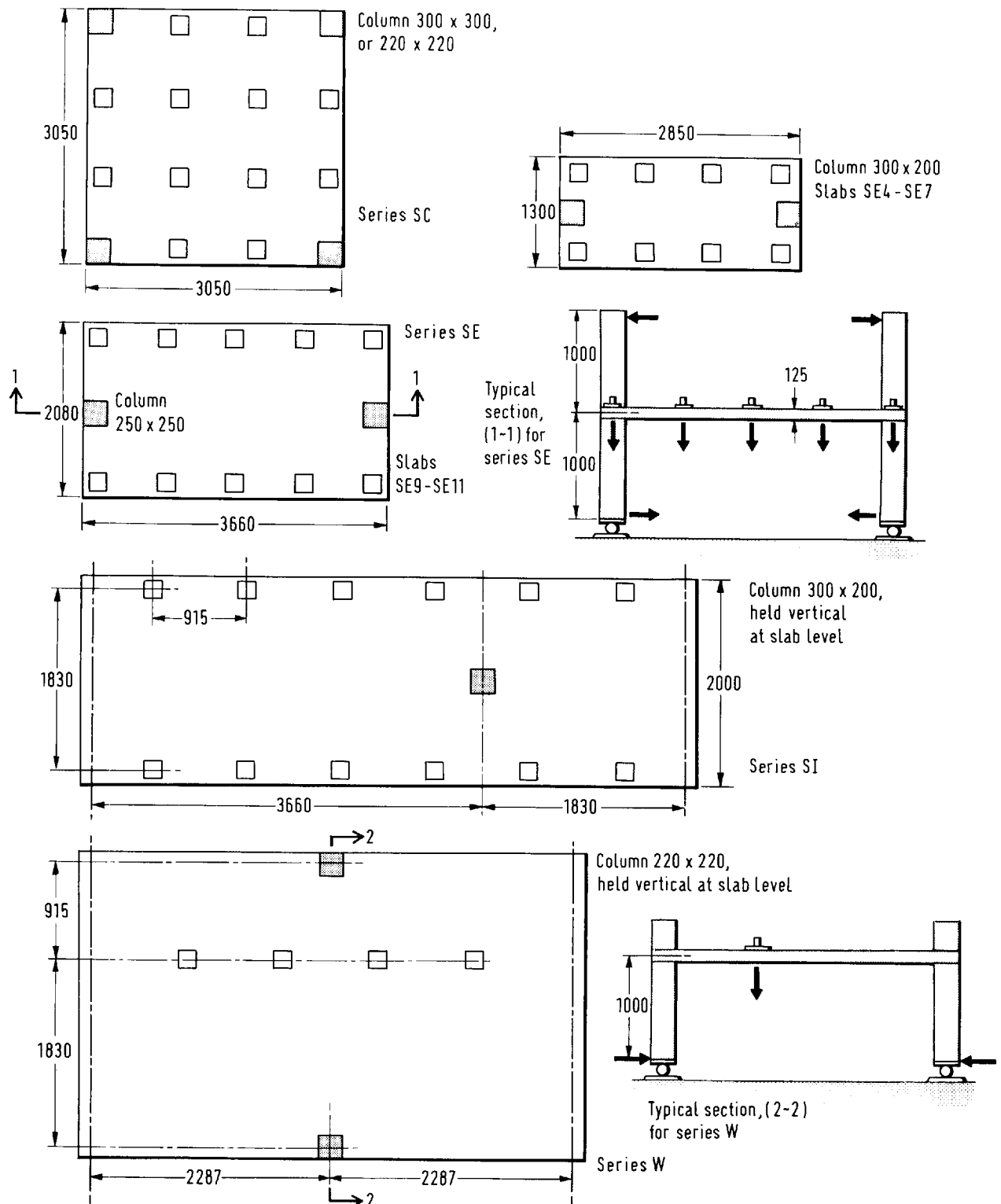


Figure 1 Slab specimens in test programme

This CIRIA research project was primarily initiated to obtain experimental information in a number of areas where published data were scarce. The main emphasis was on the behaviour of slab/column connections in statically indeterminate arrangements where shear forces could continue to increase after the formation of local yield lines had limited the moments transferred to columns. Details of the specimens used for this work are shown in Figure 1, and the numbers of tests made were as follows:

- | | |
|------------------|---|
| Series SC | — 12 slabs supported by corner columns (Figure 2) |
| Series SE | — 18 slabs supported by edge columns (see front cover illustration) |
| Series SI and SR | — three statically indeterminate slabs with interior columns (Figure 3) |
| Series W | — two slabs with mixed wall and edge column supports. |

In general, the test slabs were 125 mm thick, and could thus be regarded as small prototypes rather than as models.

In addition to the work described above, a further 25 statically-determinate slabs with interior columns were tested to study a number of particular points such as scale effects, the influence of concentration of reinforcement towards columns, and the influence of column shape on the resistance of connections subject to shear and unbalanced moments.

Full details of the experimental work are given in the project record⁽¹⁾ available on loan to members from CIRIA. The Report summarises the information obtained from the tests, and from a literature study of flat slabs. Although it contains a number of proposals for design methods, it is not intended as a design guide or alternative code of practice.

Figure 2
*Series SC slab,
showing local flexural
cracking at corner
columns*

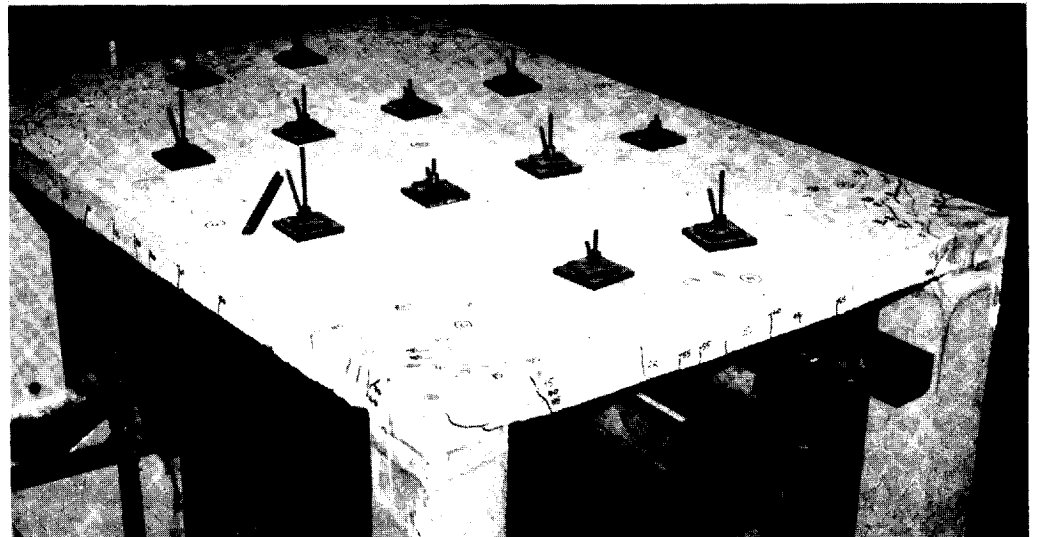
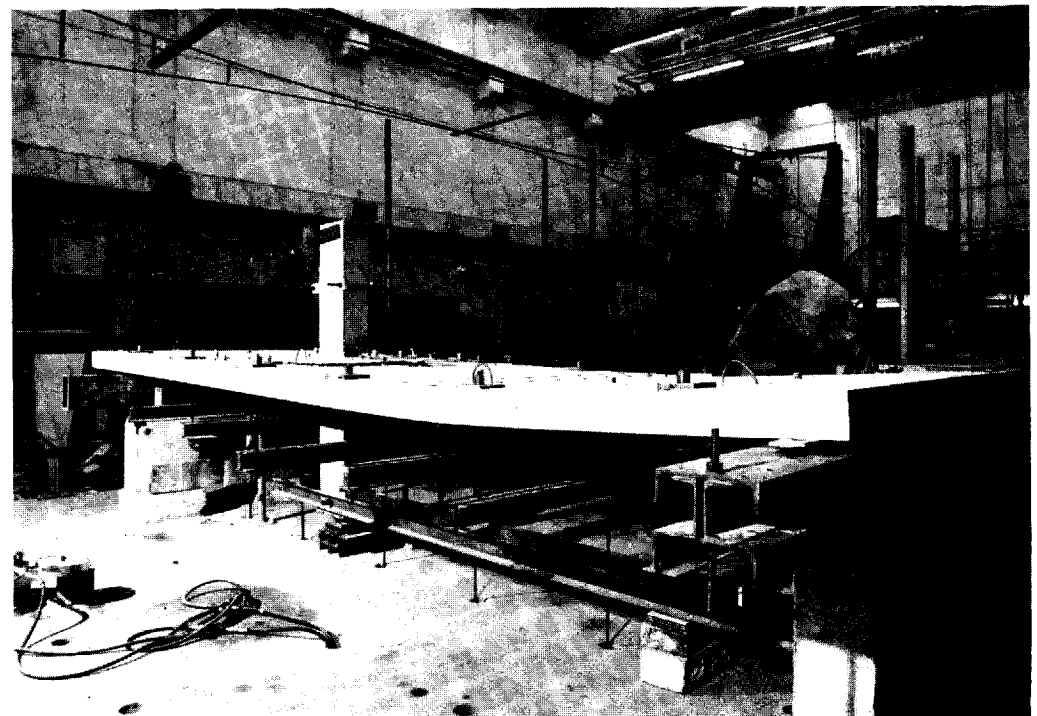


Figure 3
*Series SI slab, showing
punching failure
resulting from
combined shear and
moment transferred to
column*



2. Two-way slab systems

2.1 OVERALL EQUILIBRIUM

The description 'two-way' applies to slab systems ranging from panels with rigid beams on all sides to flat slabs directly supported by columns. With the exception of slabs on walls, all such systems are subject to common requirements of equilibrium. Neglecting the finite widths of supports, for any uniformly loaded span with a width defined by lines of zero shear, as in Figure 4

$$\int m_y dx + \frac{1}{2} (\int m'_{y1} \cdot dx + \int m'_{y2} \cdot dx) = \frac{1}{8} Q l_y^2 \quad (1)$$

where m_y is the positive moment per unit width at midspan in the y direction
 m'_{y1} and m'_{y2} are the negative moments per unit width at support lines 1 and 2
 and Q is the total load on the width in question.

The integrals are for the full width, and include the moments in any y-direction beams. A similar equation can be written for x-direction moments.

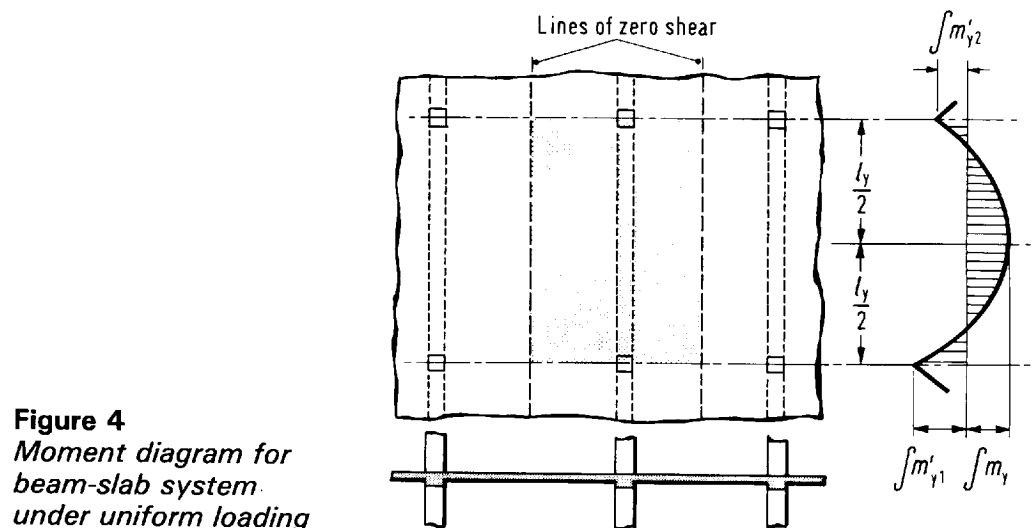


Figure 4
Moment diagram for beam-slab system under uniform loading

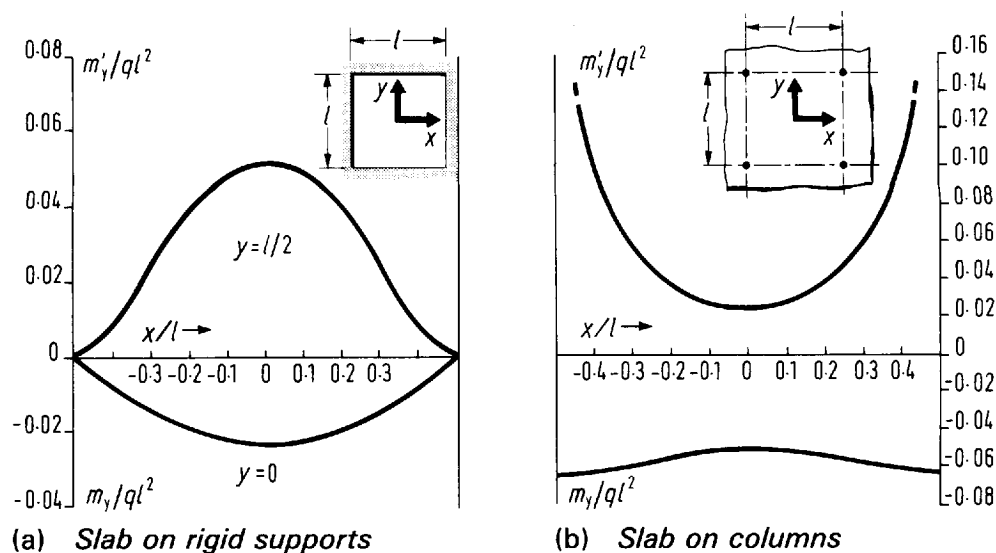
The division of moments between the slab and beams can vary greatly, depending on their relative stiffnesses and strengths. At one extreme, a slab on rigid beams need only provide $\frac{1}{3}$ of the total moment resistance, $\frac{2}{3}$ being provided by the beams. At the other extreme, a flat plate slab must provide the whole resistance.

An infinite variety of intermediate cases is possible with beams of reduced stiffness and strength or with beams at some, but not all, sides of the slab panels. In every case, the basic equilibrium requirement expressed by Equation (1) must be respected for both directions, and the total moments in orthogonal directions are independent of one another.

2.2 DISTRIBUTION OF MOMENT

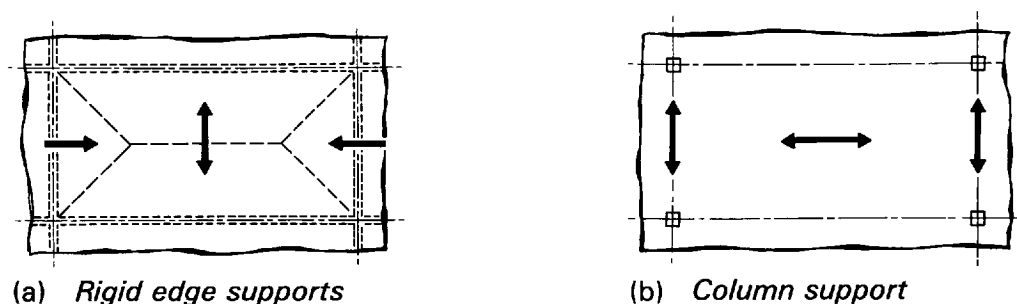
Within the overall constraints of equilibrium, there are large differences in behaviour between the types of two-way systems. For a slab on rigid beams, the maximum positive elastic moments are at the centre of the panel, and when there is fixity or continuity at the boundaries, the maximum negative moments are at the centres of the edges (see Figure 5(a)). By contrast, in a flat slab, the maximum positive and negative moments are on the column lines (Figure 5(b)). Intermediate situations arise where edge beams have appreciable flexibility in the vertical plane, and where boundary restraint is dependent on the limited torsional stiffness of the beams.

Figure 5
Distribution of moment
in continuous two-way
slab



In rectangular panels, slabs on rigid beams span predominantly between the long beams, and for an aspect ratio of 2 the central region is curved practically only in the short-span direction. In a flat slab, the central section spans in the longer direction, and the transverse moments are confined to a limited width on either side of the columns as indicated by Figure 6.

Figure 6
Behaviour of elongated
panels of continuous
slabs



2.3 DEFLECTION

For the same slab stiffness and same span, the central deflection of a flat slab is much greater than that of a slab on beams. Figure 7 shows the variation of the elastic central deflection of an isolated square panel as a function of the ratio EI/ID of the slab and beam stiffnesses. In comparison with a pure flat plate, the deflection is halved by the

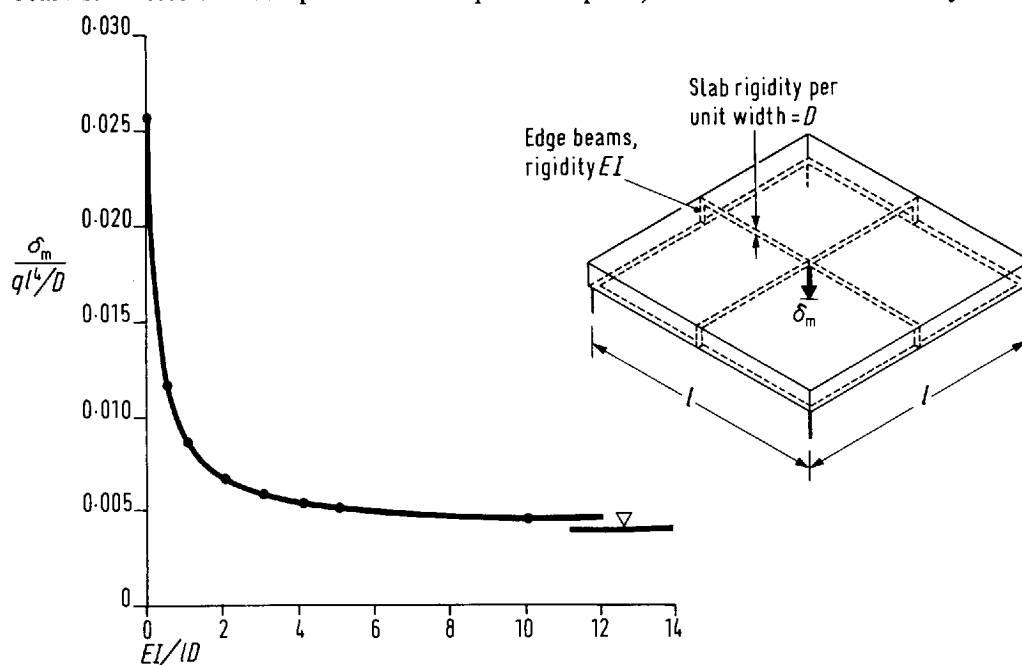


Figure 7
Influence of edge beam
stiffness on central
deflection of square
panel simply supported
at its corners

introduction of beams with a stiffness ratio of only about 0.4. With a beam width equal to 1/20 of the span, this stiffness is obtained for a total beam depth equal to twice that of the slab.

The curve of Figure 7 is drawn for uniform loading on an elastic structure on point supports and for beams without torsional stiffness. The conditions in a reinforced concrete structure are naturally more complex, but it remains true that even relatively shallow beams have a very marked effect on deflections, as can be seen from Figure 8.

As the aspect ratio of the panels increases, flat slabs are at a further disadvantage because they span in the long direction. Deflection increases in proportion to the cube of the major span, while for a beam-supported system it depends on the cube of the short span.

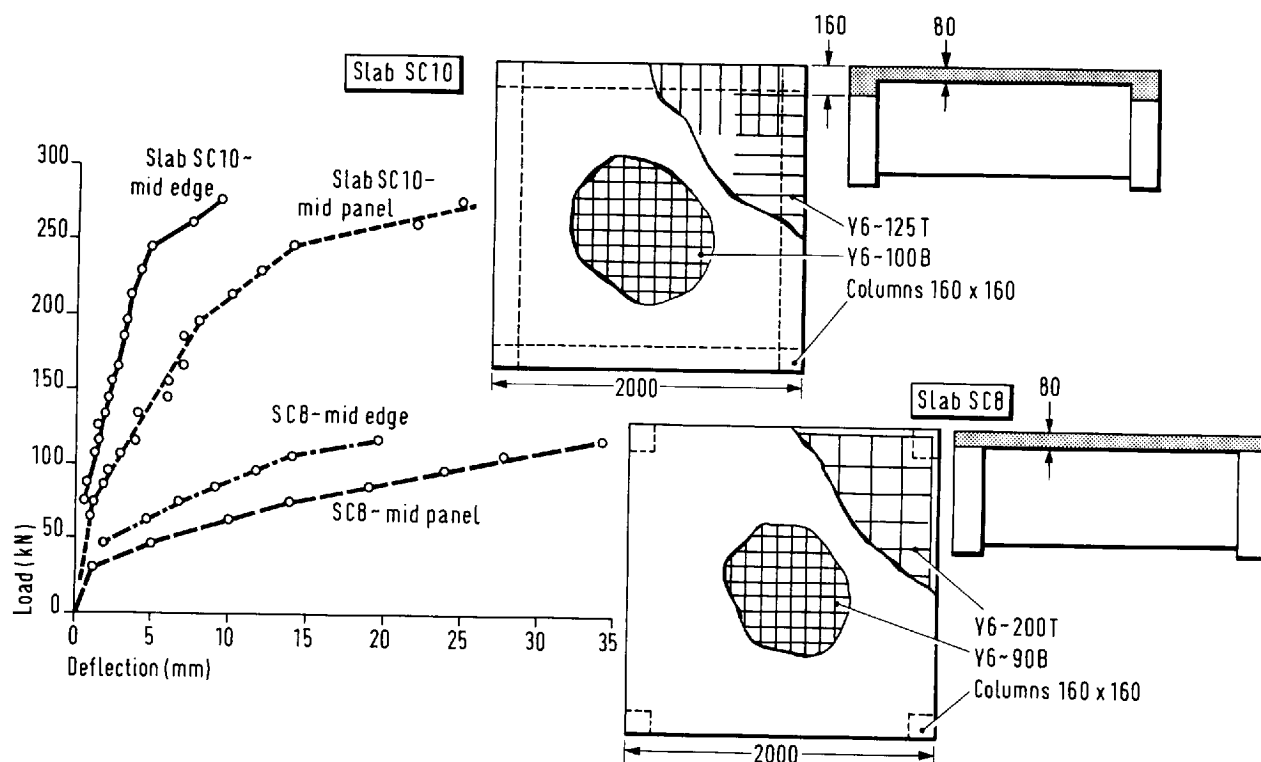


Figure 8 Deflection of square slabs on corner columns with and without edge beams

2.4 SHEAR

In a slab on rigid supports, the maximum shear resulting from uniform loading is concentrated toward the middle section of the edges. This edge shear is relatively well distributed, and, in practice, shear failure is unlikely. By contrast, in a pure flat plate, the shear is necessarily concentrated to the columns, and punching is the commonest mode of failure.

Distribution of shear in slabs with flexible beams can be analysed on the basis of elastic theory, but there is no really satisfactory method of determining the proportions of the total shear supported by the beams and slab near the columns once cracking has occurred. For practical purposes, it is probably wisest to design the beams for the whole force and to provide stirrups accordingly.

The situation in a flat plate as compared to a beam structure is somewhat anomalous, in that codes require beams to be provided with stirrups, while in a flat plate where the area of concrete is reduced by the loss of the downstands, the provision of shear reinforcement is unusual.

2.5 FRAME ACTION

In the design of reinforced concrete slab/beam systems, it is common to neglect the torsional stiffness of the transverse beams. This is generally reasonable, since their torsional stiffness in the cracked state is very low unless heavy stirrups are provided. The frame action developed is essentially that assumed in design, with interaction between the columns and the longitudinal beams.

Normal design assumptions are also fulfilled in systems where slabs are supported by monolithic walls. Here, as in a beam/column frame, the connections of the vertical and horizontal members pose no very special problems.

In flat slabs, while there is full continuity between consecutive slab spans, that between the slab and the columns is less complete. Under vertical loading, the effects of this reduction of continuity are most pronounced in external panels, but for horizontal loading the whole structure is affected.

Taking the example of a slab edge, according to elastic analysis, when the slab is vertically loaded, the parts of it in immediate contact with the column faces remain perpendicular to them, but along the rest of the edge the slab rotates relative to the columns as indicated in Figure 9. The overall effect is a reduction of continuity, so that even if the columns remain vertical, the total negative moment at the slab edge is less the normal fixed end moment.

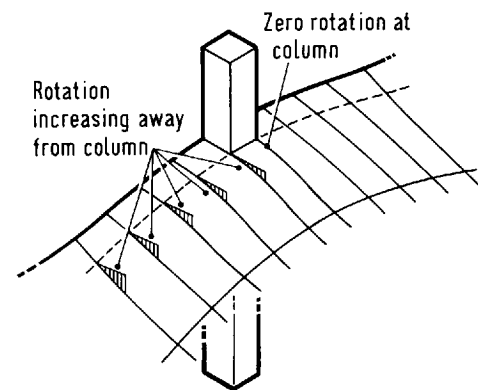


Figure 9
*Deformation at edge of
an elastic plate near a
column*

Another view of the same phenomenon comes from considering the effect of a moment transmitted from a column to a slab. Because of the limited contact between the two elements, the moment per unit width in the flat slab near the column is much higher than in a slab to which a similar moment is applied by a wall. The higher moment produces higher curvatures (and thus a greater rotation in the flat slab).

The overall influence of this connection behaviour is similar to that obtained by the insertion of elastic hinges between continuous beams and columns, the 'stiffness' of the hinge depending on the geometry of the slab/column interface.

3. The background of the flat slab design

3.1 OVERALL DISTRIBUTION OF MOMENT

As can be appreciated from Section 2, in a flat slab (and particularly a flat plate) there are a number of disadvantages in comparison with other floor systems. In terms of direct material consumption, it is seldom the most economical way of achieving a specified structural performance. However, there are positive compensating features, which include the economy of formwork because of the absence of beams, the provision of a flat soffit, which can simplify the installation of services or allow direct decoration without the need for a false ceiling, and the reduction of floor thickness,

which gives a saving in the cost of cladding and can allow an extra storey to be included in a building of limited height. On balance, flat slabs have proved advantageous, and very large numbers have been constructed since their introduction in the early years of this century.

The earliest flat slabs were built by Turner in the USA from 1906 onwards, and the first European example seems to have been by Maillart in Zurich in 1910.

The first code of practice recommendations appeared in the American Concrete Institute (ACI) Code of 1920, so there was a considerable period in which the method of design depended only on the judgement of the individual engineer. Little is known of Maillart's approach, except that it was derived from tests to failure of large-scale prototypes, the results of which were analysed by comparing deflections with those observed in simple slab strips.

Turner's work was more influential, but appears to have lacked a valid theoretical basis. Amazingly small amounts of reinforcement were used, top steel being designed for moments as low as $Ql/50$. Turner was very successful, and had been responsible for more than 1000 buildings by 1914 when his design methods were challenged by Nicholls⁽²⁾, who stressed the equilibrium requirement that the sums of the positive and negative moments in each direction should be $Ql/8$.

The major theoretical misconceptions were eventually cleared up in 1921 by a paper by Westergaard and Slater⁽³⁾, giving a rational elastic analysis for interior square panels, together with some information on other panels. They also explained the reasons for the good results obtained in proof loadings of inadequately designed structures. In most cases, load was applied to only a few panels, and the level of loading was not much above the working range. With some restraint from unloaded areas, the cracking was minimal, and tension stiffening by the concrete meant that the bar strains recorded on long gauge lengths were far below those corresponding to simple cracked-section theory.

Unfortunately, their work seems to have come too late to influence the 1920 ACI Code, which recommended an 'empirical' approach calling for a total design moment:

$$M + M' = 0.09Ql \left(1 - \frac{2c_1}{3l} \right)^2$$

where c_1 is the dimension of a column in the direction of the span l , and the term in parentheses allows for the effective reduction of the span because of the finite size of the column.

So-called empirical methods persist even to the present, and in the last edition of CP114⁽⁴⁾ the total design moment was still only $Ql/10$, although CP110⁽⁵⁾ has at last corrected this.

These methods, which give simple coefficients for bending moments irrespective of the details of the structure, have long been recognised as being of limited applicability. To overcome the restrictions, a more general approach was developed and adopted in the Californian Code of 1933. With minor modifications, it became the well known Equivalent Frame Method, which was given in ACI codes from 1941 to 1963 and is still used in CP110.

This equivalent frame approach has two principal disadvantages. First, it makes no allowance for the partial lack of continuity between the slab and columns, second, it offers no prospect of a unified approach to the design of two-way slabs. Codes which employ it have totally separate provisions for slabs on rigid beams or walls, and give no guidance on slabs with flexible beams.

In view of these shortcomings, a major reconsideration of slab design was undertaken in the USA in the late 50s and early 60s, and a large research programme

was conducted by the University of Illinois and the Portland Cement Association. As a result of this work, the ACI recommendations were revised in 1971 to the form in the current (1977) Code⁽⁶⁾. The approach adopted is a modified equivalent frame method, and unifies the design of all two-way slab systems. Its application to flat slabs is reviewed in some detail in Section 4.

The main international alternative to the ACI Code is the CEB/FIP model Code⁽⁷⁾. This gives no detailed recommendations for flat slabs, but does specifically permit the use of yield-line theory.

Codes of practice are not the only sources of information for designers, and there is a considerable literature on flat slabs, mostly concerned with elastic analysis. The earlier work used classical methods based on Fourier series expansions, but the cases which could be treated were originally rather limited. The range was greatly extended by the introduction of computers, which also made possible the use of finite element and finite difference methods.

Apart from the inherent shortcomings of applying elastic theory to reinforced concrete, the major problem was to present the results in a general way so that they can be of direct use in design. Recent American and Australian work has sought to do this by modifying the ACI Code method for cases of vertical loading, and by giving effective slab widths to be used in frame analyses for horizontal loading. The difficulty of more direct use of elastic plate solutions is illustrated by the fact that Pfaffinger and Thürlmann's 'tables for flat slabs'⁽⁸⁾ is a 331-page book, but does not treat any case of slab/column continuity.

An interesting series of papers by Brotchie^(9 to 12) develops a general alternative to equivalent frame methods, and uses the concept of a slab on elastic foundation to which loads and reactions are applied separately. The magnitudes of the reactions are determined by the conditions that the total load on the imaginary foundation resulting from the applied loading on the slab and the column reactions should be zero, and that slab/column continuity should be maintained. At present, the approach seems less attractive than frame methods where the latter are applicable, but it has the advantage of being able to deal with non-rectangular arrangements of columns.

Plastic methods can, at least in theory, be applied to flat slabs, and yield-line treatments are given by Kinnunen⁽¹³⁾ and by the CEB^(14, 15). Possible, but as yet less developed, lower bound approaches include Hillerborg's strip method⁽¹⁶⁾ and the modified 'strip deflection method' recently presented by Kemp and Fernando⁽¹⁷⁾. The problem with plastic theory is that flat slabs do not possess unlimited ductility as their deformations are frequently curtailed by shear failures. This means that it is unsatisfactory to ascribe arbitrary values to the moments transferred to columns, and that some form of compatibility analysis is necessary. The implications on service load behaviour of using plastic methods of strength design would require considerable study. Kemp and Fernando's work is a move in this direction, but has not yet solved the problems of moment transfer.

3.2 RESISTANCE TO PUNCHING SHEAR

Code recommendations on punching are nearly all empirical and were for many years limited to concentrically-loaded internal connections, although they were presumably applied in other circumstances. All such methods make use of nominal shear stresses calculated by dividing the shear force by an area, A , equal to the product of the length of a critical perimeter and the effective depth of the slab. They differ in regard to the distance from the column faces to the perimeter, and in the expressions used to define the limiting value of the stress.

When the perimeter is drawn close to the column, the corresponding stresses are very high. If the perimeter is moved outward, they reduce and, in CP110, the critical section is defined as being at a distance from the column equal to 1.5 times the slab

thickness, so that the stress limits can be the same as for one-way slabs. The more remote perimeter can also be argued to have the advantage of making allowance for the effects of stress concentrations at the corners of columns, which must otherwise be accounted for by some sort of correction factor as in the ACI and CEB/FIP Codes.

In recent years, permissible stresses have been modified to allow for the influence of the flexural reinforcement, expressed either by a steel ratio (as in CP110 and the CEB/FIP Code) or by the ratio of the punching load to the yield-line strength of the slab (as in Moe's method, on which the ACI Code is based). Scale effects are also included in recent codes.

The other development is the extension of empirical methods to deal with external column/slab connections and with internal connections transmitting unbalanced moments as well as shear forces. In most cases, this was done by assuming a part of the moment to be provided by unevenness of the distribution of shear around the perimeter, and requiring that the maximum shear should not exceed a limiting value equal to that for a concentrically loaded connection. In the ACI and CEB/FIP codes, the distribution of shear stresses, v , is found from equations which are essentially:

$$v = \frac{V}{A} + \alpha \frac{\bar{M}y}{I}$$

where V and \bar{M} are the shear force and unbalanced moment at the joint
 α is the proportion of \bar{M} assumed to be resisted by uneven shear
 A is the shear area defined above
 y is the distance from the centroid of A to the point considered
and I is the second moment of area of A about its centroid.

The CP110 method is somewhat different. For external connections with moments perpendicular to the slab edge, the maximum stress is taken as 1.25 times the average, while at internal columns, to which moments are transmitted, the ratio of maximum to average shear stress is defined in terms of the ratio of the eccentricity (M/V) to the span of the slab, rather than to the column dimensions. However, for typical column sizes and slab spans, the results produced are not very different from those of other codes.

The only code recommending a more theoretical approach to punching seems to be the Swedish one⁽¹⁸⁾, which is based on research at the Royal Technical University (KTH) Stockholm^(19, 20). The theory was originally developed for axi-symmetric loading at internal connections. In this case, the slab is analysed as a series of radial segments, such as that shown in Figure 10. Each segment is assumed to rotate as a rigid body, while the shear is supported by the vertical component of the force in the compression zone at the face of the column. The criterion of failure is taken as the attainment of a limiting tangential strain at the soffit of the slab below the root of the shear crack. In recent years, the theory was extended to deal with edge and corner columns, while internal connections with unbalanced moments can be designed on the basis of the original theory applied to the quadrant with the highest shear.

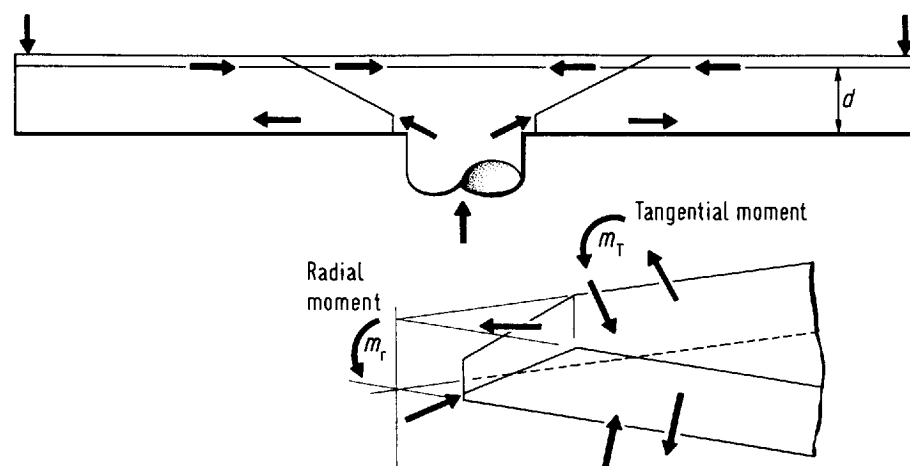


Figure 10
*Model of slab
behaviour in Kinnunen
and Nylander's
treatment of punching*

The method is not as simple as those in other codes, and although the deformation model is a good one, the criterion of failure is open to question. Some of the extensions to load conditions other than those of axial symmetry are also doubtful.

An approach based on the theory of plasticity was developed by the Technical University of Denmark^(21, 22). In this, the ultimate movement in a punching failure is assumed to be a vertical one occurring at a shear crack. The external work done is equal to the shear force multiplied by the vertical movement, while the internal work is expressed in terms of the failure criterion for concrete and the shape (inclination) of the failure surface. A minimum upper-bound solution is obtained by adjusting the shape of the surface so as to minimise the internal work. At present, the method is fully developed only for axi-symmetric punching.

Long and his co-workers at the Queen's University Belfast^(23 to 26) developed a theory by which punching resistance is related to flexural conditions in the slab. The basic case analysed is again the axi-symmetric one. Elastic plate theory is used, and the solution for the moment distribution is obtained by interpolation between limits corresponding to fixity at the column faces and to ring loading without fixity, the latter being approached as the circumferential crack at the column face widens. Shear failure is taken to occur as a result of a critical stress state being reached at the neutral axis at some distance from the column or at the compressed surface adjacent to the column. In a simplified version, the punching load is predicted as either 1.3 times the load causing the first yielding in the tangential direction or the load corresponding to a simplified form of the original expression based on shear stresses at the neutral axis. The approach was extended to deal with internal connections subjected to unbalanced moments and to edge columns.

Although the above and other theoretical approaches are of interest, they are all open to various criticisms, and none as yet deals with the full range of cases of punching. For the present, it seems that design for punching is best based on empiricism, although the method developed in Section 5 departs from current code treatments by relating its nominal stresses to the area of the failure surface instead of the product of an arbitrary perimeter and the slab depth.

3.3 LOCAL FLEXURAL STRENGTH

Although the formation of local yield lines is not a criterion of failure for a slab as a whole, it can limit the moment transferred to a column. Thus, where a slab is designed by a frame method, it is necessary that the arrangement of the reinforcement be such that local yielding does not invalidate the design distribution of moments. Unfortunately, this is not guaranteed by the detailing requirements of either CP110⁽⁵⁾ or ACI 318-77⁽⁶⁾. The subject is discussed further in Section 4.6.

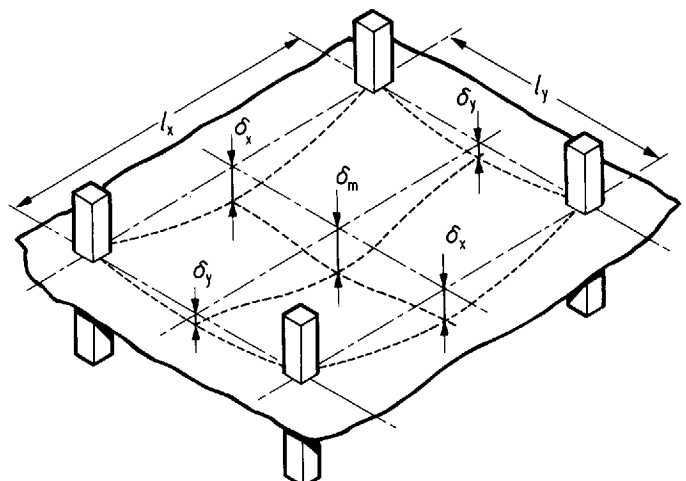


Figure 11
Deflections of an interior panel

3.4 SERVICEABILITY

Deflection of flat slabs can be critical, particularly with the general use of higher grades of reinforcement. The subject is poorly covered by CP110, which simply makes reference to tables of span/depth ratios devised for one-way members and slabs with rigid boundaries. Although it cannot be intended, the clause in question could be interpreted as referring to the ratio for the shorter span of a rectangular panel.

Various more realistic treatments of the subject have been published which model the true deflected shape of Figure 11. Ingvarsson⁽²⁷⁾ presents elastic deflection coefficients for seven arrangements of bays and for various aspect ratios of panels. By comparing these with equivalent analysis of other slab systems, he concludes that the basic method of the Swedish code can be applied to flat slabs. Thus:

$$h_{\min} = \gamma \sqrt{\frac{7m_{\text{span}}}{\sigma_{\text{bd}}}} \text{ (SI units N \& mm)}$$

where h_{\min} is the minimum slab thickness required, m_{span} is the maximum positive moment at the service load, σ_{bd} is the permissible flexural tension for the concrete taken as $0.55 \sqrt{f_{\text{cu}}}$, and γ is a coefficient varying between 1.0 and 1.2, depending on the configuration of the structure.

The analysis is somewhat limited as only overall uniform loading is considered, continuity with columns is neglected, and the deflections treated are those at the centres of column lines and not in the middle of panels. Furthermore, the constants of equations of this type are only valid for a particular working stress in the reinforcement, and so by inference for a particular grade of steel (probably $f_y \simeq 450 \text{ N/mm}^2$ in this case).

Another approach based on plate theory was devised by Jofriet⁽²⁸⁾, who gives expressions for mid-panel deflections based on numerical analyses of typical slabs with account taken of cracking at higher loads.

Other authors have treated deflections in the context of equivalent frame design. Similar approaches are given in References 29 to 31. In each, the frame used is that of the ACI code, and the mid-panel deflection is calculated as the sum of the deflection of a column strip in one direction and that of a middle strip in the other. The differences between the methods arise from their assumptions regarding slab stiffness and the influence of cracking.

A rather different sort of frame was considered in the University of Illinois study⁽³²⁾ of two-way slabs. Deflections were determined by dividing the flat slab into beam and simply-supported slab components. While the modelling of behaviour may be rather more detailed than in other frame methods, from a design point of view, it seems unreasonable to model the same structure in two different ways: one for determining moments, the other for deflections.

The approach to deflection control given in Section 4 is based on the same frame analogy proposed for the calculation of design moments for the ultimate limit state.

Crack widths should be controlled at service loads, but there are no publications dealing specifically with cracking in flat slabs. In design, reliance is thus placed on detailing requirements, normally expressed in terms of bar size, spacing and cover. For these to be effective in controlling crack widths, the service load stresses in the steel should be similar to those in simpler structures. This means that the arrangement of reinforcement should be such that excessive redistribution of moments is not required between the serviceability and ultimate limit states.

4. Flexural design

4.1 DETERMINATION OF GROSS FRAME MOMENT

The flexural design of a flat slab structure can be divided into two processes:

1. the determination of gross moments across the widths of slab associated with lines of columns (frame analysis)
2. the determination of the distributions of moments across those widths (see Section 4.2)

The two are inter-related, as the frame action differs from that of an ordinary beam/column or slab/wall structure because of differences in the transverse distributions of moments. However, the simplification obtained by the division of design into two stages is worthwhile.

As in other concrete structures, the distribution of moments in flat slabs is influenced by cracking and, in the cracked state, by the details of the reinforcement. The effect of cracking is discussed in some detail in Section 4.1.3, so, for the present, it suffices to observe that there is no really practical alternative to the use of 'uncracked' elastic theory as a design approach, and that the moment distributions calculated by it can be realised at least approximately, if the reinforcement is suitably arranged. The reality of cracking means that any apparent extra accuracy in a refined analysis (as compared to a crude one) is likely to be misleading, and that a simple and comprehensible approach is preferable.

4.1.1 Equivalent frame analysis

The use of an equivalent frame analysis seems reasonable in view of three facts:

1. It satisfies the absolute equilibrium requirements discussed in Section 2.1, i.e. that in any span of the slab:

$$M + (M'_1 + M'_2)/2 = Ql/8$$

where M is the positive moment at midspan

M'_1 and M'_2 are the negative moments at the supports

and Q is the total (uniformly distributed) load on the span.

2. The moments in one orthogonal direction are not significantly influenced by those in the other, which means that bending actions in the two directions can be treated separately. An example demonstrating the lack of influence in a full elastic plate analysis is shown in Figure 12.

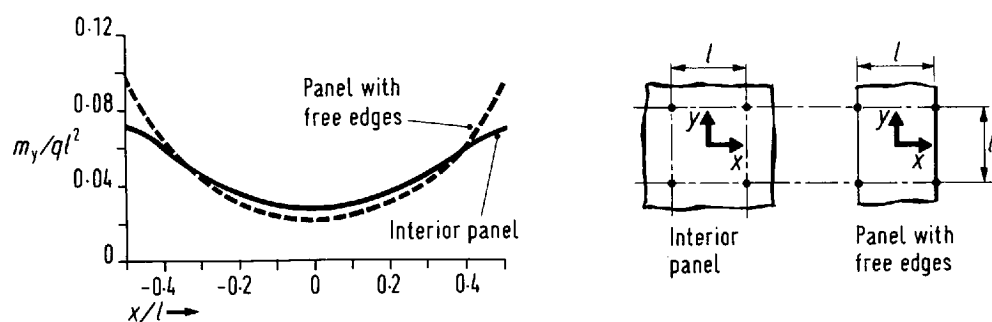


Figure 12
Positive moments at midspan for an edge panel and an interior panel

3. For a slab on point supports with a regular array of panels of equal size all subjected to uniform loading:

$$M = Ql/24 \text{ and } M' = Ql/12$$

for an elastically analysed plate and for a continuous strip or frame member. Similarly, for pattern loading with alternate bays loaded and unloaded, the two solutions agree with:

$$M = Ql/12 \text{ and } M' = Ql/24.$$

The difference between the 'frame' of a flat slab structure and a normal frame is the relative lack of continuity between the slab and columns. If the vertical members of the two substructures of Figure 13 are acted on by equal moments, the resulting rotation (θ_s) in the flat slab of Figure 13(a) is greater than the equivalent beam rotation (θ_b) in the beam/column arrangement of Figure 13(b).

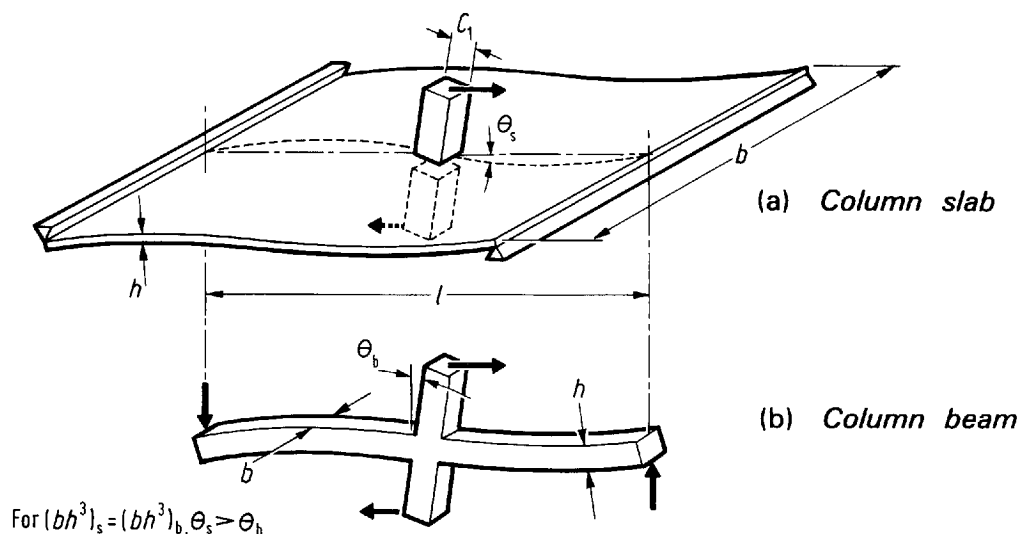


Figure 13
Deformations of slab-columns and beam-column structures

The situation in a flat slab is in some ways reminiscent of that in a steel frame with elastic or elastic-plastic joints (e.g. in a bolted or riveted structure rather than a welded frame). However, in the steel frame, the connection of one span to the next involves two deformable joints, while in the flat slab there is full continuity between spans and only the connections to the columns are deformable. A model of the flat slab arrangement shown in Figure 14(a) may be compared with the steel frame model of Figure 14(b).

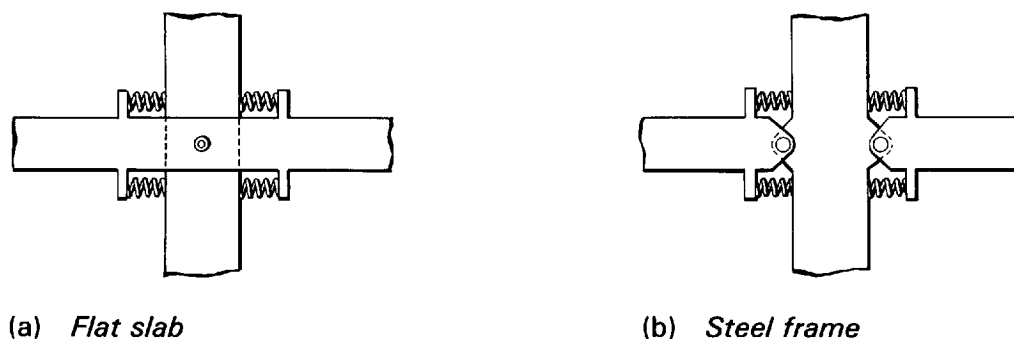


Figure 14
Models of structures with deformable joints

The representation of Figure 14(a) is essentially that used in both the current ACI method for flat slabs and in the proposed approach developed in Section 4.1.3. It has the weakness of treating members of finite dimensions as being purely linear. This is an error which is commonly not considered in all types of frame analyses, and it is not peculiar to flat slabs. It raises particular problems in the definition of the stiffnesses of slab/column connections.

The flexibility of a connection can be regarded as the difference in deformation between a flat slab structure and a basic frame (e.g. between the arrangements of Figure 13). For the flat slab, θ_s can be determined by elastic plate theory, provided that assumptions are made about the behaviour of the slab/column interface. A rather common assumption is to assume that the slab undergoes no deformation within the area of the column. For the basic beam-column frame, the corresponding rotation can be calculated either ignoring or taking account of the finite dimensions of the column. Using the example of Figure 13 in the former case:

$$\theta_b = \overline{M}l/12EI$$

where EI is the rigidity of the horizontal member.

If the column size is taken into account and the beam is assumed to be rigid within the area of the column

$$\theta_b = \overline{M}l \left(1 - \frac{c_1}{l}\right)^3 / 12EI \quad (2)$$

The difference between the above two Equations can be appreciable when the 'effective rotation of the joint' is calculated as the difference between the actual slab rotation and that of the equivalent beam, such that

$$\theta_j = \theta_s - \theta_b$$

The use of linear frame analysis for beam/column structures can be justified by the fact that in reality there are deformations of beams because of stresses within the joints. On one hand, there is a shortening across the column at the level of the compression zone of the beam, and, on the other hand, the beam reinforcement remains stressed within the column, and the extension appears in cracks at the faces of the column.

These same effects exist in flat slabs, possibly magnified by the concentration of moments causing relatively early yielding of the reinforcement near columns and correspondingly large crack widths at the column faces. Well before failure, there is a transition from a condition in which the slab is wholly elastic and encastré at the column faces to one in which an otherwise elastic slab is acted on by known actions (shears and yield moments) at the column faces.

In developing an 'equivalent frame' to represent a flat slab structure, it is thus only correct to compare like with like (i.e. to determine θ_j values as above, using compatible methods of calculating θ_s and θ_b). By ignoring this, Ingvarsson and Sundquist⁽³³⁾ showed that column moments in vertically loaded flat slabs were comparable with the results of frame analysis. However, the conclusion that a frame analysis of the CP110 type is a correct representation of flat slab behaviour is misleading.

If a correct comparison is made, a flat slab joint is always more flexible than that in a normal frame, and flat slab structures under vertical loading develop smaller column moments than normal frames, except in the short span directions of elongated rectangular panels.

The condition of compatibility at a slab/column joint, represented as in Figure 15, can be expressed as

$$\theta_s = \theta_c + \theta_j = \frac{\overline{M}}{K_c} + \frac{\overline{M}}{K_j} \quad (3)$$

where \overline{M} is the moment transferred from the slab to the column via the joint

K_c is the stiffness (\overline{M}/θ_c) of the column

and K_j is the stiffness (\overline{M}/θ_j) of the joint.

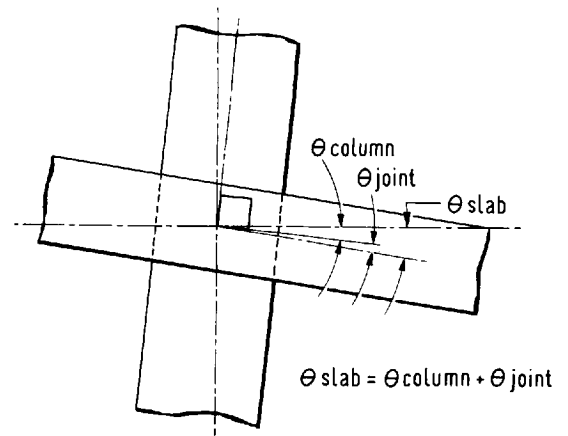


Figure 15
Compatibility of slab and column rotations

Thus, as far as loading on the slab is concerned, the presence of a deformable joint has an effect directly equivalent to that of a reduction of column stiffness to an 'effective value', K_{ce} , such that

$$\frac{1}{K_{ce}} = \frac{1}{K_c} + \frac{1}{K_j} \quad (4)$$

This simple treatment of the influence of joints is used in both the ACI approach and in the proposal of Section 4.1.3.

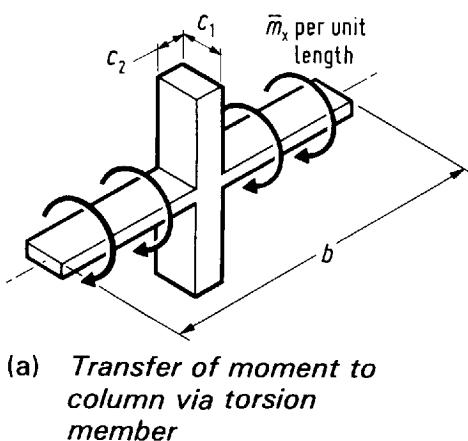
In view of the similarities between the proposal made in this Report and in the ACI method of design, the latter is reviewed in some detail below to explain the reasons why a new proposal is made.

4.1.2 The ACI equivalent frame method

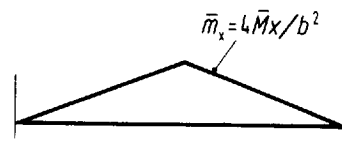
The official commentary on the ACI Code refers to a paper by Corley and Jirsa⁽³⁴⁾ for an explanation of the equivalent frame method. The following comments relate to that explanation.

The transfer of a moment between a slab and a column is assumed to be made by the imaginary torsional member shown in Figure 16(a). The distribution of moments acting on this member is assumed to be linear as in Figure 16(b), so that the moment at a distance x from the edge of the equivalent frame is

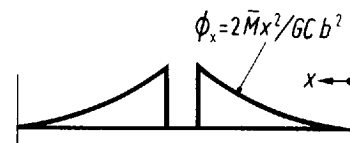
$$\bar{m}_x = 4\bar{M}x/b^2$$



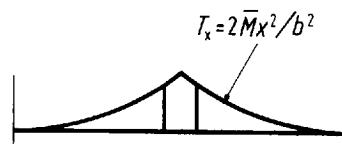
(a) *Transfer of moment to column via torsion member*



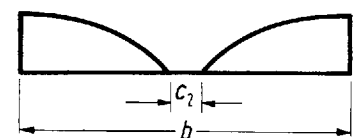
(b) *Moments from slab to edge strip*



(d) *Twist per unit length of edge strip*



(c) *Torque in edge strip*



(e) *Rotation of edge strip relative to column*

Figure 16 *American Concrete Institute equivalent frame method*

From this, the torsion at section x is

$$T_x = \int_0^x \bar{m}_x dx = \frac{2\bar{M}x^2}{b^2} \quad (5)$$

and the corresponding twist per unit length is

$$\phi_x = \frac{T_x}{GC} = \frac{2\bar{M}x^2}{GCb^2}$$

where GC is the torsional rigidity of the member.

The total twist at point x is then correctly

$$\Phi_x = \int_0^x \phi_x dx = \frac{2\bar{M}x^3}{3GCb^2}$$

If the column remains vertical, the variation of rotation across the width of the slab is as shown in Figure 16(e) and reaches a maximum $\bar{M}(b - c_2)^3/12GCb^2$ at the edges of the strip.

For the equivalent frame analysis, an approximate average value of Φ_x is used as the rotation of θ_j of the joint

$$\theta_j = \frac{\bar{M}(b - c_2)^3}{36GCb^2} \quad (6)$$

This choice of an ‘average’ seems surprising, and the explanation that the average rotation is equal to the area under one branch of the twist diagram of Figure 16(d) is of little help. There appear to be two sources of error: first, the integration of twist with respect to length gives a total rotation, while an average could only be obtained by the integration of rotations and subsequent division by length; second, the rotations obtained by the integration of Figure 16(d) are relative to the edges of the strip and not to the column.

It is hard to say how important these anomalies are, since some irregularities in a more or less pictorial representation need not necessarily mean that there is anything wrong with the expression for θ_j . However, they are rather disconcerting.

There are other more definite disadvantages in the ACI approach

1. The distribution of moments at the lines of the column faces used to determine the torque is unrealistic for rectangular panels. Where the moments are in the long span direction, they need not drop to zero at the edge of the strip, and where they are in the short span, they do not extend over the full width between columns.
2. If the width of the torsional member is reduced, the joint stiffness reduces too rapidly. In the limit, if the connection with the slab is only at the inner face of the column, the ACI joint stiffness becomes zero, while, according to elastic theory, there is still a very significant transfer of moment to the column.
3. The method of expressing compatibility conditions in terms of ‘average rotations’ is misleading, since what is required is compatibility of deformations between the column and the part of the slab in contact with it.
4. At least as expressed in the ACI Code, the US approach becomes very complicated because of the use of fixed end-moment coefficients and stiffness and carry-over factors different from those of normal frame analysis.

In view of these disadvantages and of the difficulties of extending the ACI approach to deal with horizontal loading, a proposal for a new treatment of the equivalent frame is developed below.

4.1.3 Proposed method—vertical loading

Considering the simple case of a single-bay structure simply-supported on edge columns and deflected by uniform vertical loading, the rotation of the slab at the columns is greater than that in an otherwise similar slab supported across its full width. The increase can be treated by the use of an effective slab width less than or equal to the full value defined such that:

$$\theta_s = \frac{qbl^3}{24b_e D} \quad (7)$$

where θ_s is the rotation of the slab at the columns, according to elastic plate theory

l is the span of the slab

b is the full width of the equivalent frame (i.e. the width from which the loading is determined)

b_e is the effective slab width

D is the slab rigidity per unit width ($D = E_c h^3 / 12$ if Poisson's ratio is neglected)

and q is the load per unit area of slab.

Figure 17 shows the ratio b_e/b for Equation (7), calculated by elastic plate theory as a function of b/l . It can be seen that a reasonable approximation is obtained if b_e is taken as the lesser of b and l .

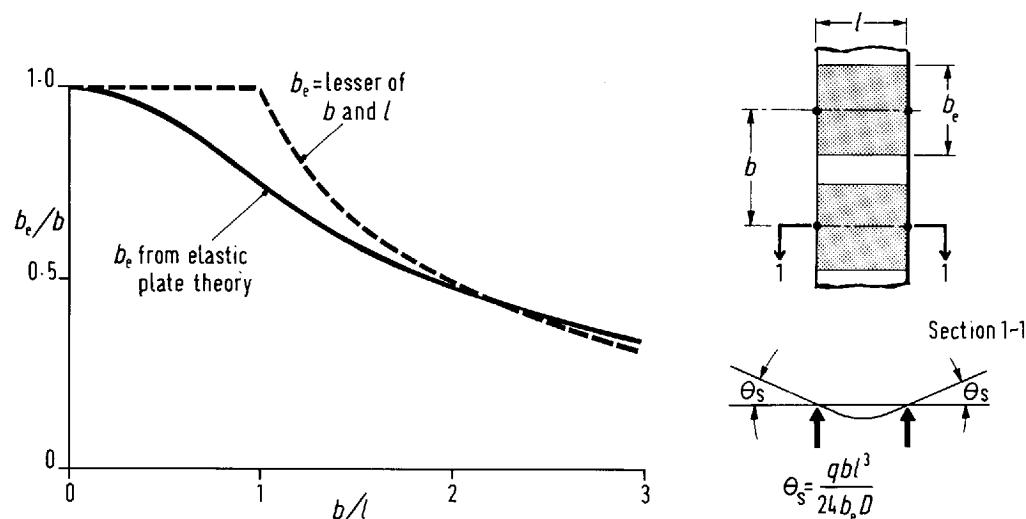


Figure 17
Rotations at edges of
a simply supported
slab strip

Now consider the same single-span structure but with the vertical loading removed and replaced by moments \bar{M} acting on the slab at the positions of the columns. As before, the rotations of the slab at the columns are greater than the uniform rotation produced if the same total moment were distributed along the edges of the slab. For uniform edge moments, the corresponding rotation is $\bar{M}l/2bD$. Thus, the slab rotation at the column can be expressed as

$$\theta_s = \theta_b + \theta_j = \frac{\bar{M}l}{2b_e D} + \frac{\bar{M}}{K_j} \quad (8)$$

where K_j is the stiffness (inverse of flexibility) of the joint between the slab and column.

The moments producing the additional deformation represented by \bar{M}/K_j are highly concentrated around the column, and are practically independent of the breadth of the slab.

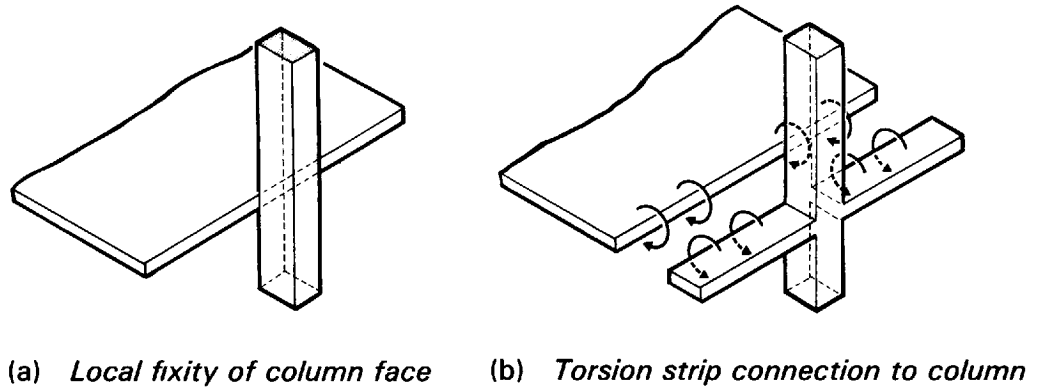
A theoretical evaluation of θ_j , using elastic plate theory, is given by Andersson⁽³⁵⁾, who considers an infinite strip of slab supported by edge columns. The uniform moment rotation term is subtracted from this slab rotation at the column to give values of θ_j as below. For the basic case of a slab contacting the columns only at their inner faces (or of columns with finite stiffness but no finite dimensions in the direction of the span) and for normal column dimensions parallel to the edge ($0.05 \leq c_1/b \leq 0.20$), a satisfactory approximation is obtained with

$$K_j = 1.5D$$

The situation arising when the slab contacts the column at three faces can be treated approximately by superposition:

1. of the previous case
2. equal and opposite moments applied to the main slab and edge strip
3. torsion of the edge strip between the columns (see Figure 18(b)).

Figure 18
Proposed approach—
addition of torsion strip
to slab contacting
column at inner face
only



The results obtained depend somewhat on the torsional properties ascribed to the edge member (i.e. on whether it is treated as a separate 'beam' or as a part of the slab). Adopting the latter assumption, which gives better agreement with other elastic approaches, and by giving a higher stiffness makes some allowance for the existence of a moment $Vc_1/2$ as a result of shear around the column, the total stiffness can be represented approximately as

$$K_j = (1.5 + 20c_1/b_e)D$$

where c_1 is the column dimension parallel to the moment and b_e is the effective slab width.

The case where moments are transferred from an internal column is somewhat more complex than the mere addition of the connections of two half edge columns (i.e. the summation of two 'inner face' stiffnesses and two torsional effects in strips of width $c_1/2$). A better correlation with elastic solutions is obtained by taking an interior joint to be twice as stiff as an edge connection to a column of the same dimensions giving

$$K_j = (3.0 + 40c_1/b_e)D$$

Connections of corner columns and of edge columns to strips parallel to the edge can be treated simply as halves of the corresponding connections with slabs to both sides of the column as indicated by Figure 19, which shows a range of slab-column connections and the relevant joint stiffness expressions.

The flexibility represented by the joint rotation, $\theta_j = \bar{M}/\bar{K}_j$, is equivalent to a reduction in the stiffness of the restraint given to the slab by the column. Thus, the effective stiffness of the column is given by Equation (4), page 23. This reduced column stiffness can be incorporated into a moment-distribution analysis.

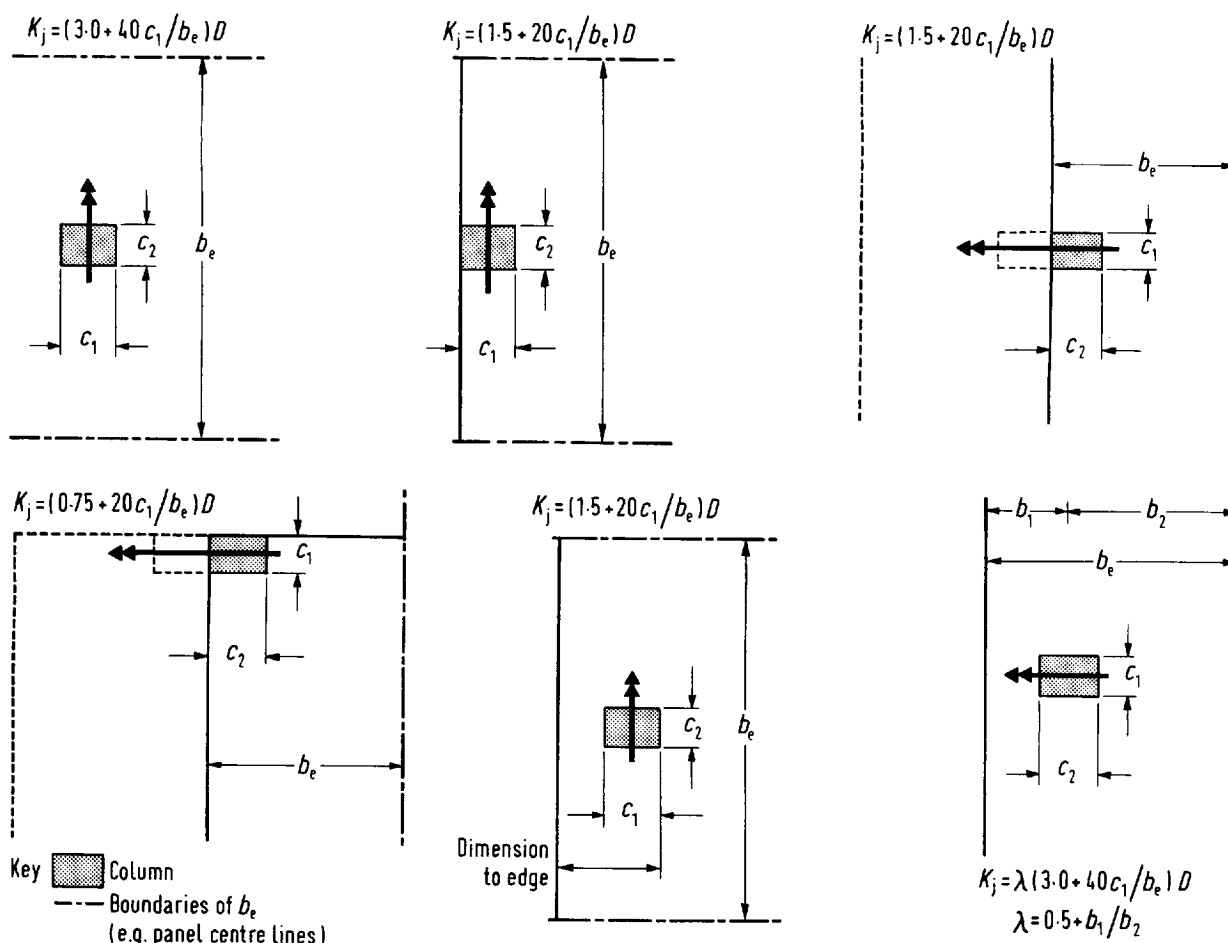


Figure 19 Joint stiffness— K_j

4.1.4 Proposed method—horizontal loading

When horizontal or sway loading is considered in a stiffness analysis, the initial fixed-ended situation is one with the external fixing moments applied to the columns. In this case, the restraining influence of the slab on the column is reduced by the flexibility of the joint. The slab stiffness should be reduced according to

$$\frac{1}{K_{se}} = \frac{1}{K_s} + \frac{1}{K_j} \quad (9)$$

where K_s = slab stiffness over the effective panel width
and K_{se} = effective slab stiffness for horizontal loading.

At an end column, Equation (9) is applicable, but at an internal column, two separate effective stiffnesses are required for each span. Thus the effective slab stiffness (K_{s1e}) on one side of the column is given by

$$\frac{1}{K_{s1e}} = \frac{1}{K_{s1}} + \left(\frac{K_{s1} + K_{s2}}{K_{s1}} \right) \left(\frac{1}{K_j} \right) \quad (10)$$

where suffices apply to spans 1 and 2 respectively.

4.1.5 Comparison of design methods

By introducing the notion of finite flexibility at slab/column connections, the proposed approach gives smaller values than CP110⁽⁵⁾ for the moments transmitted to columns when a slab is subjected to vertical loading.

For square bays, the moments predicted are similar to those obtained by the ACI method. This is demonstrated by the first part of Figure 20 which shows moments for a square internal column in a sub-frame loaded on alternate panels. For very small column sizes ($c/h \approx 1$), the proposal, ACI 318-77⁽⁶⁾ and CP110 all give some small column moments as the behaviour of the frame is determined by the very low stiffness of the column. When the column size is increased, the proposed and ACI moments

increase less rapidly than the CP 110 values, since the stiffness of the restraint to the slab is increasingly limited by the flexibility of the connection rather than that of the column. With $c/h \approx 4$, the proposed and ACI moments are about 40% below those obtained from CP 110.

In a practical case in which there is dead load on all panels, the difference is a smaller percentage but it is still significant, particularly in terms of the influence of the transferred moment on the shear capacity of the connection.

The remainder of Figure 20 shows the situation for rectangular bays, still with square columns. In the short span direction, the proposal gives moments significantly higher than those from the ACI code. The reason is the limitation of the slab's effective width to $b_e \leq l$, which reduces the stiffness of the slab relative to that of the column and also limits the value of b_e/c used in determining the connection stiffness. The predicted behaviour is in accordance with elastic plate theory. In the long-span direction, the moments from the proposed analysis are smaller than the ACI values, but the differences between all three methods are reduced.

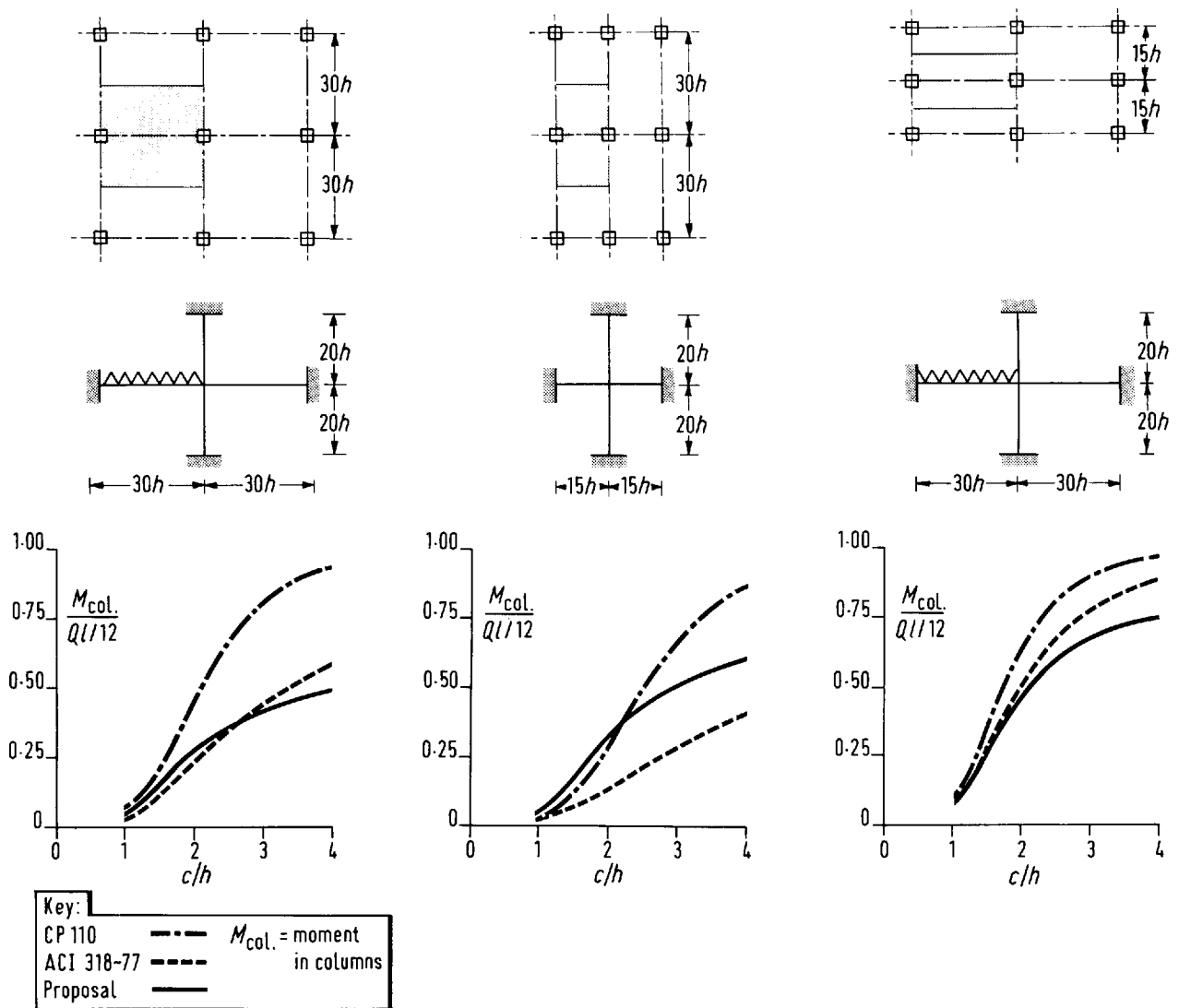


Figure 20 Comparison between various equivalent frame methods, for moment attracted to columns

Figure 21 presents similar data for external columns. From the first part, it can be seen that the column moments predicted by the proposal are similar to those for the ACI equivalent frame for smaller column sizes ($c/h \leq 2$), but fall below them for larger

columns. Both methods give column moments distinctly lower than those from CP 110⁽⁵⁾. The second part of Figure 21 shows the negative moments for which the slab would be designed, and here the proposal and the ACI Code⁽⁶⁾ give very similar results, since the ACI method allows a far greater reduction between the column and slab moments. It allows the slab to be designed for the negative moment at the inner face of the column, while the proposal made above is to treat the centroid of the slab/column interface as the critical position. Both slab moments are well below those of CP 110.

The last part of Figure 21 is drawn for the corner column case. Here, the proposed and ACI moments are very similar, and are again distinctly below those from CP 110 (about 30% lower for $c/h = 3$ to 4).

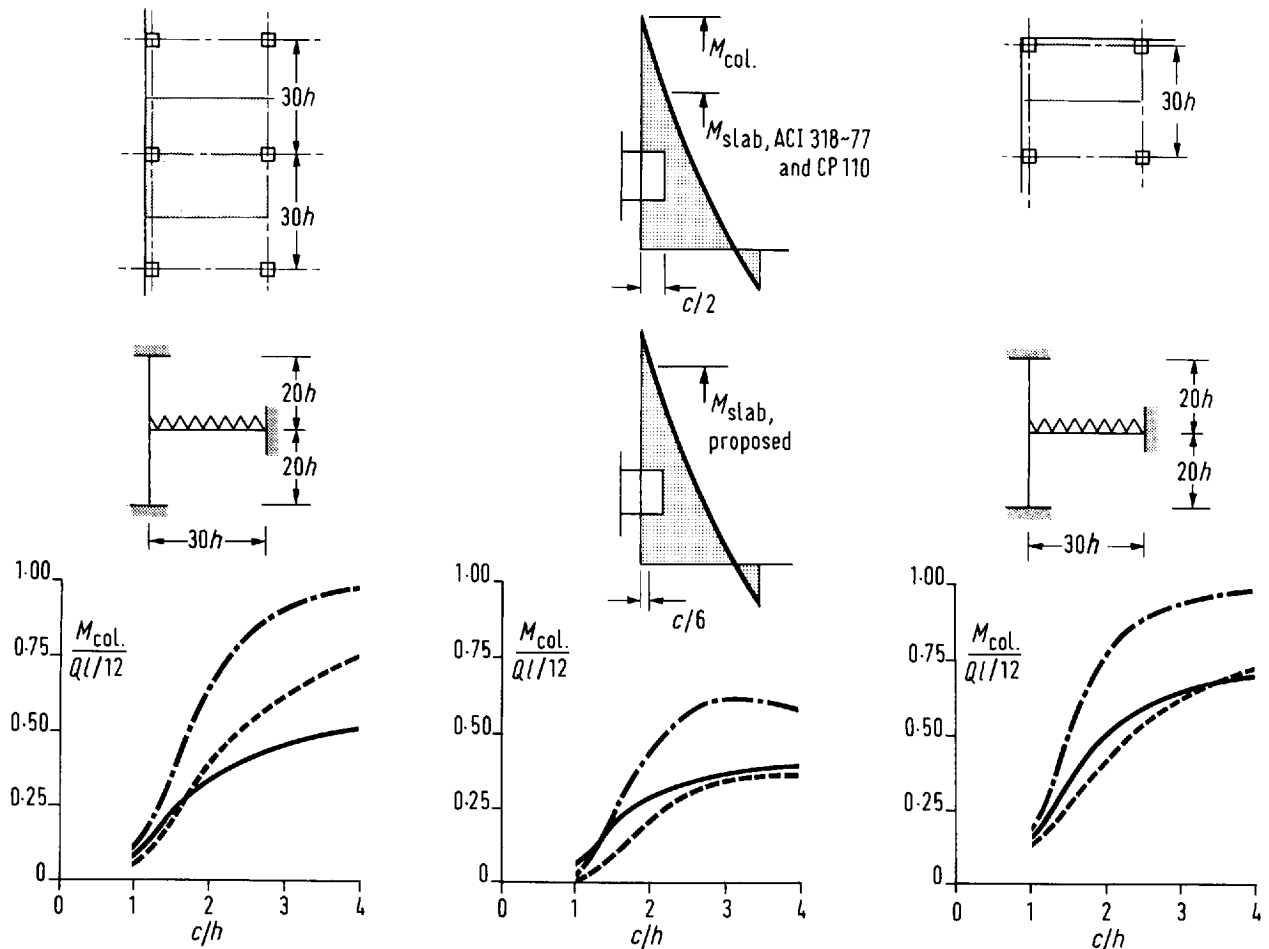
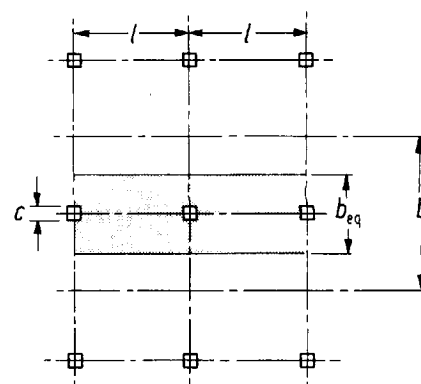
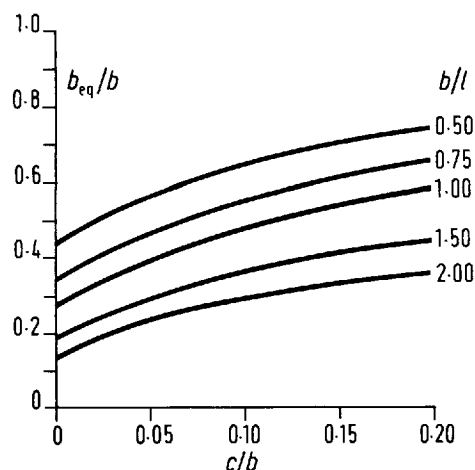


Figure 21 Comparison between methods, for moment attracted to perimeter columns

The relationship between moments calculated by the proposed method and moments from the CP110 simple equivalent frame method necessarily vary from case to case, depending on column size, panel shape, ratio of dead to live load, etc., but a reduction of about 30% is probably typical for multi-storey construction. For low-rise buildings with large spans, thick slabs and relatively small columns, the difference is less.

Finally, Figure 22 presents some results for cases of horizontal loading expressed in terms of the ratio b_{eq}/b , where b_{eq} is the equivalent width of slab defined such that an ordinary frame with horizontal members of rigidity Db_{eq} would have the same deformational characteristics as the flat slab (i.e. $b_{eq} = b(K_{se}/K_s)$). The case considered is again one with square columns. It can be seen that b_{eq}/b increases with increasing panel aspect ratios l/b and with increasing c/b . For a square bay and a column size, $c \approx 0.1b$ to $0.15b$, $b_{eq} \approx 0.5$, which agrees with the CP 110 recommendation for calculations related to horizontal loading.

Figure 22
Proposed treatment of
horizontal loading
expressed in terms of
equivalent slab
breadths



4.1.6 Comparison of proposed method with test results—discussion

Table 1 summarises comparisons between column moments measured in the CIRIA tests and values predicted by the proposed method of analysis of Section 4.1.3 and by the CP 110 equivalent frame method. In general, the moments given are those at approximately 95% of ultimate load. Actual ultimate load values are not given for two reasons:

1. where there was a brittle failure, it was not possible to record them
2. in some more ductile modes, the connections deteriorated very close to failure (primarily because of shear cracking) and the column moments decreased.

Results for a few specimens were omitted for the following reasons:

- | | |
|-------------|---|
| SC7 and SE9 | — column moments were applied externally |
| SC10 | — the specimen was not a flat slab but had shallow beams |
| SC11 and 12 | — the moments were possibly incorrectly recorded |
| W1 and W2 | — the moments given are those for the columns nearer the loads, those for the remote columns being small and in some cases affected by previous loadings. |

A fuller description of these tests is given in the Project Record⁽¹⁾.

In considering the significance of these moment ratios, a number of facts should be borne in mind:

1. The tests covered a wide range of reinforcement details and the variations involved clearly influenced the moments. This cannot be taken into account by any design method based only on the concrete dimensions. The behaviour for extreme steel details is rather unimportant as they would not correspond to design by the proposed approach (nor to most others).
2. Neither over- nor under-estimation of column moments can be regarded as 'erring on the safe side'. In general, neither leads to the use of more or less total reinforcement, only to changes in its arrangement. In some cases, overestimation of moments is 'safe' for shear design, but it is always unsafe for the estimation of deflections.
3. Any accuracy in the assessment of frame moments may be misleading as there are many unknowns involved in practice (e.g. settlements, load patterns, etc.).

Table 1 Comparison of experimental column moments with values predicted by the proposed method and by CP110 (CIRIA tests at 95% of ultimate test load)

Series	Ratios of calculated and test moments (M_{calc}/M_{test})		Remarks
	CP 110	Proposed	
Corner columns			Span steel below minimum ratio Diagonal top steel at corner
SC1	1.39	0.98	
SC2	1.28	0.91	
SC3	1.10	0.78	
SC4	1.67	1.18	
SC5	1.85	1.31	
SC6	1.29	0.91	
SC8	1.50	0.82	
SC9	1.43	0.86	
Edge columns			} Exceptionally light top steel } perpendicular to slab edge Column projecting beyond slab edge } Load <90% of ultimate, plastic } hinge formed
SE1	1.64	1.23	
SE2	2.05	1.54	
SE3	2.77	2.08	
SE4	1.56	1.32	
SE5	1.35	1.14	
SE6	1.44	1.22	
SE7	1.11	0.94	
SE8	1.11	0.97	
SE10	1.63	1.32	
SE11	1.58	1.22	
SE12	1.22	0.91	
SE13	1.22	0.91	
SE14	1.15	0.85	
SE15	1.91	1.00	
SE16	1.47	1.09	
SE17	1.28	0.96	
SE18	1.20	0.89	
W1/1	1.29	0.72	
W1/2	1.51	0.85	
W2/1	1.27	0.72	
W2/2	1.42	0.80	
Internal columns			
SI1	1.86	1.42	
SI2	1.54	1.14	

Referring to Table 1, if data for extreme and unlikely details are ignored, the ratios M_{calc}/M_{test} vary from 1.11 to 1.85 for CP 110 and between 0.72 and 1.42 for the proposed approach. Thus, the proposal does not really reduce the overall scatter of values. It does somewhat increase the number of cases for which M_{calc}/M_{test} is near the mean—more than half the values are within -15% and $+20\%$ of 1.0. More importantly, it generally gives reasonable estimates of column moments, whereas CP 110 consistently overestimates them.

A point of interest not covered by the presentation of Table 1 is the extent to which it is reasonable to treat flat slab systems as elastic when determining moments (i.e. principally the reasonableness or otherwise of using the same moment distributions for both the serviceability and ultimate limit states).

Figures 23 and 24 present some relevant examples of the ways in which column moments increase with increasing load. All the slabs for which data are shown were reasonably well detailed. The corner-column slabs of Figure 23 were lightly reinforced, and it can be seen that, following cracking of the slabs at a load of about 85kN, there was a tendency for a more rapid rise of moments in the uncracked columns.

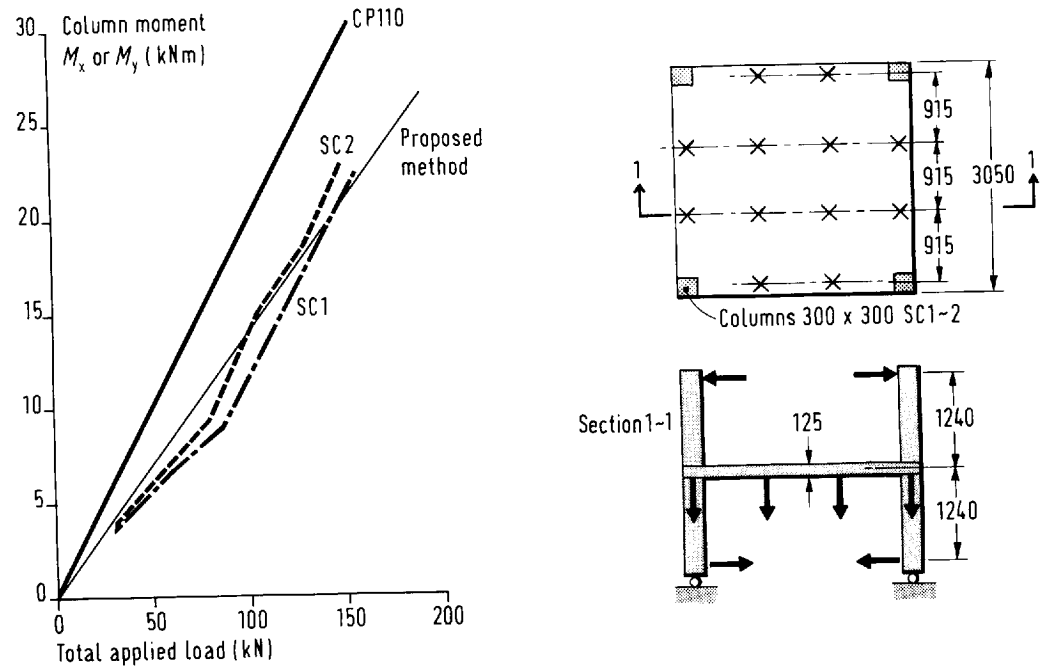


Figure 23
Actual and predicted
column moments for
test series SC

The edge-column slabs of Figure 24 were more heavily reinforced, and here the cracking had very little effect on the moment distribution. However, near failure, there was a decrease in the rate of growth of the column moments as a result of the start of plasticity in the slab/column connections.

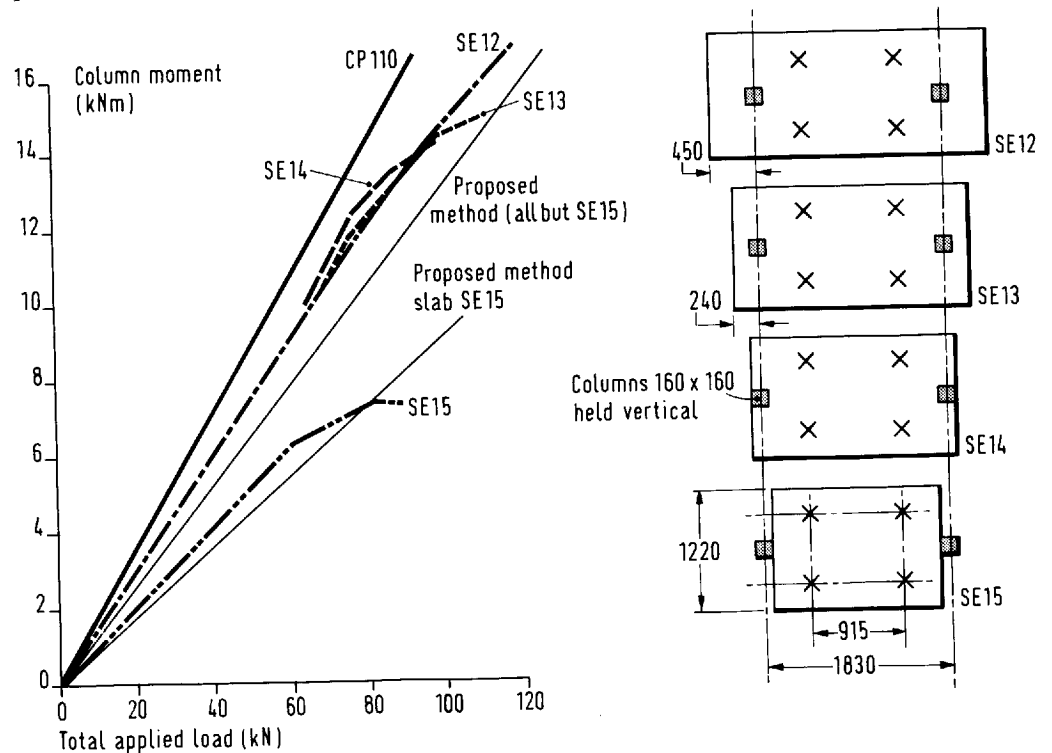


Figure 24
Actual and predicted
column moments for
test series SE 12
to 15

Although, as these examples demonstrate, there clearly can be redistribution of moment as loading proceeds, the deviation from linearity is small enough to be neglected in practice.

In general terms, the proposed treatment of Section 4.1.3 seeks to establish compatibility between the deformations of three 'elements': the span regions of the slab, the columns, and the joint/negative moment zones of the slab. An elastic approach based on overall dimensions alone should only be expected to work at high loads if the deteriorations of stiffness in all three elements are approximately proportional.

This is not wholly true in most flat slabs. Cracking generally starts in the joints, which thus lose stiffness before the other elements. This transfers moments to the span sections which then crack and lose stiffness at a faster rate than the joints, because of their generally lower ratios of reinforcement. The columns frequently do not crack at all, and there is thus a general tendency for negative and column moments to increase more rapidly after cracking than in the initial stages. In some cases, there is a reverse tendency just near to failure when the joints lose stiffness because of shear cracking.

Often, in the cracked state, the major compatibility condition is that relating the span and joint deformations as the rotations of the uncracked columns are small. An example is shown in Figure 25, which relates to a lightly reinforced specimen typical of much normal construction. Where the column deformations are negligible, it should be possible to make analyses on the basis of the cracked section stiffnesses of slab spans and joints. Such an approach is worth pursuing, but the results are unlikely to be of immediate interest to designers who wish to make their analyses before determining reinforcement. For the present, an allowance can be made for the influence of reinforcement—by accepting, say, 20% redistribution of calculated moments.

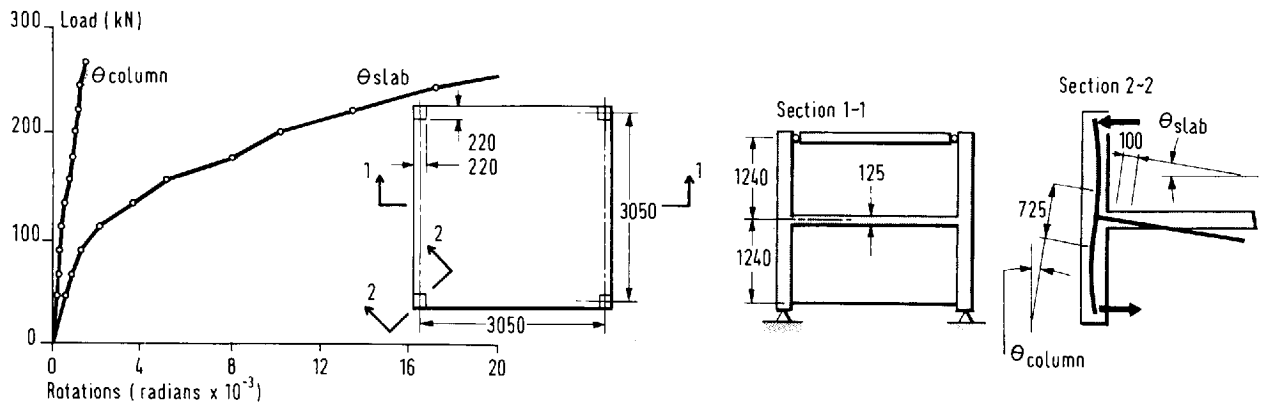


Figure 25 Slab and column rotations for test SC 6

Apart from questions of relevant stiffnesses, there are other variations between actual behaviour and that envisaged in elastic plate analysis. One relates to the pattern of deformation in the neighbourhood of columns. Elastic analysis is phrased in terms of distributed deformation, and the ACI method is very clearly of this type. In practice, there are gross deformations in cracks close to columns such as the 'local yield lines' at edge columns shown in Figure 60 (page 62), while the remainder of the slab edge undergoes practically no torsional deformation. This lack of torsional deformation can be seen clearly from the equality of rotations along slab edges shown in the example of Figure 26.

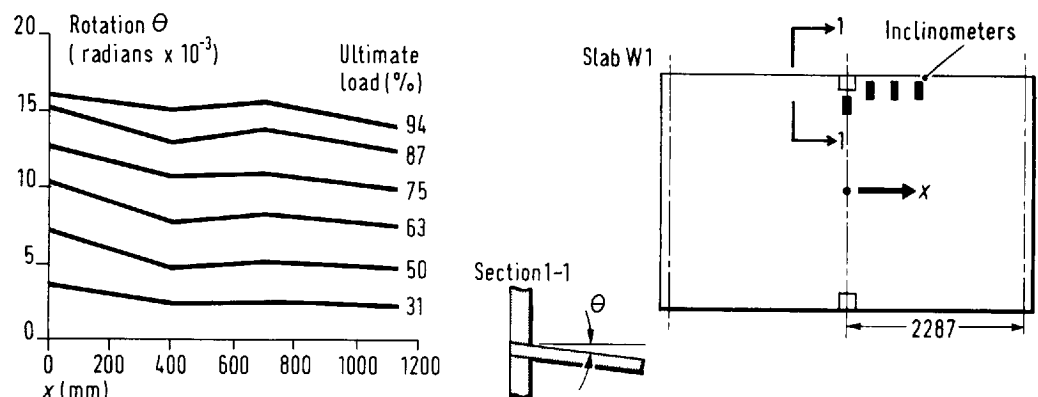
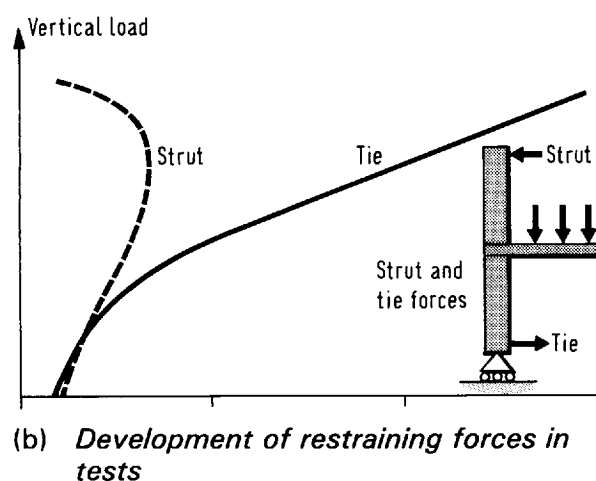
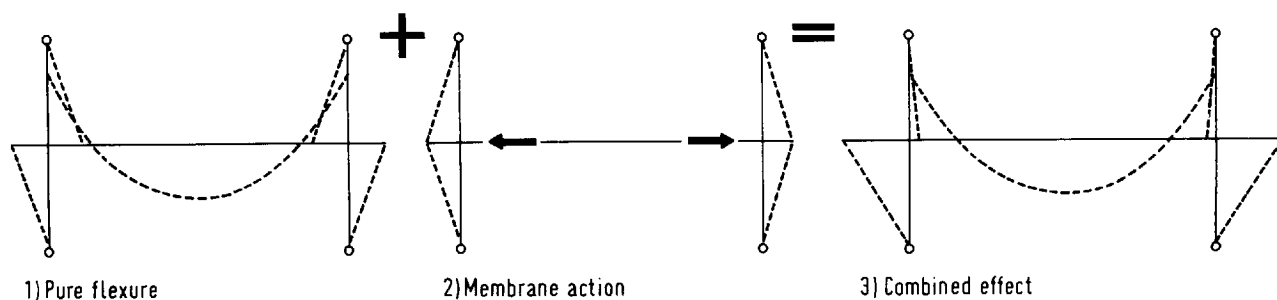


Figure 26
Rotation along edge of
slab at perimeter
column

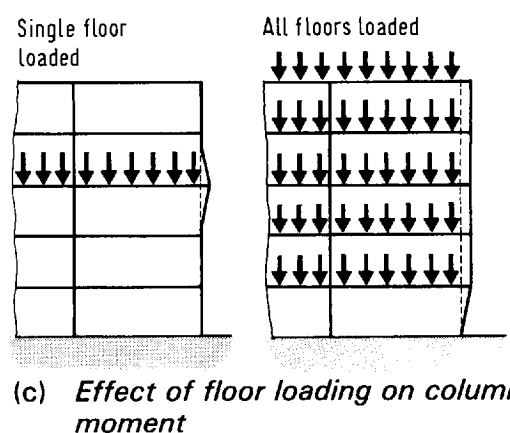
This is an aspect where the proposed approach could be helpful in the future. If joint deformations are eventually able to be expressed in terms of reinforcement, it is easy to incorporate such information in expressions for K_j .

A final point here concerns the correctness of purely flexural analyses. Throughout the CIRIA tests, where there were columns above and below slabs, it was observed that, after cracking, the strut forces associated with moments in the upper columns stabilised and then decreased. The forces in the ties between the lower columns increased more rapidly than in the earlier stages. These are the outward signs of the development of a compressive membrane action in the slab as a result of its expansion on cracking and the restraint afforded by the columns. An example of such behaviour is shown in Figure 27.

(a) *Bending moment diagrams (test specimens)*



(b) *Development of restraining forces in tests*



(c) *Effect of floor loading on column moment*

Figure 27 *Compressive membrane effects*

In a multi-storey structure, a similar effect occurs if a single floor is loaded, but if all the floors are loaded simultaneously, the columns are simply displaced outwards and only the lowest slab develops an appreciable compression. In general, the influence of membrane action can well be ignored in the design of the slabs, as the forces induced are small in relation to those in the reinforcement. For the design of the columns, the effect may be more of a problem. In the simple examples of the tests, the virtual removal of the moments in the upper columns was accompanied by an almost 100% increase of those in the lower columns. In practice, the situation illustrated at the bottom right of Figure 27 could have a still greater effect.

The phenomenon is not unique to flat slab construction, but it is worthy of consideration, and brittle column sections should be avoided. As a precautionary measure, it could be worthwhile to design the upper parts of the columns for twice the moments obtained from flexural analyses.

4.2 DISTRIBUTION OF MOMENT ACROSS FRAME

The distribution of moments over the widths of frames proposed here are essentially those of elastic plate theory.

Considering first the case of a large array of similar bays all subjected to a uniformly distributed load, let the frames in each direction be sub-divided into bands as follows:

- Band I extends on each side of the column line for a distance equal to the lesser of half the distance to edge of the frame and a quarter of the span
- Band II extends on either side of Band I for a distance equal to the width of Band I on the side in question
- Band III extends from the outside of Band II to the edge of the frame and exists only in the short span directions of rectangular bays.

This banding is illustrated in Figure 28. In the simple case for $l_x > l_y$ and where the frame is symmetrical about a column, the total band widths in each direction are:

- Band I $l_y/2$ } i.e. $1/4$ of shorter span banded on each side of column
- Band II $l_y/2$ }
- Band III $(l_x - l_y)$ residue of width
- Band III only applies to steel in the y direction.

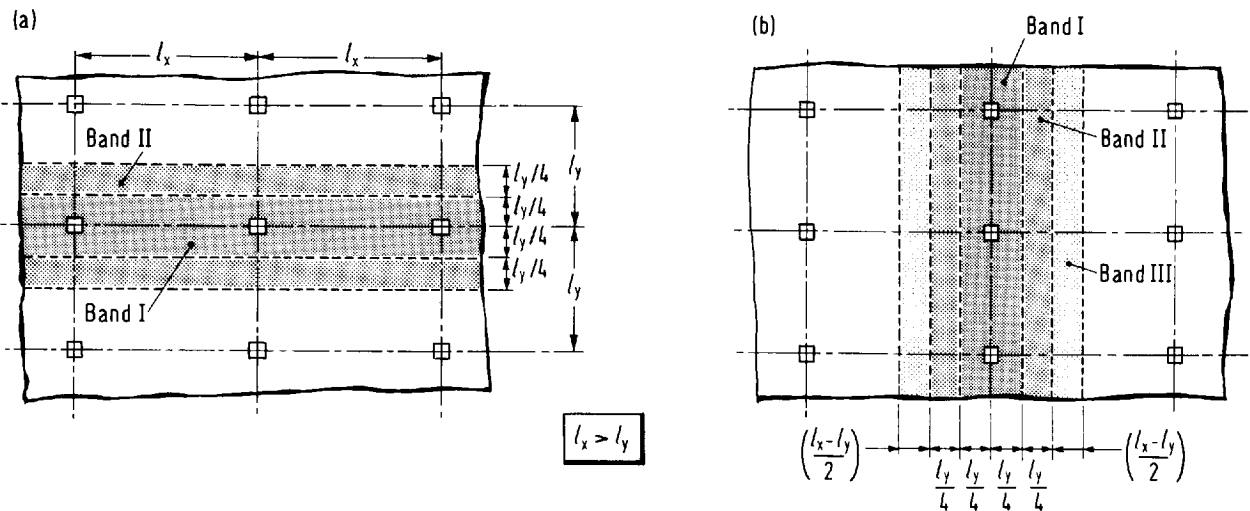


Figure 28 Bands for detailing of reinforcement

Theoretical distributions of moments between these bands are given in Tables 2 and 3. These distributions are calculated for a slab on point supports, but are not greatly changed for normally practical column sizes. The detailed variation of negative moments within Band I is more sensitive to column details. If a circular column and an isotropic plate are considered, the tangential moments at the column are zero, provided there is complete fixity between the slab and column. At this stage, the distribution of radial moments (m_r) is extremely peaked at the column as in Figure 29(b). Once cracking occurs, the tangential moments (m_t) develop, tangential yield occurs (Figure 29(c)) and then spreads outward (Figure 29(d)), while the radial moments diminish, except at the column face.

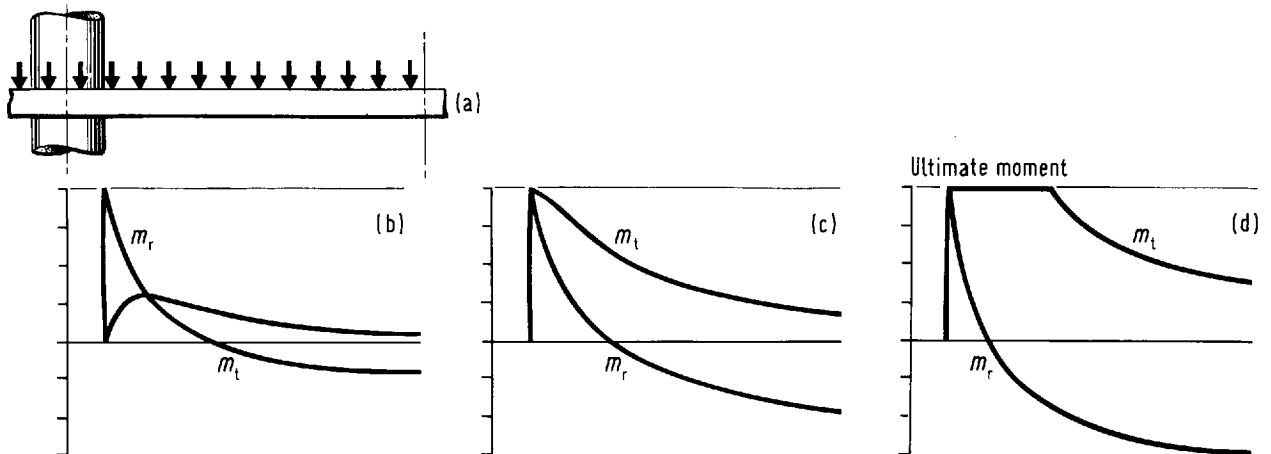
Table 2 Distributions of positive moment at midspan

Aspect ratio	Long span moments		Short span moments		
	Band I	Band II	Band I	Band II	Band III
1.00	0.61	0.39	0.61	0.39	—
1.25	0.56	0.44	0.59	0.31	0.10
1.50	0.53	0.47	0.58	0.30	0.12
1.75	0.51	0.49	0.58	0.29	0.13
2.00	0.51	0.49	0.58	0.29	0.13

Table 3 Distributions of negative moment at column lines

Aspect ratio	Long span moments		Short span moments		
	Band I	Band II	Band I	Band II	Band III
1.00	0.77	0.23	0.77	0.23	—
1.25	0.72	0.28	0.76	0.19	0.05
1.50	0.69	0.31	0.75	0.19	0.06
1.75	0.66	0.34	0.75	0.18	0.07
2.00	0.64	0.36	0.75	0.18	0.07

The moment distributions of Figure 29 are drawn for a uniform elastoplastic slab. In practice, to restrict the need for moment redistributions, and to avoid problems with serviceability, it is wise to concentrate the steel towards the columns. The situation of Figure 29(c) serves as a reasonable model. A satisfactory design approach is to concentrate the Band I steel in the ratio 2:1 towards the central half of the band as in CP110.

**Figure 29 Distribution of radial and tangential moments in an elastic-plastic flat plate**

The moment distributions resulting from moments transferred from an internal column to a slab are fairly similar to the above distribution of negative moments, and need not be considered separately if the possibility of a local flexural failure is treated as in Section 4.3.2.

The final basic case for interior panels is that where alternate spans are loaded and moments are redistributed from the column lines to the centres of the panels. The pattern (though not the magnitude) of the negative moments remains as above, while the additional midspan moments are uniformly distributed. It is thus appropriate that the coefficients of Table 2 should be applied to the span moment corresponding to end fixity ($Ql/24$ for uniform loading), while the excess moment (design moment – $Ql/24$) should be uniformly distributed across the width (see Figure 30).

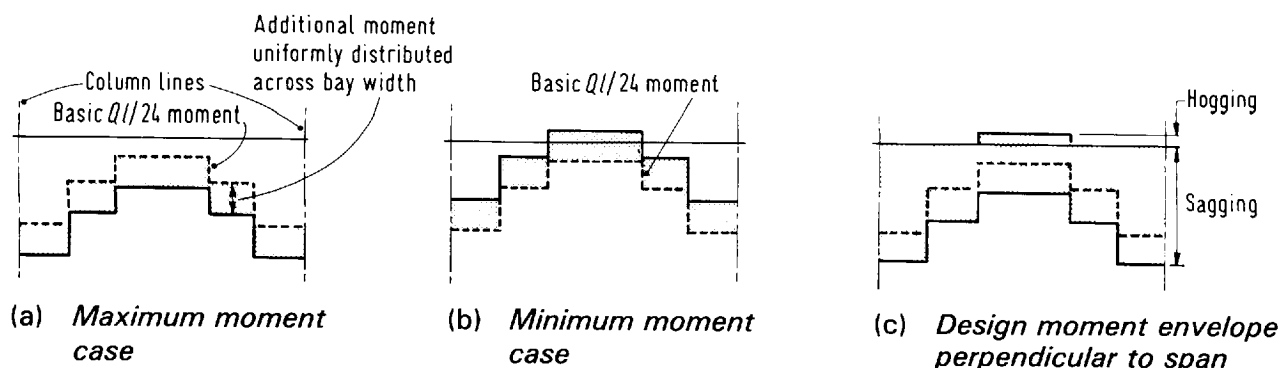


Figure 30 *Combination of basic and additional mid span moments*

Where pattern loading produces negative span moments, their distributions can be obtained from the same expression, if the signs are correctly treated.

In exterior panels with support on edge columns, the negative moments at, and perpendicular to, edges are governed by very local conditions at columns which are treated in Section 4.3.3 and 4.4, while the midspan moments are similar to those in the interior. Where support is by walls or beams, the elastic mid-span moments are rather more uniformly distributed, but the proportions of Table 2 (page 36) should still be satisfactory.

The proposals made here differ from the recommendations of CP110⁽⁵⁾ in a number of respects. Two are particularly significant. The first of these is the treatment of rectangular panels, for which CP110 retains the same distribution between column and middle strips irrespective of the panel aspect ratio. In effect, the proposal limits the active width of slab in the short span direction to b_c . This is fully in accordance with plate theory, and in practice produces satisfactory behaviour. An example is presented in Figure 31(a), which shows the CP110 arrangement of span reinforcement for a 1.5:1 rectangular panel, and also the arrangement used in a test which approximated to the proposed distribution. Figure 31(c) plots measured steel strains across the centre line, and it can be seen that even with the greater concentration of steel towards the column lines, the lowest strains were still recorded near the panel centre. The peak strains were probably more or less uniform over the width, and the variation seen is probably a result of the significant tension stiffening by the concrete in the very lightly reinforced central zone.

In many cases, the calculated steel requirements for Band III zones are less than code requirements for minimum reinforcement. In such cases, the code minimum should be provided.

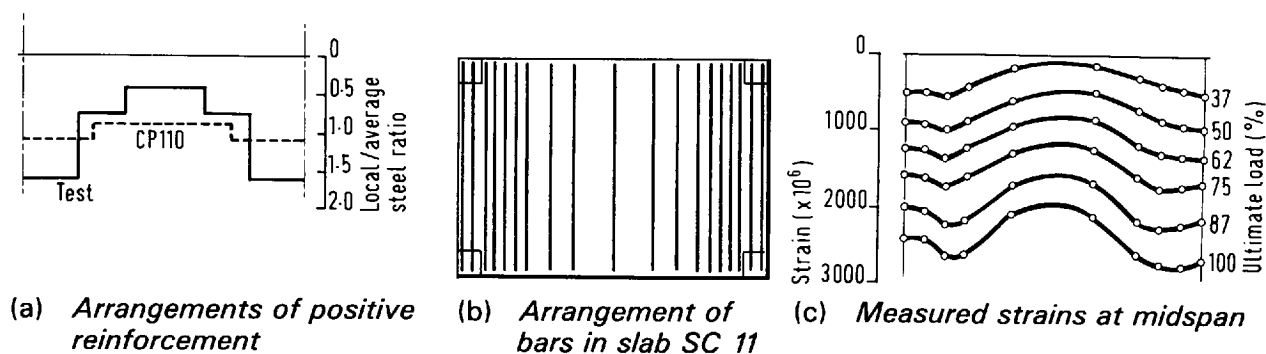


Figure 31 *Reinforcement arrangements and steel strains—rectangular slab SC 11*

The other major difference from CP110 is in the arrangement of top steel at slab edges, where the proposal elaborated below calls for an extreme concentration of steel towards the columns, while the Code spreads its reinforcement to a far greater extent. Figure 32 shows examples of measured strains, from which it can be seen that the effective reinforcement is only that local to the column.

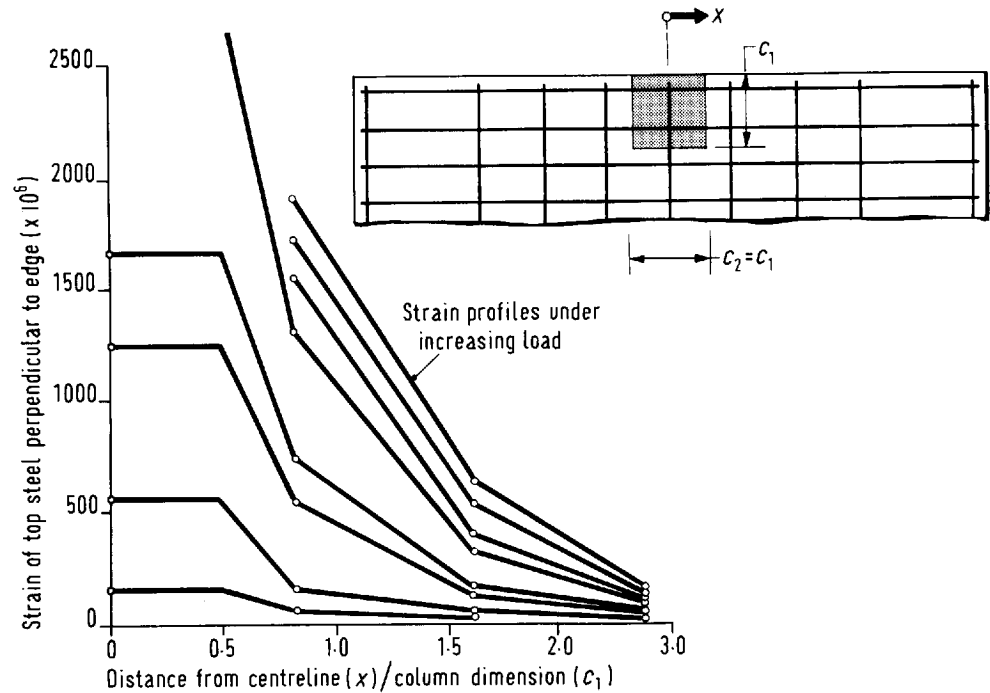


Figure 32
Reinforcement strains near an edge column for slab SE 9

The severe limitations of zones of cracking (and thus of effective reinforcement at slab edges) can also be appreciated from Figure 33, which shows the final pattern of cracking in one of Tankut's⁽³⁶⁾ tests.

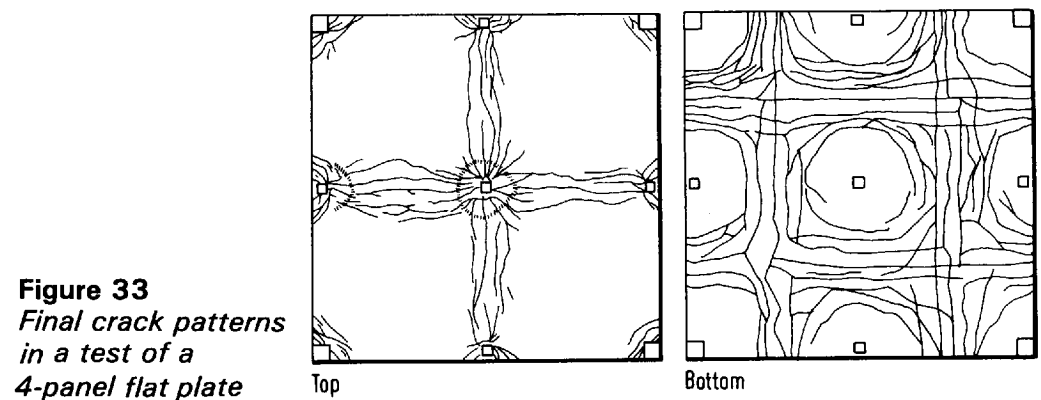


Figure 33
Final crack patterns in a test of a 4-panel flat plate

4.3 LOCAL FLEXURE AT SLAB/COLUMN CONNECTIONS

The use of a frame analysis implies the expectation of a flexural collapse mechanism with full width yield lines causing yielding of all the design reinforcement at sections of maximum moments. Such a mode of failure can be pre-empted by punching. It can also fail to materialise if other yield lines are formed, permitting plastic deformations without fully mobilising the reinforcement.

Such alternative yield lines can occur where reinforcement is prematurely curtailed or in the vicinity of columns. Situations produced by curtailment can be investigated systematically by yield-line theory, but in practice it is normal to rely on detailing rules. Local yield lines around columns require more specific consideration.

4.3.1 Concentrically-loaded internal connections

The local mechanism here is the ring and fan pattern of yield lines shown in Figure 34. Formulae for the general case of an elliptical ring and orthogonal reinforcement are given in Reference 37, but only the circular pattern for square bays and isotropic reinforcement is considered here. For this case:

$$m + m' = \frac{ql^2}{2\pi(1 + 4\frac{c}{l})} \quad (11)$$

where l is the radius of the ring yield line such that $r/l = 0.65 \sqrt[3]{c/l}$

c/l can be conservatively taken as zero in Equation (11), and r/l can be taken as 0.25, corresponding to the width of Band I. If the recommendations of Section 4.2 are followed, $m' \approx 0.125ql^2$, and the required value of m is only $0.034ql^2$ which is less than $ql^2/24$. If m' is reduced by redistribution, m is automatically increased, and this sort of mechanism should not be a problem if the negative steel is appropriately banded. With the proposed banding, though not necessarily with that of CP110, this conclusion remains valid for rectangular panels.

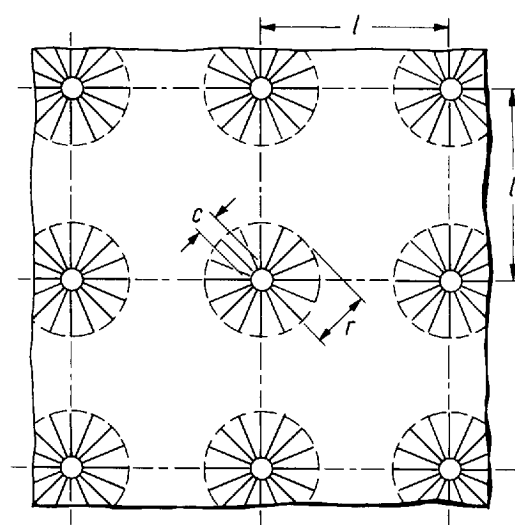


Figure 34
Local ring and fan mechanisms

4.3.2 Eccentrically-loaded internal connections

Figure 35 shows local mechanisms for this case with the eccentricity of loading decreasing from Case (a) to Case (d).

The mechanism of Case (d) is virtually the same as that for a concentrically-loaded connection, and should require no special consideration if the detailing rules are followed.

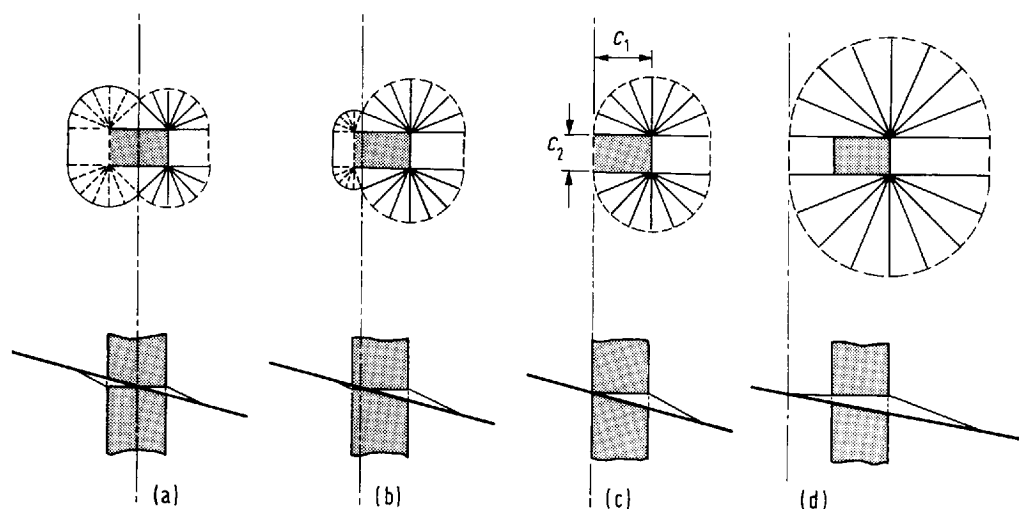


Figure 35
Local yield line patterns and slab deformations at internal columns with eccentric loading

The limiting case for which the transferred moment to the column (\bar{M}) requires specific consideration is thus that in Figure 35(c). With reinforcement equal in two directions:

$$\bar{M} = (m + m') (4.7c_1 + c_2) \quad (12)$$

$$e = \frac{\bar{M}}{V} = \frac{4.7c_1 + c_2}{\pi + 2c_2/c_1} \quad (13)$$

For the remaining cases corresponding to greater eccentricities, the value of $(m + m')$ required for a given moment \bar{M} is smaller than in this instance.

Equation (12) can thus be used as a general safe method of determining the reinforcement required to prevent the premature formation of a local mechanism. However, it does not distinguish between top and bottom steel. While such a distinction may not be necessary in terms of plastic theory, it is undesirable to have either no steel or grossly inadequate reinforcement for elastic moments.

It is possible for the gross moment across a frame to be negative and yet for there to be positive moments in the immediate vicinity of a column. To prevent a sudden loss of stiffness and probable redistribution of shear when such moments cause cracking, it is proposed that bottom reinforcement should be provided at any connection where the eccentricity exceeds the value given by Equation (13).

The amount of steel required can be obtained from the case of Figure 35(a), assuming $M = M'$. The required bottom steel reinforcement may be obtained from

$$m = \frac{\bar{M}}{12c_1} \quad (14)$$

4.3.3 Edge connections

Various local mechanisms corresponding to the ring and fan pattern around an internal column are possible. With adequate detailing, only the simple case of Figure 36(a) need be considered which shows the negative moment in isolation. Here the positive yield line is the same as in a full width mechanism, and the only restriction imposed by local behaviour is the possible limitation of the negative moment.

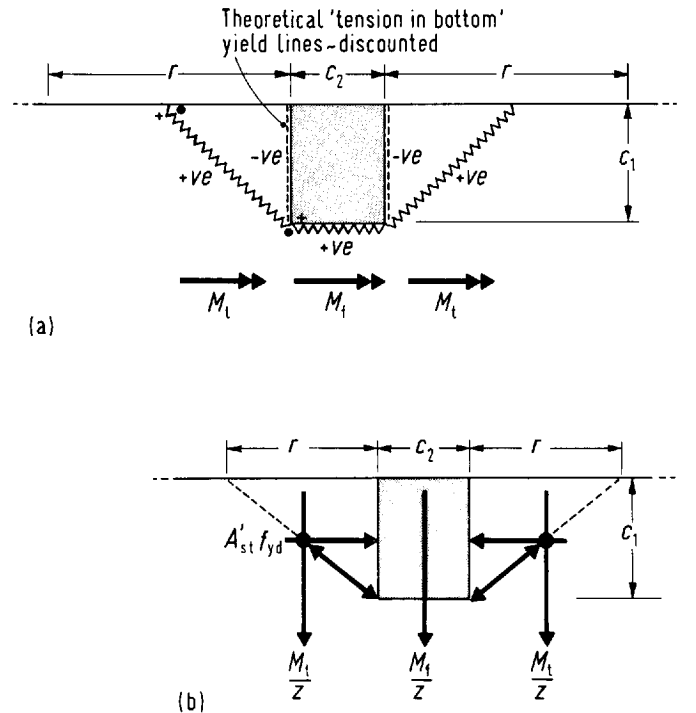


Figure 36
Local conditions at
edge column—slab
connection

The total moment at the line of the inner face of the column is made up of a component, M_t , resisted by steel passing through the column face, and two components, each M_t , resisted by steel distributed over widths r on either side of the column. The components M_t are eventually transmitted to the column as torsions on its side faces.

Solutions by Andersson⁽³⁸⁾ and Kinnunen⁽³⁹⁾ correspond to the yield lines shown in Figure 36(a) which reach the slab edges at distances $r/2$ from the column sides. The moment of resistance to be provided by the top steel parallel to the edge and passing through the column (A'_{st}) is $M_t r / 4c_1$.

This form of solution requires that half the total torque at each column side be provided by the couple formed between the vertical nodal forces indicated in Figure 36(a). In view of the condition of the slab edge following torsional cracking and uncertainty regarding the efficiency of 'vertical' reinforcement at the edge, it seems prudent to adopt a rather more conservative approach in design. This can be done by discounting the torsion resulting from vertical forces, and by designing the regions at the column sides as sections of slabs resisting torsion by horizontal forces alone as in Figure 36(b). In this case, the requirement for steel parallel to the edge and passing through the column is

$$A'_{st} f_{yd} = \frac{M_t}{z} \left(\frac{r}{c_1} \right) \quad (15)$$

This, possibly cautious, approach appears consistent with the treatment of shear in Section 5.2.3, in that the calculated resistance at the inner face is directly compared to the column reaction without regard to any extra effects resulting from the nodal forces, which are taken into account in Andersson's method⁽³⁸⁾. In this case, r is taken to be the yield-line projection c_1 . A greater value may be chosen, dependent on the provision of torsional reinforcement (see Section 4.4).

The steel required according to Equation (15) is not needed in addition to the normal frame reinforcement for bending parallel to the edge, because it automatically contributes to resistance at full width yield lines perpendicular to the edge. The requirement is only that sufficient frame reinforcement be placed within the width of the column.

It is debatable whether bottom steel 'for torsion' should be provided. In the case of a pure moment loading ($M/V = \infty$), the local mechanism is as in Figure 37, and such reinforcement should be effective. However, in more practical cases, it probably does not contribute to overall resistance, since the need for it is in effect removed by the compression because of bending parallel to the edge. It should be sufficient to require that at least two bottom bars be provided and to let their sizes be determined by the requirements of Section 5.3 for the reduction of the risk of progressive collapse.

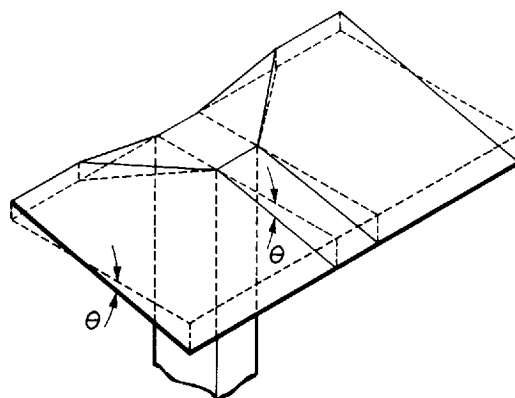


Figure 37
Failure mechanism at edge column—slab connection subject to bending

4.3.4 Corner connections

Possible yield lines near corner columns are shown in Figure 38. The local mechanism of Figure 38(a), which corresponds to the ring and fan at an internal column, is not critical unless the negative reinforcement near the column is less than the positive

reinforcement in the span. In practice, the complete absence of top steel across the line AB (Figure 38(a)) in a test with the top steel arranged diagonally had no adverse influence.

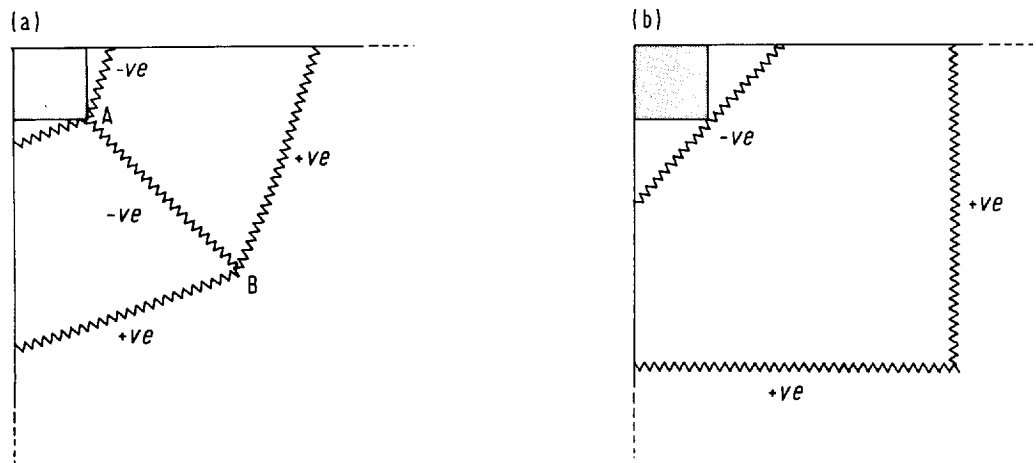


Figure 38
Local yield lines at corner columns

Concern should thus be centred on the local diagonal yield line of Figure 38(b), which can limit the moment transferred to the column. Consistent with the treatment of edge connections proposed above and the approach to shear used in Section 5.2.4, the moment across the inner corner of the column is limited to that provided by the steel crossing the diagonal yield line. Eventual transfer of moments by couples formed by vertical 'nodal' forces is again ignored, together with the additional shears such forces would create.

4.4 DETAILING

The arrangement of reinforcement across the width of an interior bay and across the midspan section of an exterior panel follows from Section 4.2. It only remains to define permissible sections for curtailment.

Under uniform vertical loading, the distance from a column line to a line of contraflexure for either set of orthogonal moments varies only from about $l/6$ to $l/4$ across the width, the greater distance applying to the centre of the width between columns, where the negative moments are in any case small. This situation is thus adequately covered by the normal practice of curtailing half the top steel at $0.2l$ from the column faces and the remainder at $0.3l$ from them.

In cases of alternate panel loading, the fixity provided by normal columns is considerable, and the risk of cracking in the top of an unloaded bay at a section more than $l/4$ from the columns can be discounted unless the live load is very high.

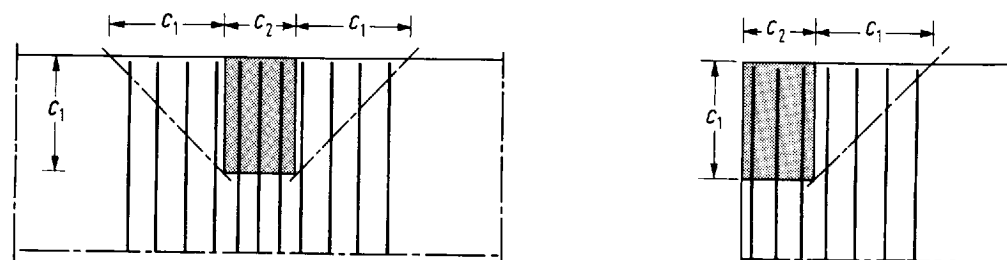
The only additional requirement for interior top steel is that bars intended to be active across the surface of an eventual shear failure need to be fully anchored beyond it. Thus, all steel within a width equal to $2.5d$ on either side of a column should be fully anchored beyond $2.5d$ from the column faces.

Conditions for interior positive reinforcement are also similar to those in other structures, and its detailing should generally be satisfactory if all the bars are extended to within $0.2l$ of the supports, and at least 50% of the steel is continued to the column lines and lapped with bars from the next span for lengths equal to 12 bar diameters.

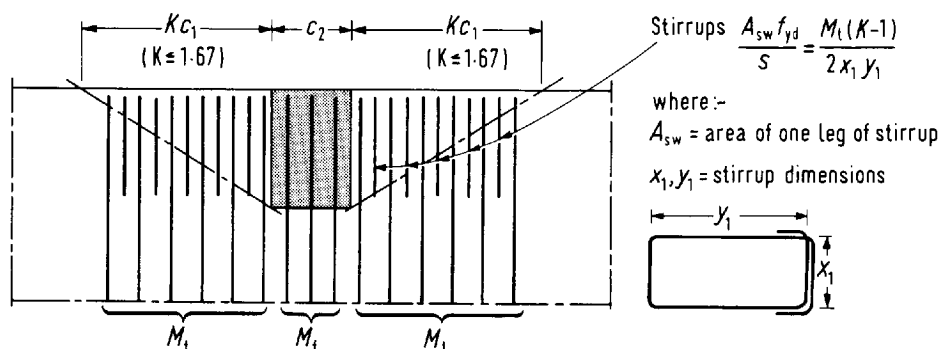
In external panels, since there are no negative moments along much of the slab edge, the positive steel should probably be extended further than in the interior, and it is simplest to continue all the bars to the slab edge.

The arrangement of the main negative reinforcement transferring moments to external columns requires more consideration. In the light of Section 4.3, the most obvious detail is to concentrate all moment reinforcement within a width $c_2 + 2c_1$ at

an edge column, or $c_2 + c_1$ at a corner column as shown in Figure 39. This is equivalent to designing for torsion based on a 45° truss analogy. If this causes too great a concentration of steel, the width at an edge column could be increased to, say, $c_2 + 3.33c_1$, corresponding to a truss with concrete diagonals at arc cot 5/3 (the greatest inclination permitted by the CEB/FIP Code⁽⁷⁾). Since the use of the variable angle truss reduces torsional stiffness, it is prudent to provide some closed stirrups in the increased breadth as indicated in Figure 39. The area of stirrups proposed is arbitrary, but corresponds to the torque in the added width ($0.67c_1$ at each end).



(a) Reinforcement detailed within 45° projection of column



(b) Reinforcement detailed over greater width using additional stirrups

Figure 39
Arrangements of top reinforcement at edge and corner columns

Tests of details such as those proposed here demonstrated that they are perfectly satisfactory in practice.

Although tests show no problems in slabs without further top steel at the edge, it is probably prudent to provide nominal reinforcement steel along the remainder of the edge outside the zones of concentration.

As far as possible, the slab edge should be protected from damage resulting from torsional cracking. The top bars also require to be properly anchored. Thus, the most natural detail is to bend the bars through 180° at the edge and to give them nominal laps with bottom steel. Within the width of a column, the slab bars can be bent down into the column, but tests show that this is unnecessary, and the previous details can be used successfully. Short U bars placed at edges and lapped into the top and bottom steel should also be adequate.

At roof level, some further caution is needed to prevent reductions of moment resistance because of the mechanisms shown in Figure 40. It is often most convenient

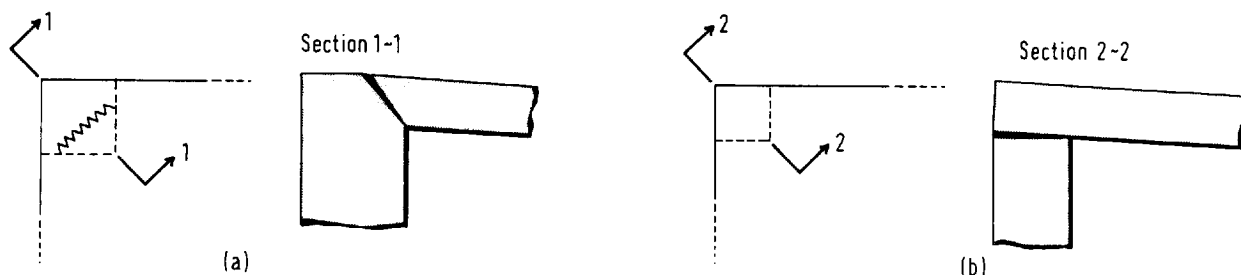


Figure 40 Local yield lines at roof level, which may reduce flexural capacity

to bend column bars over into the slab so that the area of steel crossing the failure line of Figure 40(b) is the same as that on the diagonal through the inner corner. Perfectly satisfactory results can nonetheless be obtained with arrangements of overlapping U-bars in the slab and column. In this case, the area of reinforcement within the column is greater than that on the yield line through the corner.

A last point in relation to detailing is the reduction of design negative moments to make allowance for the finite dimensions of supports. It is dubious whether this is a desirable idea, but if such measures are taken they should be consistent with the assumptions made in design for shear. Possible reductions are indicated by Figure 41.

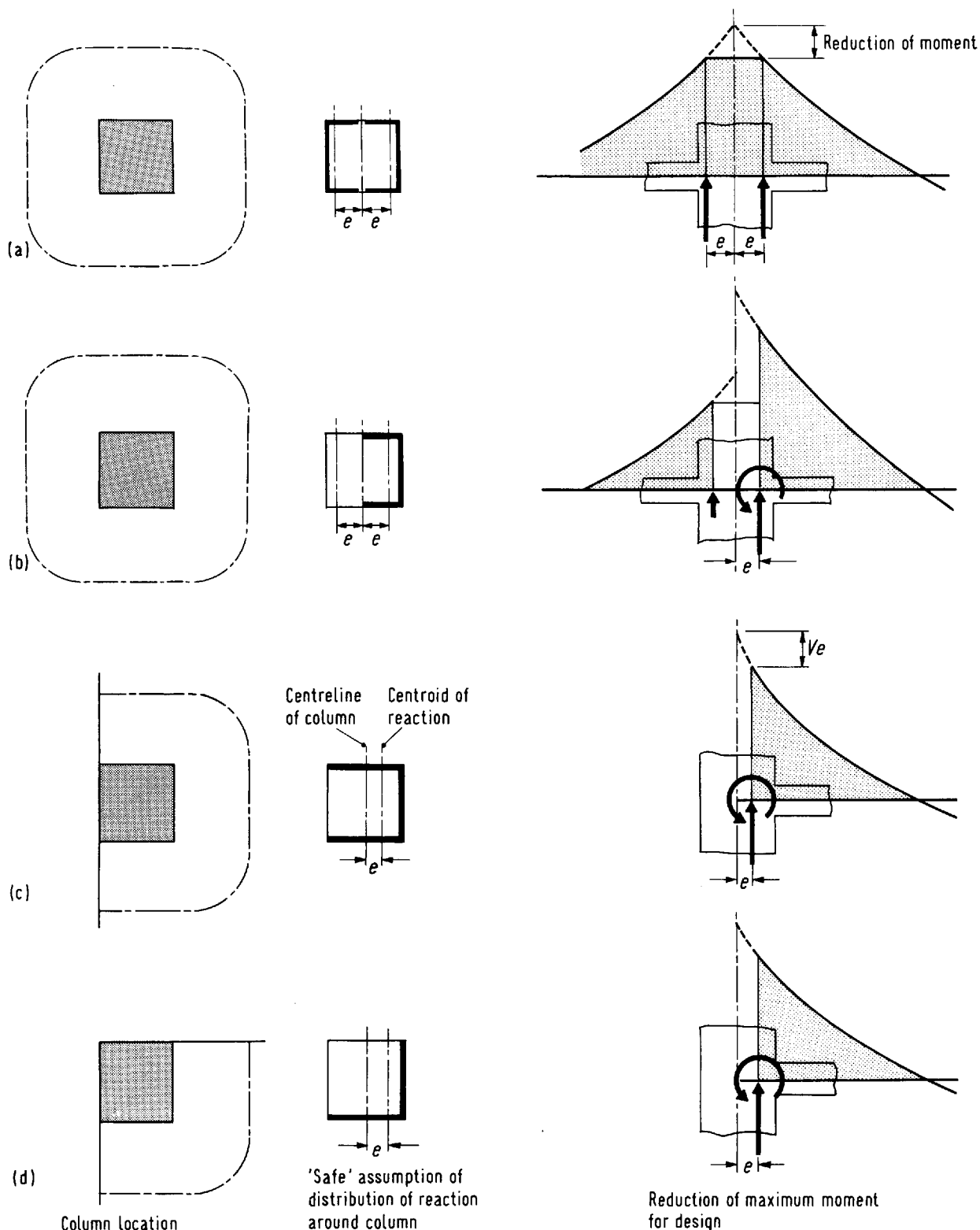


Figure 41 Reduction of maximum moments for design to take account of finite column sizes

4.5 SERVICEABILITY

4.5.1 Limits for deflections

The first question to be answered here is what deflections the designer should consider and to what spans they should be related?

CP110⁽⁶⁾ requires that the final deflection below the level of supports should not exceed the span divided by 250. It seems appropriate to apply this to any line along which the curvature of the soffit is visible. For flat slabs, the critical deflection is then that at the middle of a panel and the span to which it should be related is the diagonal distance between columns. Referring to Figure 77 (page 82):

$$\delta_m \approx \delta_x + \delta_y \leq \frac{1}{250} \sqrt{l_x^2 + l_y^2} \quad (16)$$

CP110 also states that the deflection affecting partitions and finishes (i.e. that occurring after their erection or application) should not be greater than the lesser of 20 mm and the span divided by 350. Where this limit is applied to safeguard a ceiling finish, the position of the deflection and the related span could well be as above. The same may be true for a floor finish, although the cracking of the slab on column lines is likely to be more decisive. If the limit is applied for the sake of partitions and their finishes, the relevant behaviour is that along partition lines, which are commonly parallel to the structural grid. In such a case, the design condition is:

$$\delta_x \leq \frac{1}{350} l_x$$

where δ_x is the deflection midway along a column line relative to the columns or that at the middle of the panel relative to the deflection midway between columns

and l_x is the span in the direction of the column line in question

In the interior of a floor, conditions are critical when l_x is the longer span of a rectangular panel. For an exterior panel, the critical direction is normally perpendicular to the edge, but may be parallel to it if the parallel span is significantly greater.

4.5.2 Calculation of short-term deflections

Some of the approaches mentioned in Section 3.4 seek to calculate deflections for column strips in one direction and middle strips in the other. Though this may appear reasonable, the division of the width of a span into strips with different moments and different stiffnesses is not very logical. The most critical factor in determining stiffness is the presence or absence of cracks, or at high loads the ratios of the acting moments to those causing cracking. Once cracking occurs in any part of the width, the stiffness of that part is reduced, moments are redistributed to the uncracked part, and almost immediately also produce cracking there. This being the case, it seems preferable to treat the width as a whole (i.e. to consider the action in each direction to be simply that of a wide beam as in the preceding frame analysis).

From the frame analysis, the average positive and negative moments across the effective breadth, b_e , are known

$$m = \frac{M}{b_e}$$

$$m' = \frac{M'}{b_e} \quad \text{or} \quad \frac{M'_1 + M'_2}{2b_e} \quad \text{if the support moments are unequal.}$$

For a uniformly loaded span of constant rigidity, the central deflection, δ

$$= \frac{5ql^4}{384D} \cdot \frac{b}{b_e} - \frac{m'l^2}{8D} \frac{b}{b_e} = \frac{l^2}{D} \cdot \frac{b}{b_e} \left[0.104m - 0.021m' \right] \quad (17)$$

Once cracking has occurred, the rigidity is not, in reality, constant along the span, although expressions are available giving values of effective rigidities which can be applied for a span as a whole. They relate stiffness to the maximum moment in a span or curvature region. In the latter case, separate stiffness values are computed for regions of positive and negative loading and then combined to give a single value for the whole span. Generally, deflection behaviour is principally a function of the positive moment region, and it should be sufficient to use the positive curvature stiffness throughout.

An expression for effective rigidity developed by Branson is used in the ACI Code⁽⁶⁾.

$$D_{\text{eff}} = \left(\frac{m_{\text{cr}}}{m} \right)^3 D_g + \left[1 - \left(\frac{m_{\text{cr}}}{m} \right)^3 \right] D_{\text{cr}} \quad (18)$$

where D_{eff} is the effective rigidity of the partially cracked slab

D_g is the rigidity of the uncracked gross concrete section = $E_c h^3 / 12$ (Poisson's ratio can be taken as zero)

D_{cr} is the rigidity of a fully cracked member calculated by elastic theory, with tension stiffening by the concrete ignored

m is the midspan moment per unit width

and m_{cr} is the moment per unit width to cause cracking.

The calculations of D_g and D_{cr} pose no special problems provided that the modulus of elasticity of concrete, E_c , can be estimated. In the absence of more detailed information, this can be done from Table 1 in CP110.

The moment, m , is known from the frame analysis (generally for the case of alternate spans being loaded), but the estimation of m_{cr} raises some problems. The main source of difficulty is that, in the uncracked state, the moments are not uniform across the width of the slab, and cracking is initiated by the maximum (not the average) moment. A secondary problem is that cracking normally begins in the negative moment region, and its consequent loss of relative stiffness causes a temporary redistribution of moments towards the midspan region. As a result, the average positive moment at the cracking stage is likely to be somewhat higher than the value of m from the frame analysis.

To allow for these effects, it is necessary to use a reduced value for the flexural tensile strength of the concrete when calculating m_{cr} . A reasonable estimate is

$$f_r = 0.45 \sqrt{f_{\text{cu}}} \quad \text{in N/mm}^2 \quad (19)$$

$$\text{whence} \quad m_{\text{cr}} = f_r h^2 / 6 = 0.075 \sqrt{f_{\text{cu}}} h^2 \text{ or } 0.075 h^2 \sqrt{f_{\text{cu}}}$$

Figures 42 to 44 present comparisons of experimental deflections with the result of calculations by Equations (17) to (19), with E_c taken from CP110 and experimental values used for the moments m and m' . The approach proposed can be seen to be adequate as a means of assessing serviceability loads corresponding to short-term deflections of the order of span/1000 to span/500.

Great accuracy in the prediction of deflections is not to be expected as too many parameters have to be assessed arbitrarily. In reality, E_c depends not only on the concrete strength but also on the type of aggregate and the aggregate/cement ratio. f_r is influenced by the reinforcement and by shrinkage stresses. The rigidity, D_{eff} , depends on the distribution of loads, etc.

Figure 42
Comparison of actual and predicted deflections for tests of slabs on corner columns

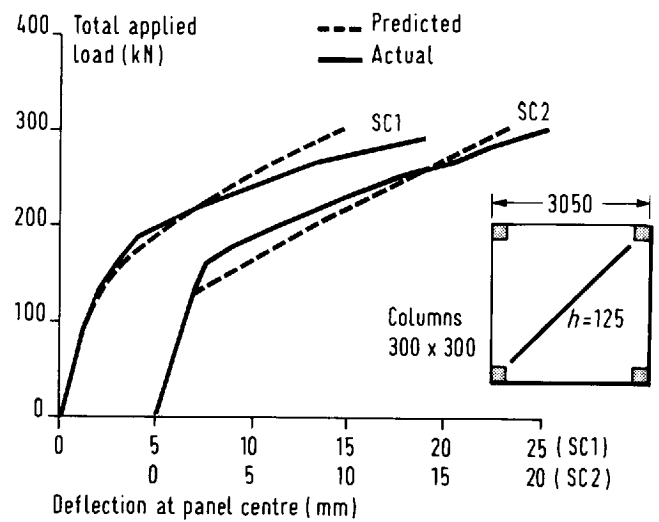


Figure 43
Comparison of actual and predicted deflections for tests by Ingvarsson⁽⁷³⁾

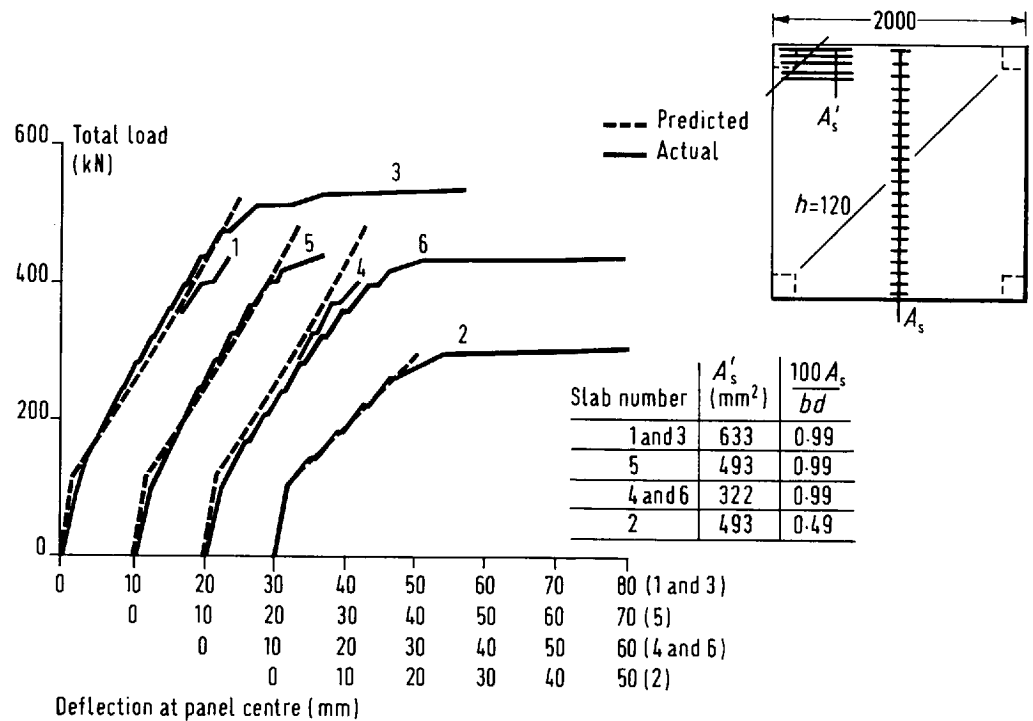
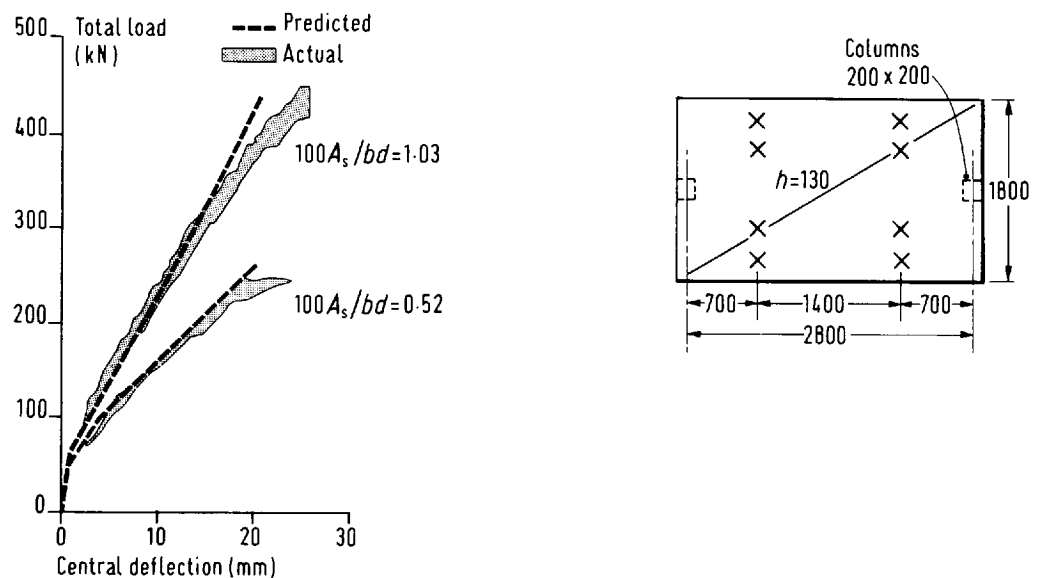


Figure 44
Comparison of actual and predicted deflections for tests by Kinnunen⁽³⁹⁾



4.5.3 Long-term deflections

Long-term deflections are greater than short-term values because of the effects of shrinkage and creep, and total deflections may be further increased by temperature differences through the thickness of the slab. Temperature effects can be important in roofs with poor external insulation and in floors with floor or ceiling heating systems, but are not discussed further here.

Deflections resulting from shrinkage can be estimated using Appendix A of CP110⁽⁵⁾. They can be relatively large (of the order of span/1500) in slender members such as flat slabs, even when there is no marked moisture differential through the slab.

Creep deflections can be estimated using the same equations as for short-term loading, but with the elastic modulus E_c replaced by an effective modulus

$$E_{\text{eff}} = \left(\frac{1}{1 + \nu} \right) E_c$$

where ν is the creep coefficient and can be obtained from the CEB/FIP model code⁽⁷⁾.

Creep coefficients for indefinite durations of loading on slabs with thicknesses less than or equal to 200 mm are as given below.

Table 4 Creep coefficients

Age at commencement of loading (days)	Humid external conditions (RH 75%)	Dry internal conditions (RH 55%)
3 to 7	2.7	3.8
7 to 60	2.2	3.0
60	1.4	1.7

If the slab is uncracked, the long-term deflection is simply $(1 + \nu)$ times the short-term value, but once cracking has occurred, the increase is a smaller proportion of the initial value.

5. Punching Shear

5.1 PUNCHING IN ABSENCE OF UNBALANCED MOMENT

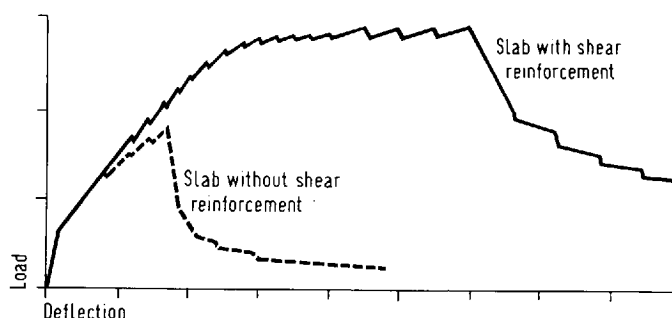
5.1.1 General

As noted in Section 3, there is as yet no fully satisfactory and comprehensive theory of punching. The proposals made here are therefore empirical, and are initially derived from data for the basic case of an internal column or load free from unbalanced moments. This is the case for which the largest body of data is available, and for which the number of variables involved is a minimum.

Punching failures are characterised by the deformations prior to failure being smaller than in flexural failures, by the violence of the failure, and by the sudden drop in resistance from the peak load which is quite untypical of flexural behaviour.

These characteristics are illustrated by Figure 45, which shows load/deflection relationships for a pair of slabs in which one had shear reinforcement and the other did not^(40, 41). Although both specimens failed at diagonal cracks, the difference between a true punching failure and a predominantly flexural response is very clear in terms of the sudden drop of resistance at peak load in the former.

Figure 45
Load-deflection relationships for slabs with and without shear reinforcement



In general, in the following paragraphs, test results are treated on the basis of the behaviour observed in the tests. This approach may run the risk that, if failures are attributed to punching when their real causes were flexural, the equations derived may be over-conservative when applied to otherwise similar slabs reinforced with stronger steels. For the present, this problem should not be serious as there are adequate data available from tests of slabs reinforced with steels having yield strengths of about 450 N/mm^2 .

Although empirical, the treatment of punching proposed here differs from that of current codes of practice in that the area of concrete by which the punching force is divided to give a nominal stress is approximately that of the true failure surface and not the product of the slab depth and a notional 'critical perimeter'.

The suggested change is motivated by two principal considerations. First, it gives the designer a better picture of what is involved and should help to avoid some of the mistakes which can be made when the critical perimeter approach is used blindly (e.g. as in Figure 46(e)).

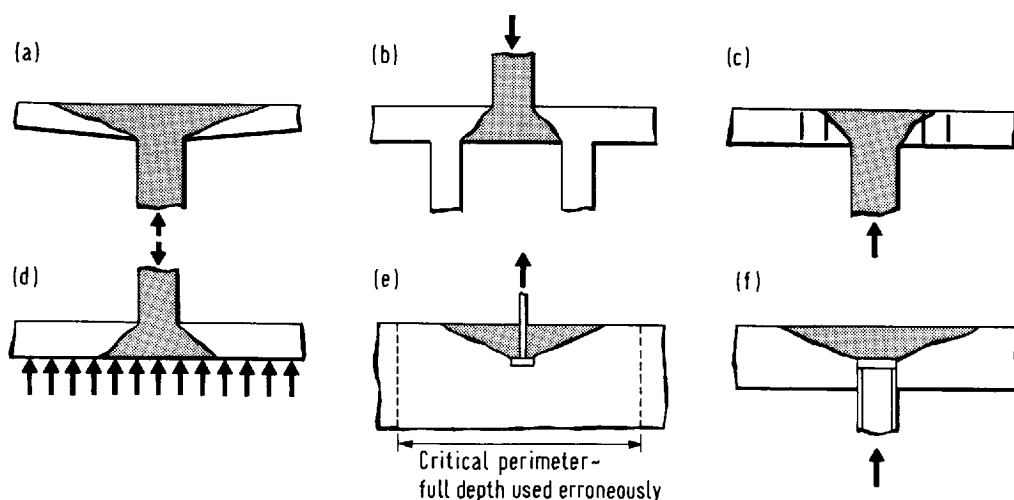


Figure 46
Use of fracture surface approach to deal with various punching situations

Second, in principle at least, the new approach makes possible the rational treatment of various cases which cannot be dealt with satisfactorily by present code methods. As shown in Figure 46, these include slabs of variable depth, cases in which the proximity of a load and support interferes with the shape of the fracture surface, slabs with shear reinforcement where failure may occur between a column and the innermost shear steel, foundation slabs where there is a counterpressure opposing the concentrated load, and pull- or push-out failures.

A general treatment requires the formulation of a relationship between the nominal ultimate stress and the inclination of the failure surface, so that conditions on various potential failure surfaces could be checked. More work is required on this subject, but it is established that the nominal stress increases quite rapidly for steeper crack inclinations. Since the fracture area decreases at the same time, the overall effect on punching resistance (stress \times area) is not great until the angle between the failure surface and the slab plane reaches about 45° .

For the present, normal flat slabs can be dealt with on the basis of a single inclination selected essentially to give correlation with the results of test series in which the main variable was the ratio of the column dimensions to the slab thickness (see Section 5.1.3).

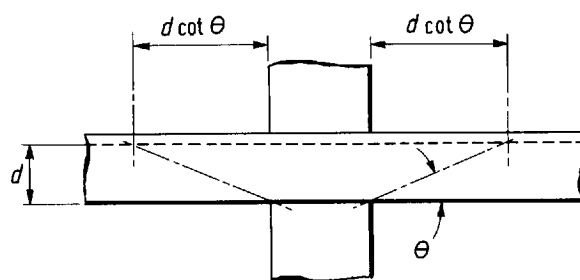
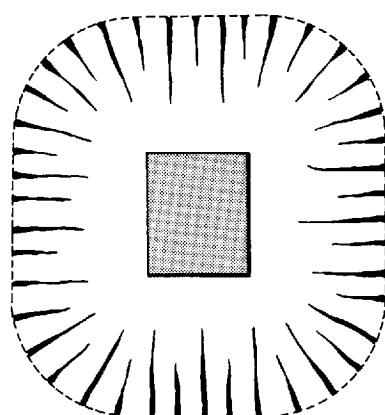
Denoting the angle between the failure surface and the plane of the slab in Figure 47 by θ , the area from which nominal stresses are calculated can be taken as either the inclined surface area:

$$A_c = d \sqrt{1 + \cot^2 \theta} (\Sigma c + \pi d \cot \theta) \quad (20)$$

or its projection on the slab plane. Although the latter is slightly simpler to work with, it has the disadvantage of tending towards zero as the surface goes towards the vertical. The inclined area of Equation (20) is adopted here, and the nominal vertical stress at punching failure is defined as:

$$\sigma_{vu} = \frac{V_u}{A_c} \quad (21)$$

where V_u is the ultimate shear force acting across A_c .



$$A_c = d \sqrt{1 + \cot^2 \theta} [\Sigma c + \pi d \cot \theta]$$

$$A_c = 2.69d [\Sigma c + 7.85d] \text{ for } \cot \theta = 2.5$$

Figure 47
*Fracture surface used
in calculation of
punching resistance*

Sections 5.1.2 to 5.1.6 discuss the effects of various parameters on the nominal stress, σ_{vu} , and present a limited amount of test data in support of the treatments proposed for the major influences. Section 5.1.7 is a more general review of the results available. Fuller treatments of some secondary parameters are given in Reference 1.

5.1.2 Concrete parameters

Surprisingly little data are available from which a relationship between punching resistance and concrete strength can be derived. The only tests with concrete strength as the sole variable seem to be Elstner and Hognestad's⁽⁴²⁾. The slabs in question were abnormally heavily reinforced and were also badly detailed. In view of the scarcity of relevant results the relationship

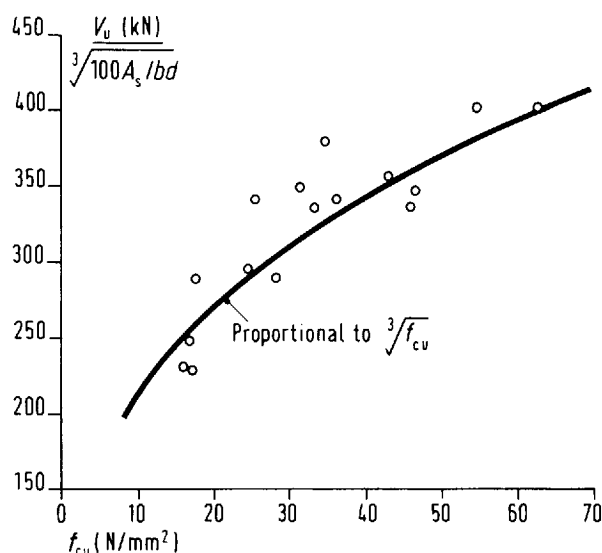
$$\sigma_{vu} \propto \sqrt[3]{f_{cu}}$$

is adopted here to be consistent with behaviour in other sorts of shear failures, as expressed by Table 5 of CP110. This relationship is compared with Elstner and Hognestad's results in Figure 48, where the experimental data from several groups of tests were combined assuming:

$$\sigma_{vu} \propto \sqrt[3]{\frac{100A_s}{bd}}$$

in accordance with Section 5.1.5. The overall agreement seems reasonable, and the proposed treatment of concrete strength causes no special problems in the overall comparisons presented later in this Section.

Figure 48
Influence of concrete strength on punching resistance



Apart from variations of strength, the concrete may vary in terms of the type of aggregate used. Beams and one-way slabs failing in shear show decreases of strength for lightweight aggregates, the reduction being of the order of 20% for those which produce concretes with densities of the order of 1700 kg/m³. The only punching tests on lightweight slabs seem to be from the USA^(43 to 46), but the aggregates were broadly similar to British ones of the type described. Where direct comparisons are available between dense and lightweight specimens, the latter show reductions of punching resistance of between 13 and 27% for similar compressive strengths of concrete. The use of the general 20% reduction in CP110 thus seems reasonable for aggregates of this type. As with beams, caution should be exercised in regard to the shear resistances of lighter materials.

5.1.3 Column or load parameters

From Equations (20) and (21)

$$V_u = \sigma_{vu} d \sqrt{1 + \cot^2 \theta} (\Sigma c + \pi d \cot \theta) \quad (22)$$

Thus, the results from two slabs with the same depth, cube strength and similar reinforcement may be compared.

Selecting a particular 'column size/slab depth' as the reference situation in Equation (22) [$(\Sigma c)/\pi d = 2.5$], $V_u/V_{u(\text{reference})}$ plotted against $(\Sigma c)/\pi d$ should be a straight line with a slope equal to $1/(2.5 + \cot \theta)$ intersecting the vertical axis at $\cot \theta/(2.5 + \cot \theta)$.

Figure 49
Influence of ratio of column size to slab depth on punching resistance

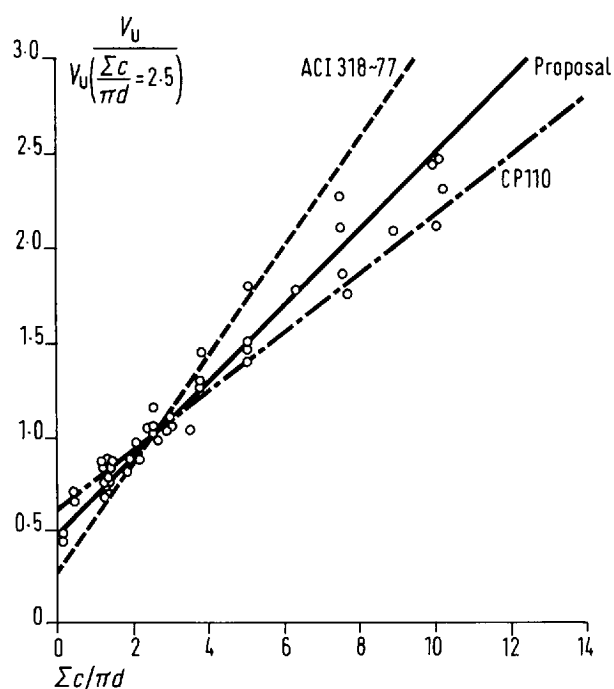


Figure 49 shows results of tests by Forsell and Holmberg⁽⁴⁷⁾, Mowrer and Vanderbilt⁽⁴³⁾, Vanderbilt⁽⁴⁸⁾ and Richard and Kluge⁽⁴⁹⁾ plotted in this way. The three lines drawn represent Equation (22) with $\cot\theta = 2.5$ and the equivalent expressions derived from the ACI Code⁽⁶⁾ and CP110⁽⁵⁾ based on their 'critical perimeters', which are at distances equal to $0.5d$ and $1.5h$, respectively, from the column. For this illustration, h was taken as $1.3d$, which is an average value for the test specimens involved.

On the basis of this comparison with test data, a value of 2.5 is adopted here for $\cot\theta$, making

$$A_c = 2.69d (\Sigma c + 7.85d)$$

In most tests of reinforced concrete slabs, the basic failure surface is confused by damage around the reinforcement. Clearly defined surfaces are obtained in push-out tests of the type illustrated in Figure 50, which also shows a typical measured profile from the work of Chan and Lau⁽⁵⁰⁾. The value of 2.5 for $\cot\theta$ can be seen to agree well with this experimental evidence.

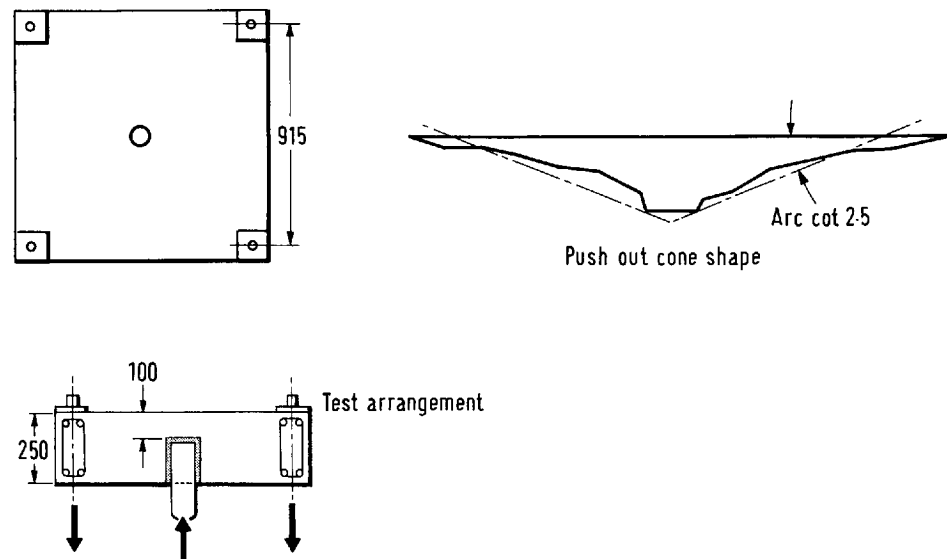


Figure 50
Punching test failure cone

While the length of the perimeter of a column is the major parameter, its shape can also influence the punching strength. The elastic distribution of shear approaches uniformity for a circular column, and generally becomes less even for more elongated rectangular shapes, although the distribution also depends on the span of the slab—short spans encouraging stress concentrations.

Test results for circular and square columns of the same perimeter generally show higher strengths in the former case, the difference being of the order of 10 to 15%. Results for rectangular columns from work by Hawkins, Fallsen and Hinojosa⁽⁵¹⁾ show some decrease in resistance for more elongated forms, but the flexural reinforcement of these specimens was not designed taking account of the column shape. Had it been so, the strength variation could have been reduced.

In view of the complex interaction of the shape of the column, the shape of the slab and the layout of reinforcement, together with the rather small variations in strength at stake, it does not seem worthwhile to go too far into shape effects. Some empirical improvement of correlation with data presently available can be achieved by multiplying the calculated strength by a shape factor:

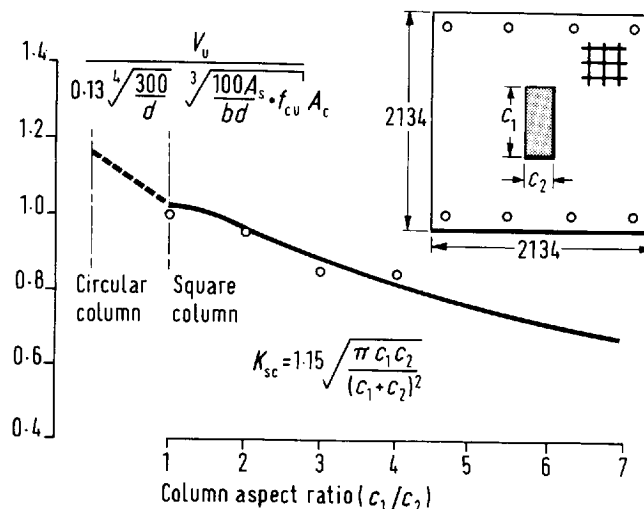
$$K_{sc} = 1.15 \sqrt{\frac{4\pi \times \text{column area}}{(\text{column perimeter})^2}} \quad (24)$$

The basic value $K_{sc} = 1$ corresponds to a square column, and the factor gives a 15%

increase of strength for circular columns. Its effect for rectangular shapes is shown in Figure 51, together with Hawkins' test results⁽⁵¹⁾.

For extreme column shapes or virtual line loads, this factor may be excessively conservative. Where higher resistances can be predicted by considering a smaller 'effective' column (with a higher K_{sc}), these values should be accepted.

Figure 51
Influence of column shape on punching resistance for a constant perimeter length



5.1.4 Scale effect

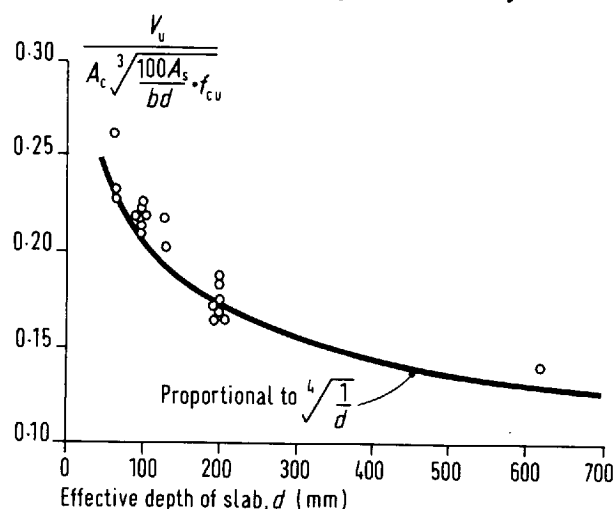
It is well established that in beams and one-way slabs without shear reinforcement the ultimate nominal shear stress (V_u/bd) decreases with increasing depth if other parameters are kept constant. If the same concrete mix is used in specimens of varying depth

$$\frac{V_u}{bd} \propto \sqrt[4]{\frac{1}{d}} \quad (25)$$

while if the maximum aggregate size is scaled along with d , the effect is somewhat reduced.

Figure 52 shows values of $V_u/A_c \sqrt[3]{f_{cu} \cdot 100A_s/bd}$ from the CIRIA punching tests and KTH Stockholm⁽⁵²⁾ plotted against d . A reasonable overall correlation is obtained with the fourth root relationship, although there is evidence of a reduction of the scale effect when the aggregate is scaled. In practice, scaling of aggregates is unlikely.

Figure 52
Influence of slab depth on punching resistance



5.1.5 Flexural reinforcement parameters

Flexural reinforcement may influence punching resistance in a number of ways. Viewed in terms of actions contributing to strength, an increase of flexural steel should increase the depth of the compression zone and thus the area of uncracked concrete available to support shear. It should reduce the widths of cracks, thus improving the transfer of forces by aggregate interlock, and should also provide an increased dowel action.

Alternatively, viewed in terms of a failure mechanism involving a vertical displacement at an inclined fracture surface, an increase of reinforcement should enhance the restraint available in the plane of the slab.

The rather ill-defined factors above are complicated by the fact that at failure some, but not all, of the flexural steel is yielding. It is unlikely that any very simple reinforcement parameter could express all the various actions involved. On the other hand, in the present state of knowledge, it is doubtful whether a rational approach could be derived, and the available test data are insufficient to substantiate a complex treatment.

The approach used here is to work first in terms of the simplest possible parameter, the ratio of reinforcement, and to establish an expression for punching strength. The effects of other factors can then be assessed by reference to this expression.

The test results considered first are from tests of slabs with uniform reinforcement equal (or nearly so) in two orthogonal directions. From Section 5.1.4

$$V_u \propto \sqrt[3]{f_{cu}} \sqrt[4]{\frac{1}{d}} \cdot A_c$$

where A_c is given by Equation (23)

Figure 53 shows V_u divided by the right side of the above Equation plotted against the ratio of flexural reinforcement for tests by Elstner and Hognestad⁽⁴²⁾, Base⁽⁵³⁾ and Kinnunen, Nylander and Tolf⁽⁵²⁾. For the last group, the experimental strengths were reduced by 1/1.15 according to Equation (24) to allow for the columns being circular and not square as in the other tests.

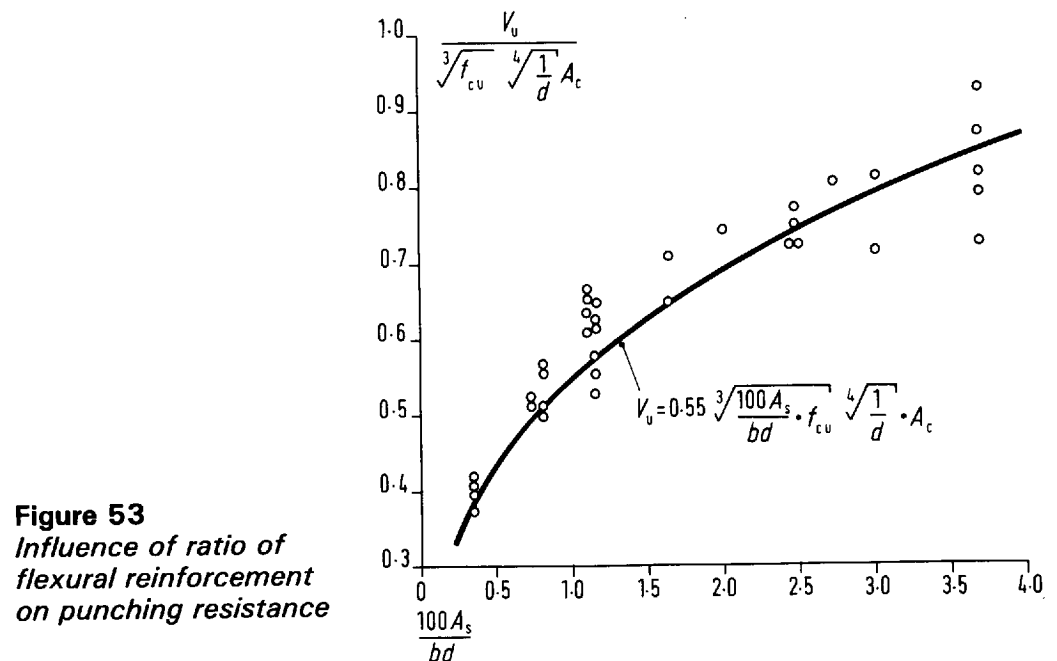


Figure 53
*Influence of ratio of
flexural reinforcement
on punching resistance*

It can be seen that there is a general agreement with the equation

$$V_u = 0.55 \sqrt[3]{\frac{100A_s}{bd} \cdot f_{cu}} \sqrt[4]{\frac{1}{d}} \cdot A_c \quad (26)$$

and the use of a cube root function is again convenient as it is consistent with what is known from other types of shear failures.

Apart from the simple ratio $100A_s/bd$, there are other reinforcement parameters which could influence punching resistance. One is the concentration of reinforcement towards the column or loaded area. For practical arrangements of bars, Moe's tests⁽⁵⁴⁾ and the CIRIA results showed decreases of strength by roughly 6% with increasing concentration, compared to those for slabs with uniform steel. The influence is clearly marginal.

The layout of reinforcement can vary in other ways than by the concentration of equal orthogonal steel. Some of Kinnunen and Nylander's slabs⁽¹⁹⁾ were reinforced only with circumferential or ring steel. For similar ratios of reinforcement, these slabs were, on average, 30% weaker than orthogonally reinforced specimens, although their flexural capacities were virtually identical.

In more general terms, there can be unequal orthogonal reinforcement. Work by Mahmood⁽⁵⁵⁾ indicates that the provision of excessive reinforcement in a direction in which it is not required for flexure does not enhance the shear capacity. This makes it difficult to formulate a simple but general method of combining orthogonal ratios to give a single value for $100A_s/bd$. However, assuming that the steel arrangement is appropriate for flexure, it should be adequate to work in terms of a simple average:

$$\frac{100 A_s}{bd} = \frac{1}{2} \left[\left(\frac{100 A_s}{bd} \right)_x + \left(\frac{100 A_s}{bd} \right)_y \right] \quad (27)$$

Predictions made on this basis are included in the general comparison of Section 5.1.7, and do not give rise to any serious errors.

The yield strength of the flexural reinforcement appears as a parameter in a number of expressions for punching resistance, and can be expected to have some influence at least where a part of it yields before failure. The question is whether the influence is small enough to be neglected in practice, and there is evidence that this is the case. Two of Moe's series of tests⁽⁵⁴⁾ were of otherwise similar slabs having steel with a yield strength of 330N/mm² in one set and 480N/mm² in the other, and there is no apparent difference between the punching strengths obtained. Further, the data of Section 5.1.7 are from tests with widely varying strengths of steel and there is no apparent effect on the results.

There are insufficient data available from which to make a proper comparison of slabs with otherwise similar plain and deformed reinforcement, but the relatively few tests of slabs with plain bars show no significant variation from the general trend of results.

All the paragraphs above relate to tension reinforcement, but slabs can contain compression steel. There are a few sets of results^(1, 53, 56), giving direct comparisons of slabs with and without compression reinforcement. The ratios of compression steel vary from 0.3 to 1.0 times the ratios of tension steel, and the maximum increase of punching resistance is only 12%, even where compression reinforcement theoretically increases the flexural strengths of the slabs.

5.1.6 Loading and/or support conditions

In most experimental work on punching, the slabs were simply supported (or loaded) at a distance from the column intended to represent the distance to a 'ring of contraflexure' in a prototype floor. Such an arrangement provides very little restraint to deformations in the plane of the slab, and it was suggested that, in practice, punching resistance is enhanced by in-plane or membrane restraints from a floor as a whole.

Where there is an absolute restraint to expansion a slab can develop a very significant 'dome' action. Tests of this type by Taylor and Hayes⁽⁵⁷⁾ showed increases of punching strength in slabs with 1.57% reinforcement, varying from 16 to 64% as the side dimension of the loaded area increased from 0.67 to 2.0 times the slab thickness. With the 3.14% reinforcement, the strength enhancement by membrane action was only 0 to 15%. These results and others by Mowrer and Vanderbilt⁽⁴³⁾ show that in-plane restraint can in a sense replace flexural reinforcement, but that the dome

action becomes less significant in more slender slabs, where the rise of the effective dome is reduced by deflection (Taylor's specimens had span/depth ratios of less than 12). In a practical flat slab floor, compressive membrane effects are thus unlikely to be significant.

Apart from in-plane restraints, slab boundaries may be subject to rotational fixity as in the test arrangements used by Vanderbilt⁽⁴⁸⁾ and Long and Masterson⁽⁵⁸⁾. The strength enhancement from a combination of in-plane and rotational restraints is probably small enough to be neglected, particularly in view of the difficulty of including membrane actions in slab analyses.

A different aspect of loading and support arrangements arises if the slab spans predominantly in one direction. Tests of this type were carried out by Elstner and Hognestad⁽⁴²⁾ and Mahmood⁽⁵⁵⁾. In the former case, the slabs were somewhat inappropriately reinforced equally in two directions and showed a 12% drop of strength compared with similar slabs supported on all four sides. In Mahmood's tests, the reinforcement was appropriate for the flexural conditions and the strengths were as normal.

5.1.7 Comparison with test results

From the preceding sections, the expression proposed for the punching strength of a slab at an internal column or load free from any unbalanced moment is:

$$V_u = K_a K_{sc} \xi_s \sqrt[3]{\frac{100A_s}{bd}} \cdot f_{cu} \cdot 2.69d (\Sigma c + 7.85d) \quad (28)$$

where V_u = the ultimate shear force (in N)

K_a = 0.13 for normal dense concrete and 0.105 for lightweight aggregate concrete with a density of about 1700 kg/m³

K_{sc} = $1.15\sqrt{4\pi \times \text{column area}/(\text{column perimeter})^2}$

ξ_s = $\sqrt[4]{300/d}$ (with d in mm)

$\frac{100A_s}{bd}$ is the average of the percentages of tensile reinforcement in two orthogonal directions, each calculated for the width of slab treated as 'Band I' in flexural design. For a simply-supported test slab, the percentages are calculated for the specimen as a whole. For slabs with reinforcement in one direction only (circumferential rings), the value of $100 A_s/bd$ can be taken as half the percentage in a plane normal to the bars

f_{cu} is the cube strength of the concrete in N/mm², and where necessary is taken as 1.25 times the cylinder compressive strength. No corrections were made for cubes of different sizes, although in principle f_{cu} is the value for a 150-mm cube

d is the effective depth of the slab to the mean plane of the reinforcement in mm, here taken as the depth to the inner surface of the outer reinforcement irrespective of any differences in bar sizes or steel ratios in the two directions

and Σc is the perimeter of the column or loaded area in mm.

Figure 54 presents a comparison between Equation (28) and relevant test data from this work and References 19, 43 to 47, 49, 51 to 57, and 59 to 62. The data taken from Reference 57 are only for specimens without in-plane restraints. In addition, some results from Elstner and Hognestad⁽⁴²⁾ are included. These are those from slabs in which the reinforcement has adequate cover. The tests by Vanderbilt⁽⁴⁸⁾ are excluded, since, although they are of qualitative interest, their quantitative significance is doubtful in view of the very large bar spacings.

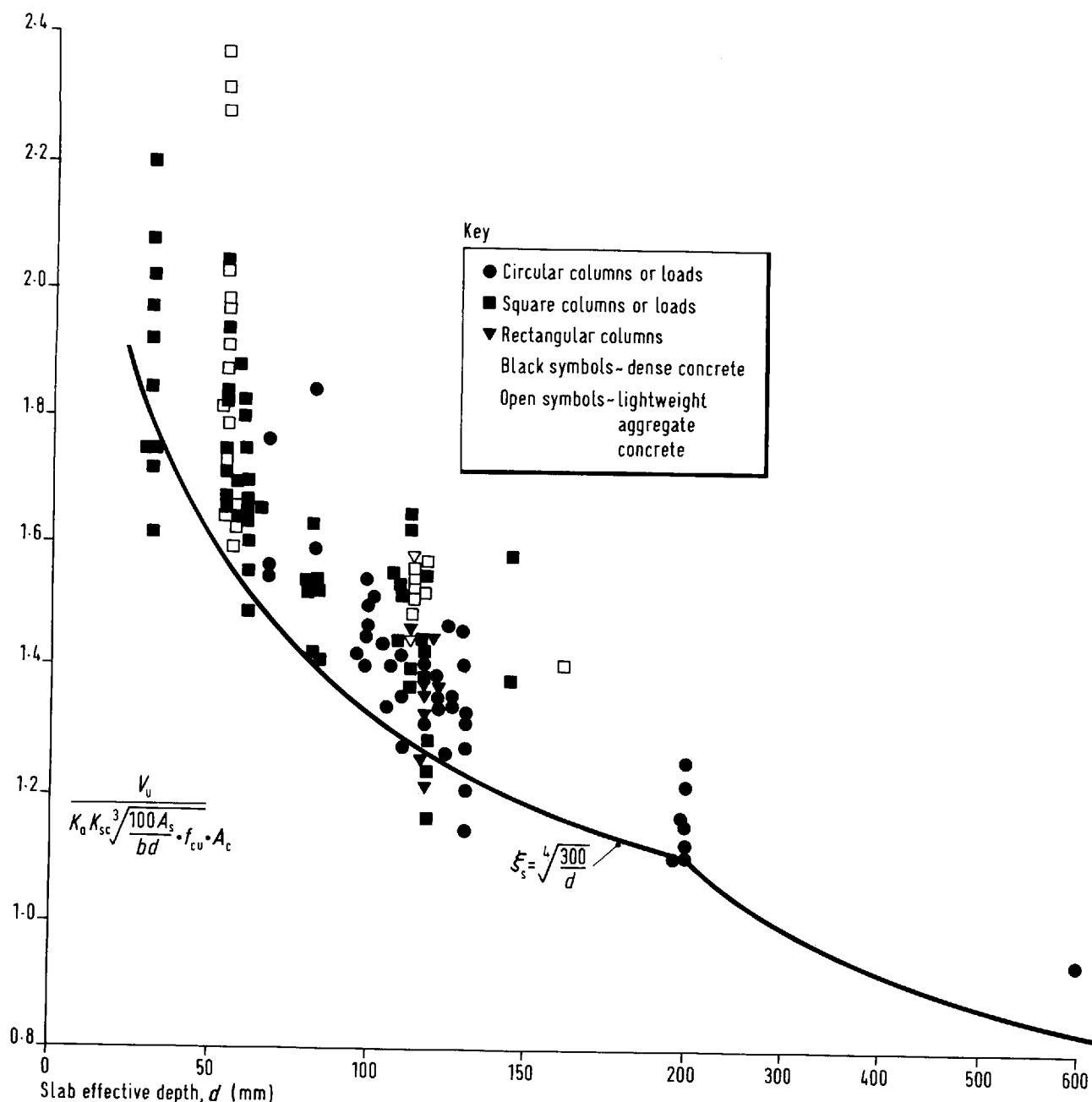


Figure 54 *Punching shear test results for internal slab-column connections under concentric load*

It can be seen that Equation (28) is practically a lower bound to the test results, and as such can be taken as an expression of characteristic strength.

The way in which the partial safety factor for materials should be applied to the equation of this type is debatable. In both the CP110⁽⁵⁾ and European codes, the factor for concrete in compression is 1.5. This could either be applied to the equation as a whole to give

$$V_{Rd} = \frac{1}{1.5} \cdot V_u$$

or to the concrete strength, which appears under the cube root, in which case

$$V_{Rd} = \frac{1}{\sqrt[3]{1.5}} \cdot V_u = \frac{1}{1.14} \cdot V_u$$

A reasonable compromise would be to make $V_{Rd} = V_u/1.3$ where V_u is defined in Equation (28).

5.1.8 Slabs with shear reinforcement

If the punching resistance of a given connection is inadequate, the design can be improved in five ways:

1. by increasing the concrete strength
2. by increasing the quantity of flexural reinforcement
3. by increasing the effective size of the column, either by enlarging the whole column or by adding a capital
4. by increasing the thickness of the slab, either throughout the panels in question or locally by the introduction of a drop panel
5. by providing shear reinforcement.

In many circumstances, the use of shear reinforcement must be the most attractive solution. If shear reinforcement is placed in a slab, the following modes of failure, shown in Figure 55, are possible in addition to flexure:

- a. punching on a surface crossed by shear reinforcement
- b. punching outside the reinforced zone
- c. punching between the innermost reinforcement and the column faces
- d. wide-beam shear failure.

It is proposed that the last of these be treated on the basis of CP110, the beam breadth being taken as equal to the width of Band I as defined for flexural design or as $l/2$, whichever is the greater, but not exceeding the full breadth, b .

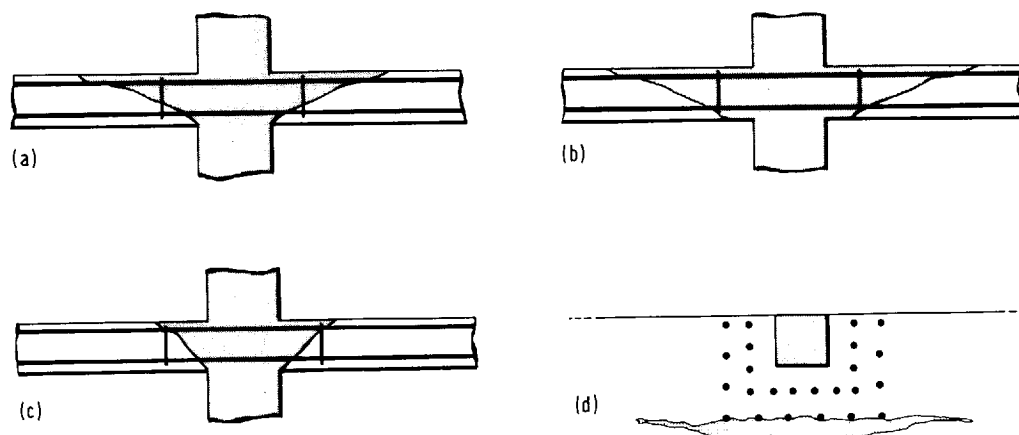


Figure 55
Possible modes of shear failure for slabs with shear reinforcement

Ideally, the various possibilities of punching should be treated by considering conditions at all possible failure surfaces, thus involving variations of both location and inclination.

The simplest case is that where the failure occurs outside the zone with shear reinforcement. In principle, conditions are similar to those at a fracture surface defined by the outermost shear bars. The only apparent difficulty here is that the assumed failure inclination of 22° (arc cot 2.5) is not necessarily a good approximation irrespective of the size of the reinforced zone. This should not be a serious problem within the range of Σc values already covered in tests of plain slabs.

Failure between the column faces and the innermost shear reinforcement can be treated on a rational basis only if the relationship between nominal ultimate stresses and the slope of the fracture surface is defined. For the present, it probably suffices to adopt a 'good detailing' approach and to place the inner shear steel sufficiently close to the column to prevent such failures occurring. The CP110⁽⁵⁾ requirements (that the bars should be at a distance from the column faces equal to $0.75h$) may well not ensure this. Such a position allows failure to occur at 45° inclination without crossing shear reinforcement. The evidence of tests of short span slabs without shear steel is that the resistance at a 45° failure surface is not very much greater than the basic value for 22° . To be cautious in a situation of uncertainty, it is better to reduce the maximum unreinforced width to about $d/2$.

In the remaining cases where the failure surface crosses at least some shear reinforcement, difficulties in relating nominal ultimate stresses to surface slopes are compounded by lack of information on the efficiency of the various possible forms of shear reinforcement. The absence of reliable data may be appreciated from the divergencies of recent codes

$$\text{CP110}^{(5)} \quad V_u = V_c + V_w$$

$$\text{ACI 318-63}^{(62)} \quad V_u = V_c + \frac{1}{2} V_w$$

$$\text{ACI 318-77}^{(6)} \quad V_u = \frac{1}{2} V_c + V_w$$

$$\text{CEB/FIP}^{(7)} \quad V \simeq 1.33 V_w$$

where V_c is the punching strength of an otherwise similar slab without shear reinforcement and V_w is the vertical component of the sum of the forces in the shear reinforcement, assumed to work together and assumed to act at yield stress.

It may be noted here that CP110⁽⁵⁾ is in reality similar to ACI 318-63⁽⁶²⁾, since only half the shear reinforcement provided is assumed to 'work together'. In practice, the differences between these recommendations are of less consequence than might be imagined, as, in many cases, the amount of reinforcement is governed by prescribed minimum steel areas. Without further and rather better test data, there is little point in making any new proposal for determining the required shear steel.

5.2 PUNCHING IN THE PRESENCE OF UNBALANCED MOMENT

Where an unbalanced moment is transferred between a slab and a column, the distribution of shear around the column ceases to be uniform. In practice, there are two possible situations. One arises at external columns where the moment is perpendicular to the edge of the slab, the other applies at internal columns and at edge columns with moments parallel to the slab edge.

At an edge column with a perpendicular moment giving an eccentricity of loading in the direction of the interior slab, the extreme credible situation is that the entire shear should act at the inner face of the column. At an internal column, however, a much greater shear couple can be developed with the forces at opposite column faces acting in opposite directions.

5.2.1 Internal slab/ column connections

The actions involved in the transfer of an unbalanced moment from a slab to a column are flexure at the faces perpendicular to the moment, torsion (horizontal forces) at the other column faces, and an unevenly distributed vertical shear.

Elastic solutions for the relative magnitudes of the three components are given by Mast⁽⁶³⁾ and the uneven shear contribution is

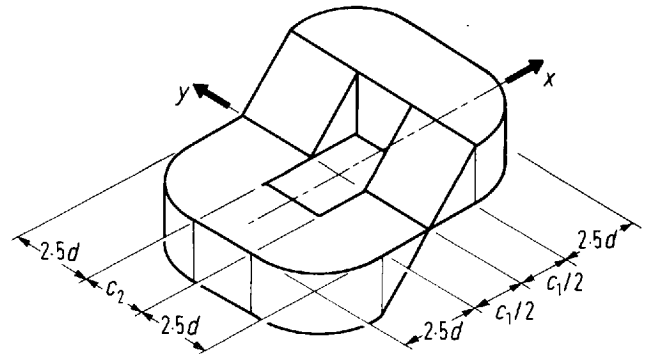
$$\bar{M} \left[1 - \frac{2}{\pi} \arctan \frac{y}{x} \right] = \alpha \bar{M}$$

where \bar{M} is the total moment transferred, and x and y are the dimensions of a rectangular perimeter parallel and perpendicular to \bar{M} .

For use with the fracture surface approach of Section 4.3.2, the distribution of shear can be visualised as in Figure 56, with the dimensions x and y taken as $(c_1 + 2d)$ and $(c_2 + 2d)$. The lever arm between the forces reaching onto the faces c_2 of the column is approximately $(c_1 + 2d)$, and the maximum nominal vertical stress because of the moment \bar{M} is

$$\frac{\alpha \bar{M}}{d \sqrt{1 + \cot^2 \theta} (c_1 + 2d) \left[c_2 + \frac{\pi}{2} d \cot \theta + c_1^2 / (3c_1 + 6d) \right]}$$

Figure 56
Distribution of stresses
on fracture surface due
to unbalanced column
moment loading



Combining this with a stress resulting from concentric shear, V , writing $e = \bar{M}/V$, and accepting the same limiting stress for the sum of the effects of V and \bar{M} as for the earlier concentric loading, it follows that

$$\frac{V_{ue}}{V_{uo}} = \frac{1}{1 + \beta \left(\frac{e}{c_1 + 2d} \right)} \quad (29)$$

where V_{ue} = ultimate shear capacity for a load eccentricity, e

V_{uo} = ultimate concentric load shear capacity

$$\text{and } \beta = 2\alpha \left[\frac{\frac{c_2}{c_1} + \frac{\pi}{2} \cdot \frac{d \cot \theta}{c_1} + 1}{\frac{c_2}{c_1} + \frac{\pi}{2} \cdot \frac{d \cot \theta}{c_1} + \frac{1}{3(1 + 2d/c_1)}} \right]$$

For practical purposes, it is probably more convenient to approximate Equation (29) and the above value for β by

$$\frac{V_{ue}}{V_{uo}} = \frac{1}{1 + 1.5e / \sqrt{(c_1 + 2d)(c_2 + 2d)}} \quad (30)$$

This approximation should be adequate for all normal column sizes, but might be less than conservative if applied to the very large perimeters which may need to be checked when shear reinforcement is provided. In such cases, the design (imposed) shear force should be increased by 10% to allow for unevenness of shear at each side of the perimeter as proposed for drop panels in Section 6.

Figure 57 presents a comparison between Equation (30) and test results from the CIRIA work and other sources^(54, 56, 60, 64 to 69) for slabs with overall depths in the range 75 to 175mm. They can be seen to agree well enough with a partial exception for very large values (c_1/d) which should be dealt with as described in the preceding paragraph.

The major difference between the proposal and CP110 in this context is the use of the ratio $e/(c_1 + 2d)$ as opposed to e/l in CP110. The present version corresponds better with the elastic shear distributions, provided that the column dimensions are small in relation to the slab spans, but for typical proportions ($c_1 \approx 2d$, $l \approx 25d$) the numerical results are very similar. The test data now available are considerably more extensive than those published before 1972, and support the new proposal in cases where the two methods diverge.

5.2.2 Edge columns with moments parallel to the slab edge

The situation here is similar to that at an internal column and can be treated as a similar case to Equation (30). The very limited test data for this case come from Stamenkovic and Chapman⁽⁵⁶⁾, and are compared with calculated strengths in Figure 58. The correlation obtained is satisfactory.

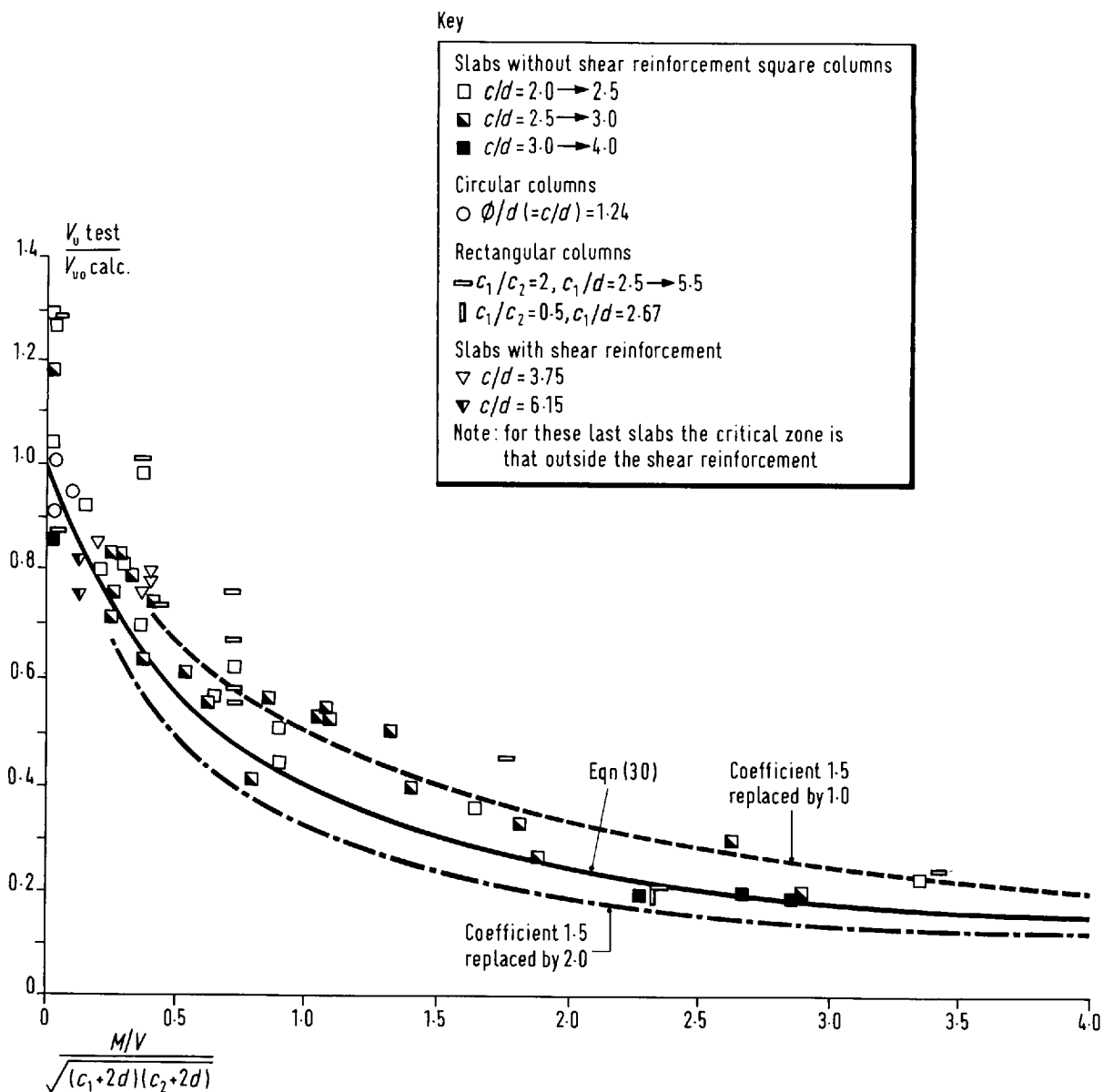
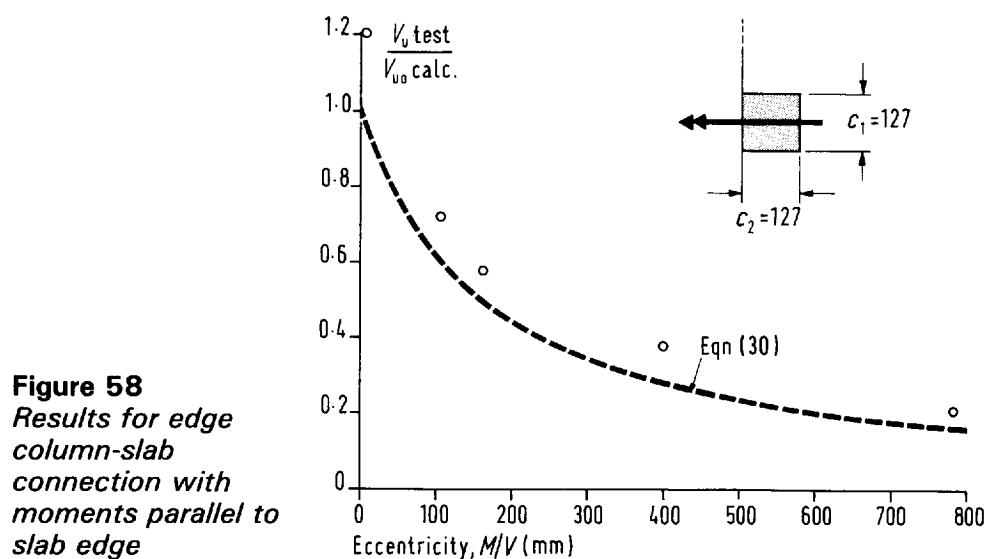
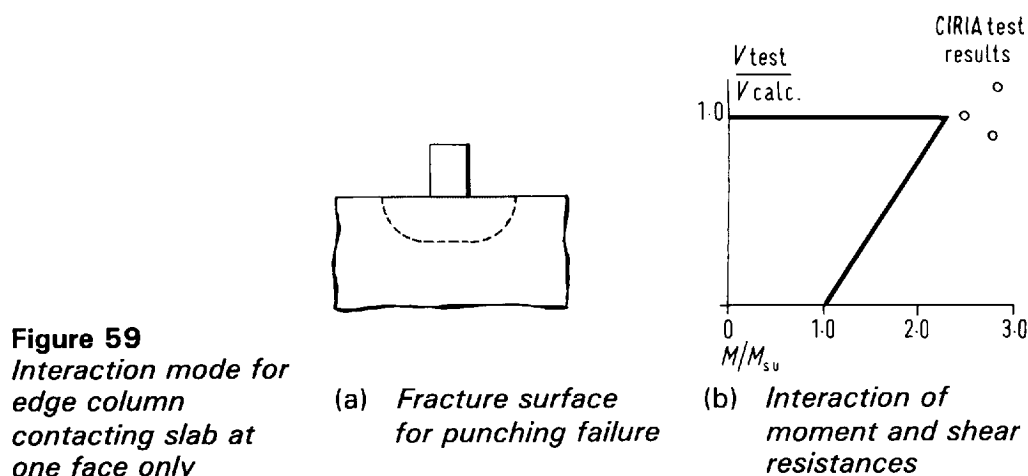


Figure 57 Test results for internal slab-column connections under eccentric loading



5.2.3 Edge columns with moments perpendicular to the slab edge

An extreme case of an edge column/slab connection is one in which the slab contacts only the inner face of the column. The shear at the face automatically produces a moment about the column centre, but the distribution of shear is independent of the transferred moment.



With the fracture surface as shown in Figure 59, the limiting shear force is

$$V_u = d \sqrt{1 + \cot^2 \theta} (c_2 + 0.5\pi d \cot \theta) \sigma_{vu} \quad (31)$$

where, as before, $\cot \theta$ can be taken as 2.5, and for dense concrete

$$\sigma_{vu} = 0.13 \xi_s \sqrt{\frac{100 A_s}{bd}} \cdot f_{cu}$$

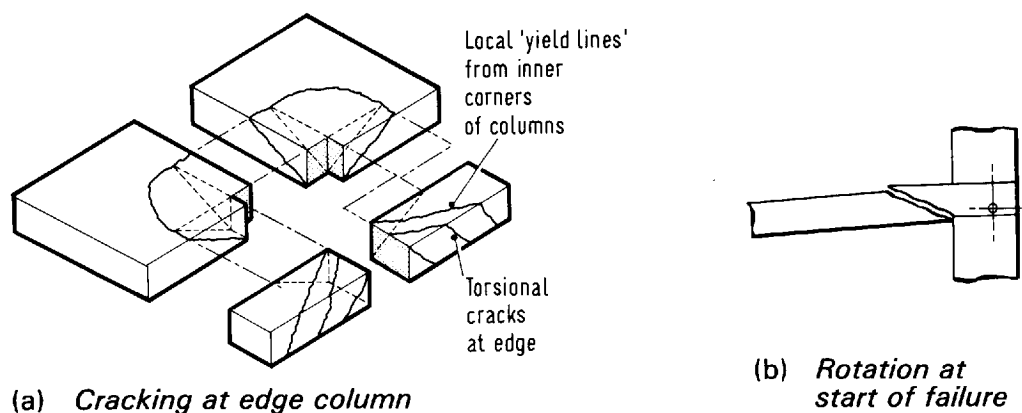
The moment about the column centre is

$$M \leq M_{su} + V \frac{c_1}{2} \quad (32)$$

where M_{su} is the ultimate moment at the column face determined by the reinforcement passing through the face and anchored on both sides of it.

The resulting moment/shear interaction is as shown in Figure 59, which also shows three relevant test results from the CIRIA programme. The proposed approach can be seen to give satisfactory predictions.

In more normal cases, the slab is connected with three column faces. The maximum moment available from the flexural reinforcement (M_{s1}) is that resulting from the bars crossing the inner face of the columns and the two local yield lines running from the inner corners of columns



As an approximation, only the simple case of bars crossing 45° yield lines is considered here. If detailing is such that bars over a greater width are mobilised in flexural resistance, the difference arises primarily in terms of bending, and the subsidiary effect on V_u can reasonably be ignored. For design purposes, shear and moment can be treated separately.

If the full flexural resistance is developed, it is improbable that there can be any shear in the triangular zones behind the yield lines, where the cracking at the slab edge is in the torsional direction shown in Figure 60. The area of the fracture surface is thus as in Figure 61(a), and with $\cot\theta = 2.5$ the limiting shear for point (a) is

$$V_1 = 2.69d (c_2 + 5.89d) \sigma_{vu}$$

At the column, this shear acts on the inner face so the limiting moment about the column centre is

$$M_{c1} = V_1 c_1 / 2$$

Thus, for $V \leq V_1$, the moment/shear interaction can be expressed as in Equation (32).

$$M_u = M_{s1} + V \frac{c_1}{2}$$

although the ability to develop the moment M_{s1} is dependent on the provision of suitable reinforcement parallel to the edge (see Section 4.3.3).

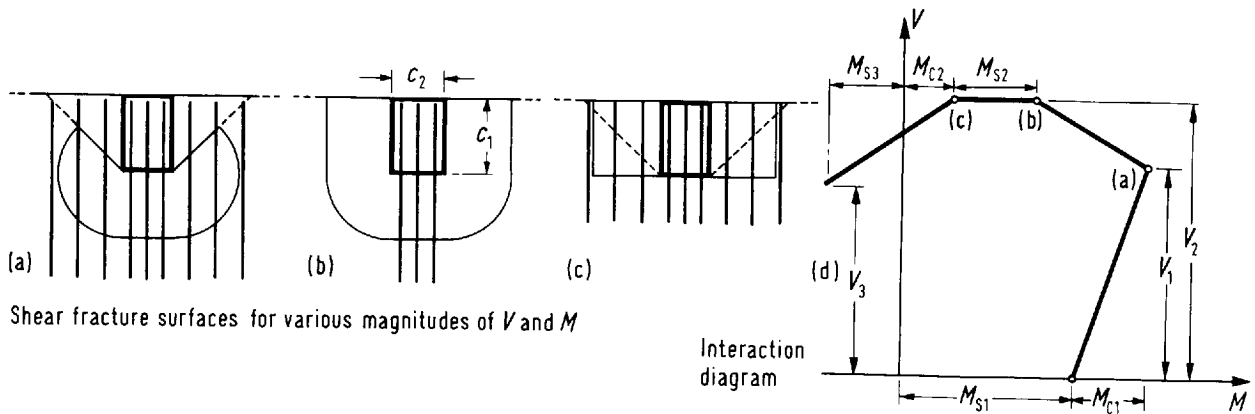


Figure 61 Limiting conditions for shear-moment interaction at edge columns

In a test specimen, where an eccentric load or a load and a moment are directly applied to a column stub, Equation (32) is a criterion of failure for all values of V .

In a statically-indeterminate system such as a normal floor or the CIRIA specimens shown in Figure 1 (page 9), the attainment of a limiting edge moment is not in itself a failure criterion provided that a yield line has not formed at midspan and the only true failure treated so far is one by shear with $V_u = V_1$.

This sort of failure is common, the most probable sequence of events leading to it being that the steel involved in M_{s1} yields. As the load increases, the steel stresses do not reduce to allow increased uniformity of shear, so when the shear force reaches V_1 , a punching failure occurs at the inner face of the column. The mechanism of failure begins with a rotation of the slab about an axis near the outer face of the column (Figure 60), but as the resistance at the inner face reduces, shear is transferred to the column sides, so that eventually the shear cracking generally propagates to the slab edge crossing the earlier torsional cracks.

Shear resistances greater than V_1 are not obtained in most realistic specimens. However, when the eccentricity of loading applied to a column stub in a simple

statically-determinate model is small, it is possible for the shear to be more uniformly distributed, but only at the price of not developing the diagonal yield lines. A simple limiting condition can be visualised as in Figure 61(b). The shear is assumed to be uniform around the three column faces, but the moment resulting from the reinforcement is taken to be limited to that provided by the bars through the inner column face (M_{s2}). Thus

$$\text{for } M_{c2} \leq M \leq M_{c2} + M_{s2}$$

$$V_u = V_2$$

$$\text{where } V_2 = 2.69d (c_2 + 2c_1 + 3.93d) \sigma_{vu}$$

$$M_{c2} = 2.69c_1d (0.5c_2 + 1.96d) \sigma_{vu}$$

If the moment about the column centre is smaller than M_{c2} , the maximum shear stress is at the edge of the slab, and for negative moments (i.e. for eccentricity towards the exterior) the connection must behave largely as a pair of beams framing into the side faces of the column. These 'beams' are subjected to bending shear and torsion. Assuming that the reinforcement parallel to the edge is correctly dimensioned, the only interaction at issue is that between the shear and torsion. For normal geometric proportions (i.e. $c_1 > 2d$), this is not great, as the maximum stresses from vertical shear are at the slab edge, while the torsional shear stresses are low there and high on the top and bottom surfaces of the slab.

A simple limiting condition can thus be taken to be defined by:

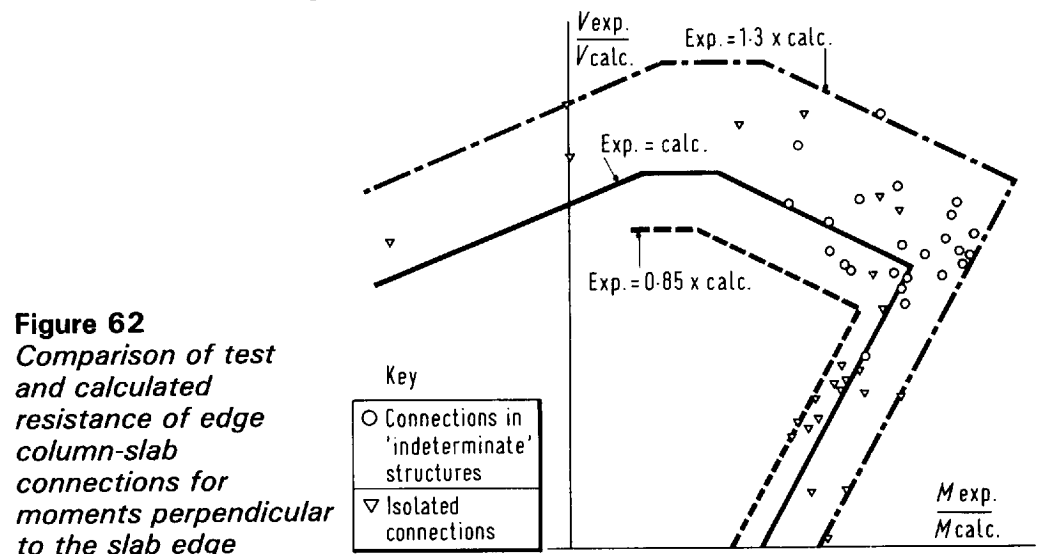
$$M = M_{s3} (M_{c3} = 0)$$

$$V = V_3 = 2.69d (2c_1) \sigma_{vu}$$

where M_{s3} is the total 'tension in the bottom' moment provided by the reinforcement crossing the local yield lines of Figure 61(c), and V_3 is the shear resistance of the two 'beams'.

The complete moment/shear interaction diagram proposed is obtained by joining the points and line derived above by straight lines and is shown in Figure 61(d).

There are difficulties in presenting an overall comparison between this interaction relationship and test results, since the relative magnitudes of M_{cl}/M_{sl} , M_{c2}/M_{sl} , etc. vary from slab to slab. Figure 62 shows a comparison in the following way. The interaction line is drawn with arbitrary but reasonable proportions, and the test data originally plotted on individual interaction diagrams is scaled onto it. The data plotted are from the CIRIA work and from various other sources (36, 38, 39, 56, 60, 66, 70 to 72). The correlation of actual and predicted strengths is adequate.



The group of points from isolated column tests which plot on the unsafe side of the theoretical line were derived from tests by Taylor and Clark⁽⁷²⁾. The apparent unsafety may not be very serious for two reasons. First, in many of these slabs, the top steel perpendicular to the edge was not properly anchored; second, the yield stress of the reinforcement is not given in Reference 72, and was assumed to be 450N/mm² (which may be too high).

Two of the points plotted are from tests of slabs which had overhangs beyond the column. The ways in which moment and shear values were calculated for these are shown on Figure 63.

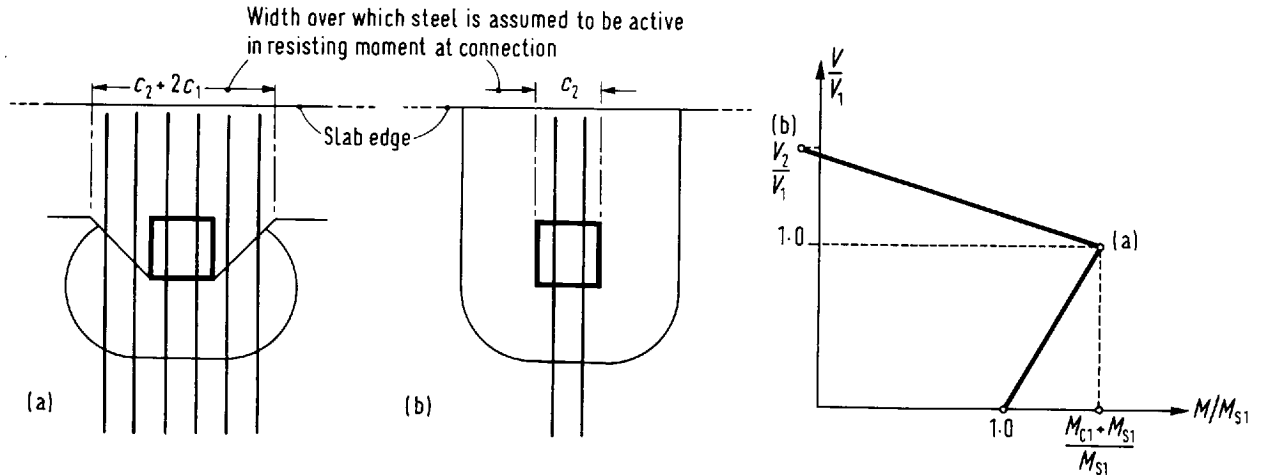


Figure 63 *Shear-moment interaction at edge column-slab connection for slab overhang*

While the approach given above seems to give good prediction of ultimate resistance, it is probably too complex to be of very general use. Various simplifications are possible. The most generally useful appears to be:

$$V \leq 0.8V_2$$

$$M \leq M_{s1} + M_{c2} \frac{V}{V_2}$$

This has the advantage of being applicable for all column shapes and of being compatible with a viable approximation for corner columns. It is also similar to CP110 in regard to the shear limit. The only obvious disadvantage is that it is not directly applicable to overhanging slabs, but these can be treated satisfactorily by calculating V_2 and M_{c2} as for a slab ending flush with the outer face of the column while determining M_{s1} as in Figure 63.

The simplified form is compared with the test data in Figure 64, and the results can be seen to be satisfactory, at least as long as the eccentricity of loading is towards the interior of the slab.

5.2.4 Corner columns

The treatment of corner connections directly follows from that of the edge situation. For biaxial bending, limiting conditions considered are as shown in Figure 65, and the resulting interaction diagram is constructed in the same way as for edge columns. A comparison with the CIRIA tests and other test results^(73, 74) yields the simplified form shown on Figure 64. All the results plotted are for biaxial bending, but the simplified formula is also valid for uniaxial bending.

In general, the comparisons show the proposals to be reasonably accurate. The only exceptions arise in rather peculiar circumstances. Two of the CIRIA slabs had unusually little top steel, and the experimental moments were almost certainly

enhanced by strain hardening. In one, the top steel was so minimal that the rather high shear resistance may have depended more on the bottom bars in the manner described in Section 5.3.

A few published results are excluded from the comparisons. These are:

1. A group of four tests by Zaghlool, de Paiva and Glockner⁽⁷⁵⁾ in which the only top steel was a splayed arrangement of bars bent over from the columns, which makes the assessment of $100 A_s/bd$ impossible.
2. A group of tests by Tankut⁽³⁶⁾ carried out on the corners of two four-bay slabs at the end of a programme of work which had already produced failures at the interior and edge columns. The results all correspond to flexural failures, but are extremely scattered, probably because of cumulative damage to the slabs prior to the final tests.

Figure 64
Comparison of test data for edge and corner column-slab connections with simplified Equation (61)

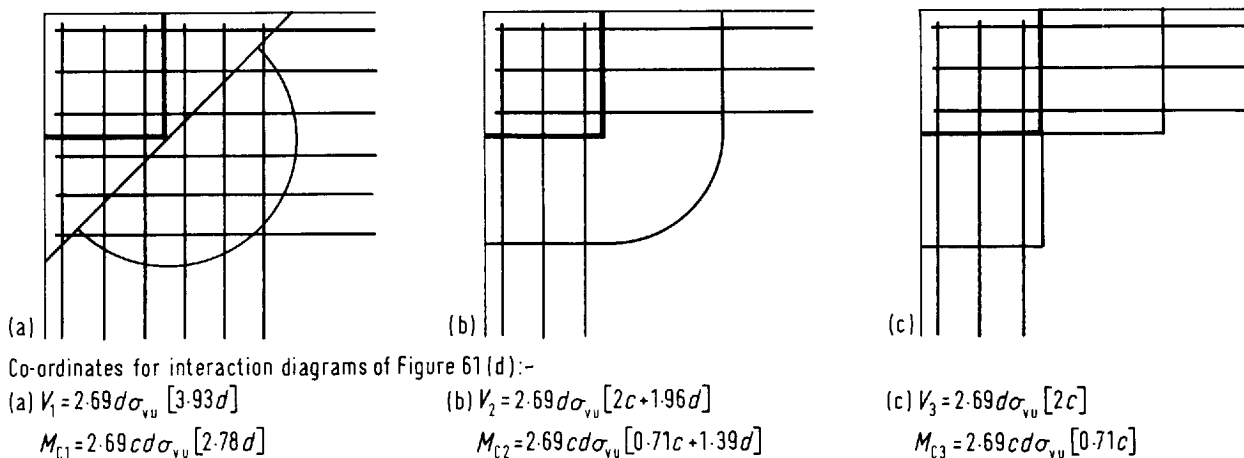
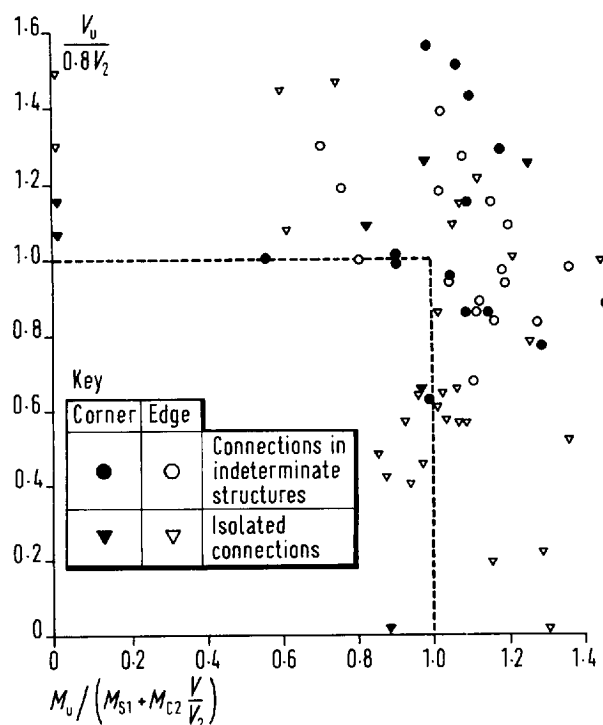


Figure 65 Limiting conditions for shear-moment interaction at corner columns

5.3 PROGRESSIVE COLLAPSE

There have been several collapses of flat slab structures. A major example was the collapse in the USA in 1973 of a block of flats in the Skyline Plaza Complex in Fairfax County, Virginia. The failure was initiated by the premature removal of props, and its cause was thus not unique to flat slab construction.

What is worrying in this case is the downward progression of the collapse through 24 floors and its horizontal extension to a neighbouring car park which was also a flat slab structure. The three suspended floors of the car park were of post-tensioned unbonded construction and collapsed completely.

The problem with flat slabs is that unless special precautions are taken, the shear resistance at a column following a punching failure is low. Punching even at a single column thus causes a major redistribution of load effects. If the failure is at an internal column, the shear at the neighbouring columns is increased by about 25%, and large eccentricities are developed because of the inequality of the residual spans.

A failure initiated at one column can thus rather easily spread horizontally, and once this happens the slab falls onto the next lower floor where the extra loading is magnified by dynamic effects.

Once punching occurs at a slab/column connection, the only reliable resistance to shear is that provided by reinforcement crossing the fracture surface. Top bars provide some resistance, but are relatively easily torn out of the slab as sketched in Figure 66(a). The tearing extends outward at an almost constant load until the remaining anchorages are inadequate and the bars are detached.

Bottom bars are much more resistant to being torn out. After an initial fall at the original punching, resistance rises rapidly with increasing vertical displacement. The final mechanism of collapse is uncertain, but probably involves the yielding of the steel in bending and the progressive destruction of the concrete on to which it bears (the areas marked A in Figure 66(b)).

The situation is fairly similar to that arising when a load is applied to a dowel projecting from a concrete surface. The latter case was considered by Rasmussen⁽⁷⁶⁾, on the basis that the criterion of failure is the development of a plastic hinge in the dowel within the concrete, while the bearing stresses on the concrete are at high and effectively plastic levels. When the load acts at the face of the concrete, as in Figure 66(c), the shear resistance for a single bar of diameter ϕ is given as:

$$V = 1.2\phi^2 \sqrt{f_y \cdot f_{cu}} \quad (33)$$

Failure in this sense does not necessarily amount to collapse, and the load may be increased with the bar kinking as in Figure 66(d).

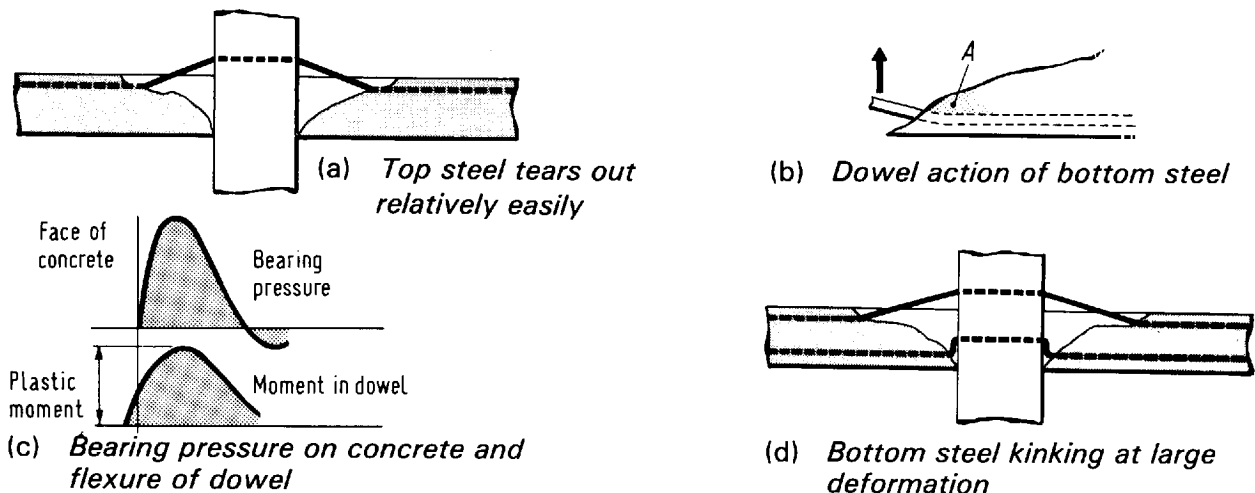


Figure 66 Behaviour of slabs after punching

It is very difficult to estimate the breaking load for such situations. In the case of post-punching resistance, the problem is made more complex by the presumably unfavourable effect of the concrete being tapered at the inclined crack.

The proposed use of Rasmussen's equation as a basis for determining the amount of bottom steel which should pass from a slab into a column, is not intended to represent any very accurate assessment of strength. However, its use of the steel area and the strengths of both the concrete in compression and the steel in tension seems preferable to the alternative of working in terms of the shear strength of the steel.

It can be assumed that in the punched condition the top steel can resist approximately 25% of the shear causing punching. Then, if the ultimate dowel capacity of the bottom bars is equal to about 75% of the punching load, V_u , there should be no great drop of resistance at punching. With the materials safety factor approximately equal to 1.3

$$V_u = 1.3 V_{ud}$$

where V_{ud} is the design shear force for the ultimate limit state.

The required dowel capacity is thus

$$V = 0.75 \times 1.3 V_{ud} \approx V_{ud}$$

It is proposed that the bottom bars passing into any column should satisfy the condition

$$1.2 \sum \phi^2 \sqrt{f_y \cdot f_{cu}} \geq V_{ud} \quad (34)$$

where ϕ is the bar diameter and the summation applies to all the bars passing through the column faces and fully anchored on either side. If a bar passes through two opposite faces, it is counted twice.

The condition is not excessive in terms of quantities of reinforcement as may be appreciated from the following example.

Internal column 300×300 mm
 Slab thickness $h = 175$ mm $d_s = 143$ mm
 Design ultimate shear $V_{ud} = 250$ kN
 Concrete Grade 30

Using 16-mm bars with a yield stress $f_y = 450$ N/mm², the number of dowels required is

$$n = \frac{250 \times 10^3}{1.2 \times 256 \times \sqrt{450 \times 30}} = 7$$

Thus two bars in each direction passing through opposite column faces making $n = 8$ is sufficient reinforcement.

Experimental evidence in favour of the proposal is admittedly meagre. Post-punching loading in CIRIA tests of internal slab/column connections gave residual strengths of between 25 and about 50% for slabs with only top steel, the high values being for cases where the bars were very heavily concentrated to the column. A test of a comparable slab with uniform top steel and two bottom bars through the column in each direction gave a residual resistance of 71% of the original punching load without failing before the test was discontinued because of problems with the load and support arrangements. This resistance is almost exactly equal to 25% of V_u plus the resistance according to Equation (33).

Two tests were carried out on edge column connections with only one face of the column in contact with the slab and with only bottom steel at the interface. The test strengths with two different amounts of reinforcement were 1.24 and 1.32 times the values from Equation (33). The conditions in these tests were favourable in that there was no diagonal cracking prior to the loading to failure.

Although the preceding paragraphs are in no sense a scientific verification of the proposal, they do indicate that bottom bars can provide an appreciable resistance, and this agrees with common sense. The proposal is not extravagant in its requirements of steel, and is put forward as a sensible measure, which should reduce the risk of progressive collapse at no great cost.

6. Flat slab variants

6.1 SLABS WITH COLUMN CAPITALS

The principal function of a column capital is to improve shear resistance by increasing the effective size of a column. CP110⁽⁵⁾ limits the dimensions of capitals for calculation purposes as follows:

1. the angle of greatest slope of the capital should not exceed 45° from the vertical
2. the dimensions of the capital used in calculations should be those at a depth of 40 mm below the soffit of the slab

With these limitations, the critical zone for shear lies outside the capital as shown in Figure 67(a), and the only modification required in calculations for punching is that the column dimensions be replaced by those of the capital.

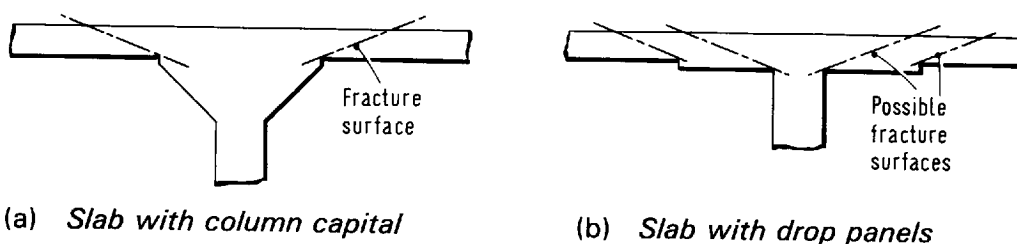


Figure 67
Surfaces used in shear calculations for slabs with column capitals and drop panels

The same replacement can be made in the determination of effective stiffnesses of joints and in calculating the design negative moments for the slab, (i.e. in making allowances for the finite support dimensions).

6.2 SLABS WITH DROP PANELS

Drop panels can be used with or without capitals. The extra thickness of slab increases the shear resistance, and to be fully effective in this respect the drop should extend for a distance from each column face, at least equal to 2.5 times the effective depth of the slab. Calculations for punching should be made adjacent to the column and at the edge of the drop as indicated by Figure 67(b). At the latter location, it would be prudent to increase the design shear force by about 10% to allow for the non uniformity of shear around the large perimeter. If the drop extends beyond the lines of contraflexure, a greater increase could be necessary.

In flexural analysis, the joint stiffness should be calculated on the basis of the depth of the drop section, and slab stiffnesses, fixed end moments and carry-over factors should, in principle, be determined for members of variable rigidity as indicated in Figure 68. However, this is probably not necessary for drop depths of the order of 25 to 30% of the slab thickness. Stiffnesses based on the variable rigidity should be used in deflection calculations if account is to be taken of the favourable effect of the drops, which can be considerable. The effect on overall moment distributions is not generally so pronounced, but the addition of drop panels⁽⁷⁹⁾ always increases gross negative moments and decreases positive ones.

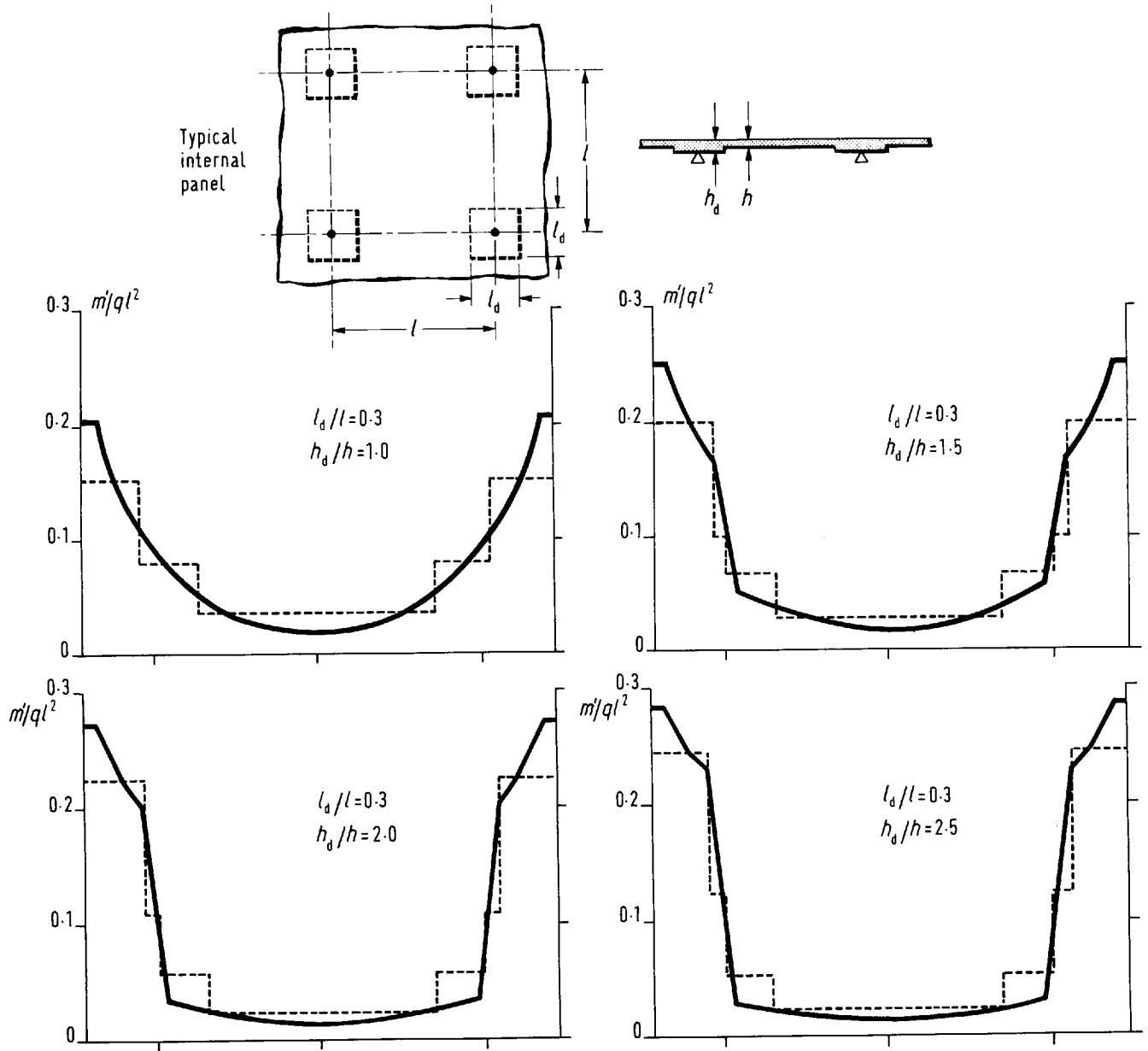


Figure 68 Negative moment in slabs with drop panels

In regard to the transverse distribution of reinforcement, CP110 recommends that where drops are used 'the width of the column strip may be taken as the width of the drop'. This tends to underestimate the moments attracted to the thickened section, and it is probably preferable to retain the normal division into bands given in Section 4.

For span sections, the design can then proceed as for a flat plate. For the support sections, Table 3 (page 36) should be taken to give distributions of reinforcement rather than of moments. This automatically allows for the influence of the drop, since, if the area of steel per unit width is unchanged across the drop boundary, the moment resistance varies in almost direct proportion to the effective depth.

An example of the proposed approach is as follows for the case of a square panel.

From Table 3 and the recommendation that two thirds of the steel in Band I should be placed in its central half, the proportions of reinforcement are:

<i>Location</i>	<i>Total reinforcement</i>	<i>Ratio of band to average reinforcement per unit width</i>
Inner half Band I	$\frac{2}{3} \times 0.77 = 0.51$	$0.51/0.25 = 2.04$
Outer half Band I	$\frac{1}{3} \times 0.77 = 0.26$	$0.26/0.25 = 1.04$
Band II	0.23	$0.23/0.50 = 0.46$

The corresponding relative moment resistances can then be determined knowing the widths and depths of the drops. For example, for a drop head width $0.2l$ and an effective depth $2d$, the following moment resistances apply:

<i>Location</i>	<i>Resistance per unit width</i>	<i>Total resistance</i>
Within drop	$2.04 \times 2 = 4.08m'$	$4.08 \times 0.2l = 0.82lm'$
Inner half of Band I but outside drop	$2.04 \times 1 = 2.04m'$	$2.04 \times 0.05l = 0.10lm'$
Outer half of Band I	$1.04 \times 1 = 1.04m'$	$1.04 \times 0.25l = 0.26lm'$
Band II	$0.46 \times 1 = 0.46m'$	$0.46 \times 0.5l = 0.23lm'$
		TOTAL = $1.41lm'$

where m' is an arbitrary moment per unit width.

If the total moment to be resisted is M' it follows that

$$1.41lm' = M' \text{ or } m' = M'/1.41l$$

The moment resistance per unit width in each part of the section is thus found by substituting for m' in the 2nd column of the last table.

Figure 68 shows examples of transverse moment distributions obtained in this way compared with elastic solutions⁽⁷⁷⁾.

6.3 WAFFLE OR COFFERED SLABS

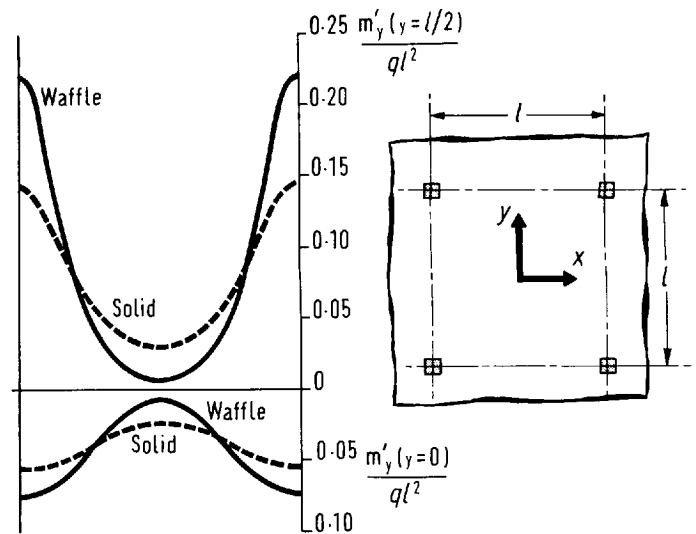
A waffle or coffered slab deviates more from the basic flat plate than slabs with capitals and/or drops. The difference arises from the anisotropy of the waffle form, which, in terms of an orthogonal system parallel to column lines, amounts to a major reduction of torsional stiffness.

In principle, waffle structures can be analysed as grids with ribs having little or no torsional rigidity. In practice, simpler approaches, based on such analyses, are required. The following paragraphs are based on two Swedish publications^(78, 79) on the subject. The treatment is derived from analyses of torsion-free grids.

The lack of torsional rigidity reduces the possibilities of redistribution of moments across the width of a section, which means that the distributions of reinforcement should match the elastic moment distributions so far as is possible. As can be seen in the example of Figure 69, the moment distributions are less uniform than those in solid slabs.

Figure 70 shows the treatment of moment distributions across critical sections at supports. The top part of the illustration shows the idealised moment profile

Figure 69
Comparison of moment distribution in waffle and solid slabs



associated with a single column line. The moment values are related to the mean moment per unit width, and the span, l , and width b , of the frame. Complete moment distributions for support lines are obtained by the superposition of the local distributions from each column line as shown in Figure 70(b) and (c).

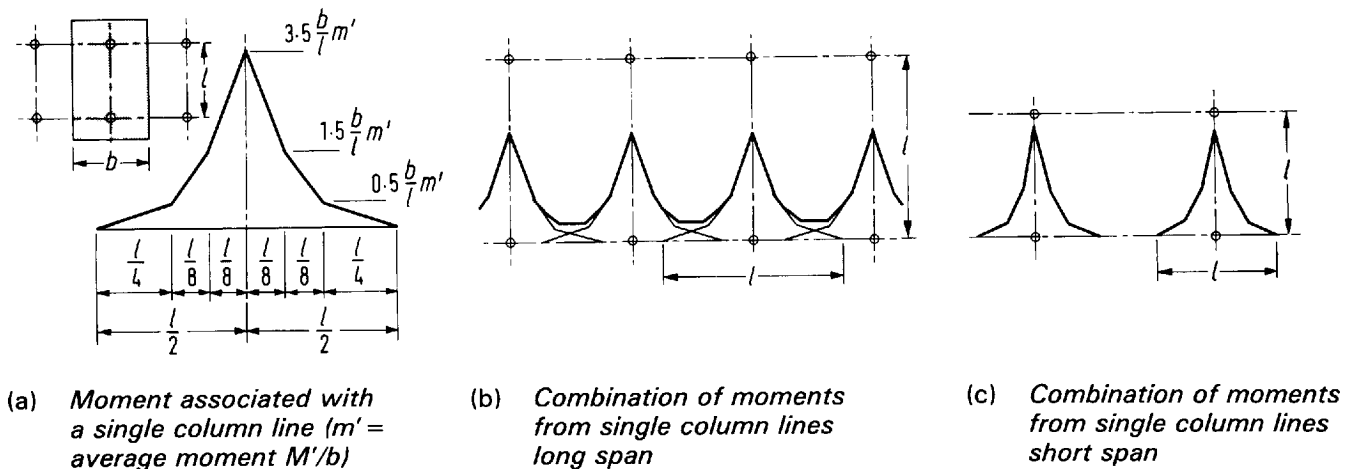


Figure 70 *Distribution of negative moment in waffle slabs*

Span section moments are treated as the sums of two components. The first corresponds to an overall uniform load equal to the dead load plus half the live load, and the moments are taken to be distributed as in Figure 71, where the process of superposition of diagrams from individual column lines can be seen to be similar to that for support moments. The second component corresponds to loading equal to half the live load applied in opposite directions to alternate spans, and the resulting moments are taken to be uniformly distributed. This subdivision of loading is equivalent to that described in Section 4.2.

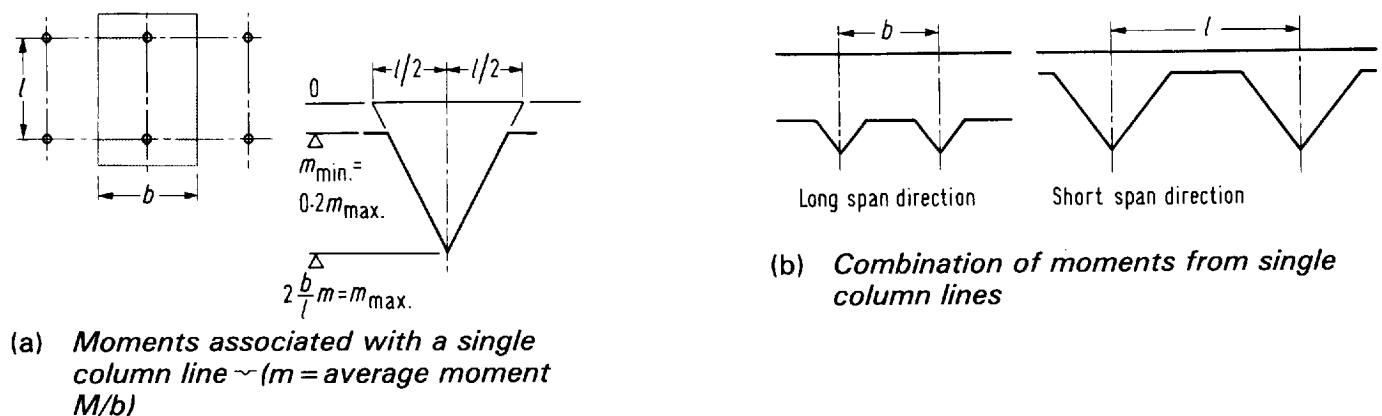


Figure 71 *Distribution of positive moment in waffle slabs*

Once the idealised distributions of moments at support lines and span sections are established, it remains to determine the reinforcement of individual ribs. Within the widths of the solid sections, the moments are averaged provided that the solid infill does not extend for a greater distance than half the distance to the line of contraflexure. Outside this width, each rib is reinforced for the total moment within the width between the centre lines of the adjacent waffles.

The top reinforcement of the rib within the breadth of the solid section can be curtailed in the normal way, but it is a characteristic of waffle construction that the points of contraflexure in the outer ribs are further away from the supports. The relatively light top steel of these ribs should generally be extended over the whole span. To allow for the unfavourable effects of pattern loading the minimum top steel should be sufficient for a moment

$$m' = \frac{(1.5p - g)l^2}{24}$$

where p = live load, g = dead load.

All the bottom reinforcement should generally extend over the full span and have full tension laps at support lines.

References 78 and 79 do not give a full treatment of a method of determining gross frame moments. It appears desirable to calculate the properties of the slab spans taking account of the (sometimes considerable) variation of inertia resulting from the presence of the infill.

The treatment of joint stiffness is more debatable, but it should probably be based on the full solid slab section, provided that this extends for at least the distance required below in relation to punching shear.

The extent of the solid section around a column may be governed by a number of factors:

1. punching resistance—to ensure that the normal punching equations of Section 5 can be applied adjacent to the column, the solid section should extend for a distance at least equal to 2.5 times the slab effective depth from each column face
2. flexural resistance of the ribs—the extent of the solid section in each direction must be such that the negative moment capacities of the rib sections are not exceeded—the critical situations are indicated in Figure 72.

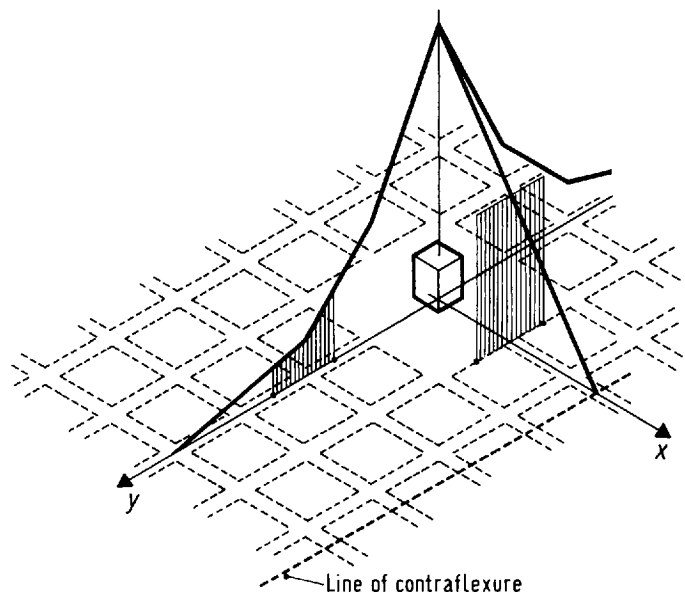


Figure 72
*Critical design moment
for rib concrete*

3. shear resistance of the ribs—provided that the solid section does not extend beyond the ‘ring of contraflexure’ around a column, the maximum shear at its periphery may be taken to be 1.1 times the average value. It may be possible by a suitable choice of infill size to avoid the need for shear reinforcement in the ribs,

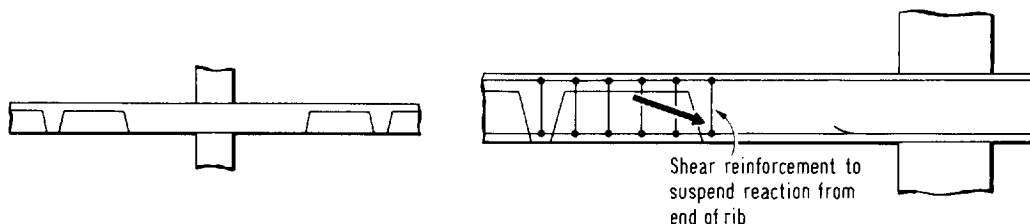
$$\text{i.e. if } 1.1 \hat{v}_d s \leq \xi_s v_c b_w d$$

where \hat{v}_d = design ultimate shear per unit length at perimeter of solid section
 s = spacing of ribs
 ξ_s = depth factor according to CP110
 v_c = design ultimate shear resistance (CP110, Table 5)
 b_w = rib width
 and d = effective depth of rib

If this condition is not fulfilled, the ribs require shear reinforcement and the maximum shear should be limited as in CP110.

If shear reinforcement is designed according to CP110, the design method is based on the assumption of direct loading and support (i.e. loading from above and support from below). For such a design to be valid, extra reinforcement must be provided at the edge of the solid section to ‘suspend’ the loads from the ribs as indicated by Figure 73.

Figure 73
Shear or suspension reinforcement at edge of solid slab



The treatment of slab edges is not covered in References 77 and 78, but it seems desirable to ensure that the top reinforcement for the entire negative moment is placed within the width of the infill panel and that the edge rib is provided with at least nominal stirrups.

6.4 POST-TENSIONED SLABS

The principal advantage of prestressing flat slabs is that cracking can be prevented at service loads, thus retaining the full stiffness of the concrete section, so allowing greater span/depth ratios than are possible with ordinary reinforced concrete construction. With curved tendon profiles, the upward component of the prestressing forces can be used to balance permanent loads and so minimise long-term deflections.

Relatively detailed guidance on the design of such slabs is given in a recent Concrete Society Report⁽⁸⁰⁾ and in earlier USA recommendations⁽⁸¹⁾, both of which contain bibliographies of specialised publications.

7. Design conclusions

7.1 OVERALL FLEXURAL DESIGN

The proposals made were developed primarily to treat the effects of vertical loading on structures in which stability is assured by shear walls or bracing. The approach can also be applied to horizontal loading and to sway corrections for vertical loading, provided that second order ($P\delta$) effects are negligible, but does not treat questions of overall stability.

Flat slabs do not generally possess the very great ductility of many concrete slab systems, principally because of the intervention of punching failure. It is thus necessary that the reinforcement is proportioned so that excessive reliance is not placed on a plastic redistribution of moments. In practice, this requires the use of an approximate elastic analysis for the ultimate limit state. An elastic basis of design is also beneficial in ensuring that steel stresses at working loads are not too high, and thus that deflections and crack widths can be controlled satisfactorily.

Gross moments can be estimated from a equivalent frame analysis, using member stiffnesses calculated for gross cross-sectional dimensions. The analysis should take account of the limited extent of the slab/column connections, which reduces the effective continuity between horizontal and vertical elements.

The slab can be analysed for the effects of vertical loading by being treated as a series of frames in two orthogonal directions, each comprising a line of columns and a strip of slab bounded by lines of zero shear, which, in the absence of more accurate estimates, may be taken to coincide with panel centre-lines as shown in Figure 74.

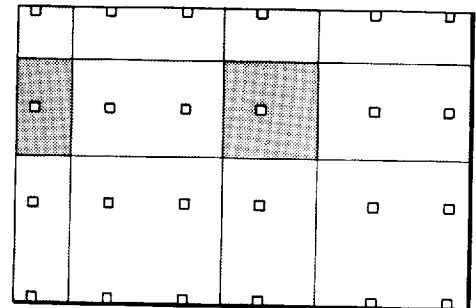


Figure 74
Widths of loading for equivalent frames

In the design, it is generally only necessary to consider two types of load patterns:

1. all spans fully loaded ($1.4g + 1.6p$)
2. each span fully loaded in turn ($1.4g + 1.6p$) while all other spans carry minimum load ($1.0g$)

In principle, the frames can be analysed with the following assumptions regarding stiffnesses:

1. slab members, $EI = Db_e$
2. column members, EI direct from column dimensions
3. slab/column joints, $K_j = \bar{M}/\theta_j$

where b_e is the sum of widths on either side of the column line, each of which is equal to the lesser of the distance to the line of zero shear and half the span

\bar{M} is the unbalanced moment transferred from the slab to the column at the joint in question

θ_j is the differential rotation between the slab and column (see Figure 15, page 23)

and K_j is the joint stiffness, values of which are given in Figure 19 (page 27) for common cases.

If a moment distribution method of analysis is employed for vertical loading, the flexibilities of the joints can be conveniently incorporated with those of the columns by treating the frame as comprising slab strips of breadth b_e and columns of stiffness K_{ce} such that

$$\frac{1}{K_{ce}} = \frac{1}{\sum K_c} + \frac{1}{K_j} \quad (4)$$

Horizontal loading and sway corrections can be treated in an analogous manner. The stiffnesses (1) to (3) above are unchanged, but in terms of moment distribution, the columns should be treated as having their full stiffnesses, while the slab spans should be treated as having reduced effective stiffnesses, K_{se} , such that

$$\frac{1}{K_{se}} = \frac{1}{K_{s1}} + \left(\frac{K_{s1} + K_{s2}}{K_{s1}} \right) \frac{1}{K_j} \quad (10)$$

With this formulation, a span may have different effective stiffnesses in relation to its two ends. The suffices 1 and 2 relate to the two spans meeting at a joint.

To allow for the fact that such analyses are merely approximations and for the influence of reinforcement on member stiffnesses, it is reasonable to accept redistributions of the moments (including \bar{M}) from the analyses by up to 20%.

The columns should then be designed for the moments from the analysis. The slab moments may be reduced to make allowance for the finite dimensions of columns as indicated in Figure 41 (page 44). The reductions, which are broadly consistent with the proposed treatment of shear, are much smaller than those allowed by CP110.

The approach to flexure proposed here is relatively well, though not precisely, supported by test data, a part of which is presented in Section 4.1.7.

7.2 DISTRIBUTION OF MOMENT ACROSS FRAME WIDTH

The transverse distributions of moments given in CP110 are essentially for square panels. To allow rectangular panels to be treated more successfully, the following approach based on elastic plate theory is recommended.

Each frame is subdivided into the bands defined on page 35 illustrated by Figure 28.

The negative moments of column lines in the interiors of frames should be apportioned according to Table 3, page 36.

Within the width of Band I, approximately two thirds of the reinforcement should be concentrated to the middle half.

In Band III, the reinforcement for the above moments may often be less than the minimum required as 'nominal steel'. In such cases, the latter reinforcement should be provided.

If the unbalanced moment, \bar{M} , transmitted to an interior column exceeds

$$Vc_1 \left[\frac{4.7 + c_2/c_1}{\pi + 2c_2/c_1} \right] \quad (12)$$

where V is the simultaneous shear and c_1 and c_2 are the column dimensions along and transverse to the axis of the frame, bottom reinforcement should be provided in the

vicinity of the column. This reinforcement should be designed for a moment, m , per unit width such that

$$m = \frac{\bar{M}}{12c_1} \quad (14)$$

The bottom steel should be extended over a width $(c_2 + 3c_1)$. (For moment direction, x under consideration in Figure 75, $c_1 = c_x$ and $c_2 = c_y$.) The area of bottom steel proposed here is based on the pure moment case ($V=0$) for which equal top and bottom steel would be provided.

In general, the design moments at midspans have maximum positive values, M_{\max} , where the span in question is loaded while adjacent spans are not, and minimum values M_{\min} , which may be negative, arising when the span in question is unloaded but an adjacent span is fully loaded.

Reinforcement for a moment equal to $Ql/24$ should be distributed across the frame in accordance with Table 2 (page 36), for which the band system is as in Table 3 (page 36). Reinforcement for the remainder of the design moment $M_{\max} - Ql/24$ should be distributed evenly across the total width as should any top steel required for $M_{\min} + Ql/24$ if this quantity is negative (see Figure 30, page 37).

The reinforcement for negative moments at the ends of frames (i.e. moments perpendicular to slab edges) must be heavily concentrated towards the columns. All the reinforcement for the design moments should be placed within the widths shown in Figure 75. The basic width $c_x + 2c_y$ at the bottom of the illustration corresponds to local yield lines at 45° to slab edges. At edge (but not corner) columns, the width may be extended as shown for the upper right column, but it is then prudent to provide some closed stirrups for torsion as indicated.

All top steel at slab edges should be anchored as shown at the right, using either 180° bends back into the bottom of the slab or 90° bends down into columns.

At edge columns, the torsional reinforcement A'_{st} should be placed in the top of the slab within the width of the column and be fully anchored beyond the width over which top steel is provided for \bar{M} . Any reinforcement provided in this zone for flexure of the frame parallel to the edge can constitute a part of A'_{st} .

At corner columns, the transverse reinforcement is generally provided by the steel for flexure of the orthogonal frame, but if this is not the case the steel area A'_{st} should be added here too.

7.3 PUNCHING SHEAR

Instead of relating punching resistance to nominal stresses on vertical surfaces defined by critical perimeters, it may be treated in terms of (still nominal) vertical stresses on surfaces approximating to the actual fracture lines. The change is motivated by the possibilities which it opens up of future semi-rational treatments of a range of phenomena which cannot be dealt with satisfactorily on the basis of 'critical perimeters' (see Figure 46, page 49) and also by the more realistic picture it presents.

Figure 76 illustrates the surfaces considered and gives expressions for the surface area, A_c , in common circumstances.

At an internal slab/column joint subjected to concentric loading, the design ultimate resistance to punching in a dense concrete slab without shear reinforcement can be taken as:

$$V_{Rd} = 0.1 K_{sc} \xi_s \sqrt{\frac{100 A_s}{bd}} f_{cu} A_c \quad (27)$$

where

$$K_{sc} = 1.15 \sqrt{\frac{4\pi \times \text{column area}}{(\text{column perimeter})^2}}$$

—for a rectangular column $K_{sc} = 1.15 \frac{\sqrt{\pi c_1 c_2}}{(c_1 + c_2)}$ (24)

$$\xi_s = \sqrt[4]{\frac{300}{d}} \quad (\text{for } d \text{ in mm})$$

$$\frac{100 A_s}{bd} = \text{average ratio of Band I reinforcement in x and y directions}$$

For structural lightweight aggregate concrete with a density of the order of 1700 kg/m³, a similar expression may be used with the coefficient 0.1 replaced by 0.08.

At an internal joint subjected to eccentric loading (shear + unbalanced moment), the design ultimate resistance (V_{Rde}) may be taken as:

$$V_{Rde} = V_{Rdo} \cdot \frac{1}{1 + \frac{1.5(e_x + e_y)}{\sqrt{(c_x + 2d)(c_y + 2d)}}}$$

where V_{Rdo} is the resistance of an otherwise similar but concentrically loaded joint
 e_x, e_y are the eccentricity of load (\bar{M}_x/V) in the x and y directions
and c_x, c_y are the column dimensions in the x and y directions

Values of the design shear V and the eccentricities e_x and e_y used together should be those arising simultaneously under a given loading.

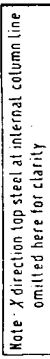
At edge and corner columns, the design ultimate punching resistance can be approximated safely by

$$V_{Rd, \text{edge}} = 0.1 K_{sc} \xi_s \sqrt{\frac{100 A_s}{bd}} f_{cu} \left(\frac{A_c}{1.25 + \frac{1.5e}{c + 2d}} \right)$$

$$V_{Rd, \text{corner}} = 0.8 \times 0.1 K_{sc} \xi_s \sqrt{\frac{100 A_s}{bd}} f_{cu} A_c$$

where the appropriate A_c values are as indicated by Figure 76, and values of $100 A_s/bd$ are calculated for widths equal to those of the columns plus $2.5d$ of slab at each face. e and c refer to the load eccentricity and column width parallel to the slab edge. For lightweight aggregate concrete, the V_{Rd} values should again be reduced by 20%.

If the slab extends beyond the edge columns, a simple and safe estimate of the design resistance can be made by ignoring the overhang. If this is not acceptable, the

$$\frac{\left[\frac{1}{2} \cdot \frac{1}{2}\right]}{\pi \cdot 2} \bigg/ \left[\frac{1}{2} \cdot \frac{1}{2}\right] \cdot 1$$


CIRIA Report 89

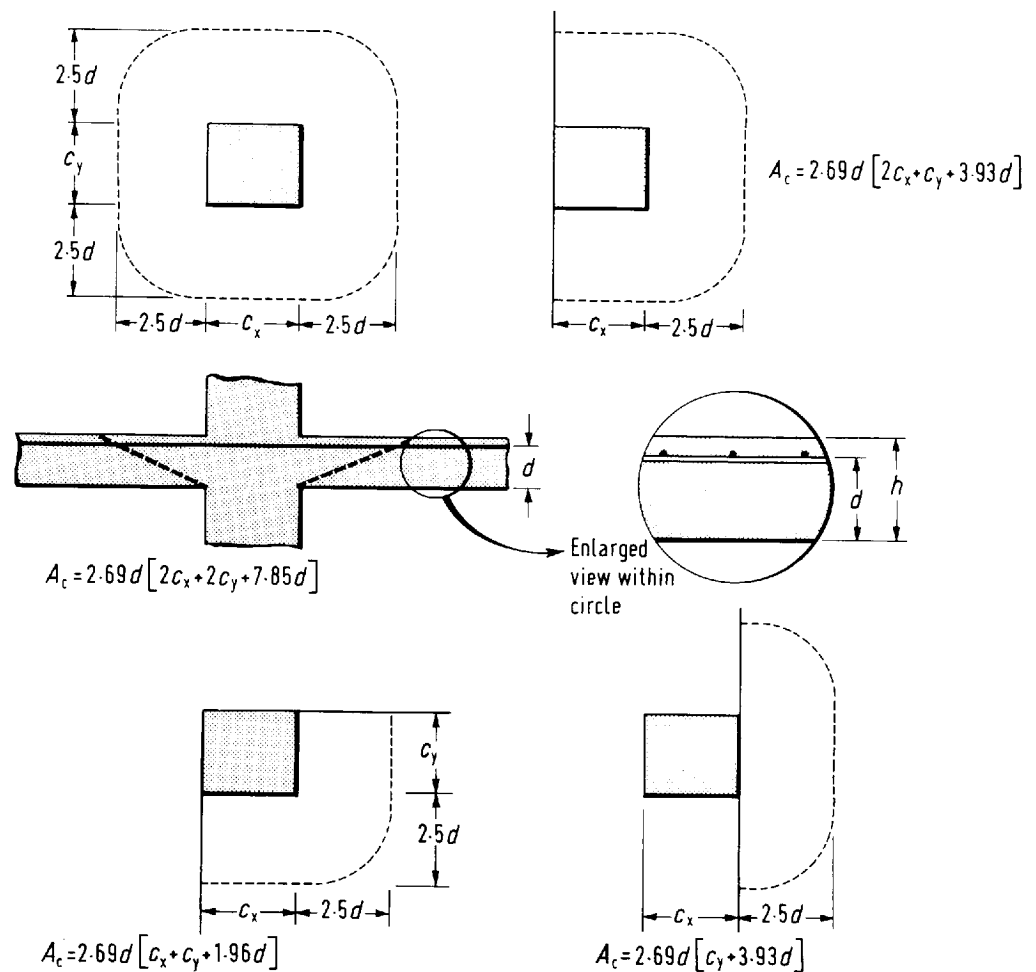


Figure 76
Concrete areas used in
punching calculations

interaction of shear and moments perpendicular to the edge should be considered explicitly as in Section 5.2.3.

The approach to shear described above is relatively well supported by test results as shown in Section 5, but it is empirical, and satisfactory test data are meagre in some areas (e.g. internal rectangular columns with eccentric loading and edge columns with slab overhangs). The treatment of the influence of the flexural reinforcement on V_{Rd} is not ideal. The effect is probably essentially that of reducing deformations, but it is difficult and may be impossible to express this in a rational and reasonably concise manner.

7.4 PRECAUTIONS AGAINST PROGRESSIVE COLLAPSE

As a precaution against progressive collapse occurring as a result of a punching failure at a slab/column joint, and the consequent increases of shear and unbalanced moments at neighbouring joints, some bottom reinforcement should be provided at all joints. It is suggested that the amount of reinforcement be determined by the condition that:

$$1.2 \Sigma \phi^2 \sqrt{f_y f_{cu}} \geq V_{ud} \quad (34)$$

where ϕ is the diameter of a bottom bar passing through a face and anchored to either side of it
 Σ the summation is for all such bars at a joint, with a bar being counted twice if it passes through two faces and is fully anchored beyond both of them
and V_{ud} is design shear force for the ultimate limit state.

The background of this proposal is described in Section 5.3. The evidence supporting the equation is minimal, but the intention is reasonable, and the adoption of such a precaution must do some good and would not be expensive.

7.5 CONTROL OF DEFLECTION

The mid-panel deflections of flat slabs are relatively large, being made up of components from the spans in two directions. A designer must thus decide, in the light of the finishes and partitions to be used, what deflections need to be controlled and in relation to what spans. Figure 77 shows that the choice is essentially between the central bay or mid-side deflection, and the rate of change of deflection.

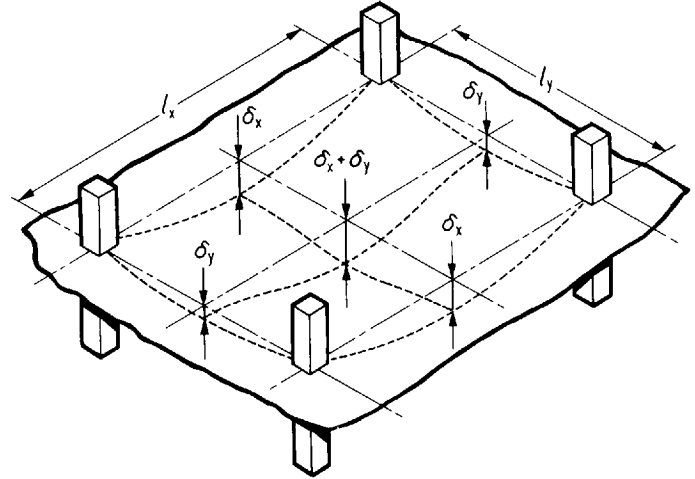


Figure 77
*Representation of
central slab deflection*

Short-term deflections resulting from loading can be calculated on the basis of the equivalent frame analysis used for flexural design, with δ_x and δ_y taken as the mid-span deflections for the orthogonal frames. For each frame, the rigidity, EI , can be taken as

$$EI = b_e D_{\text{eff}}$$

where

$$D_{\text{eff}} = \left(\frac{m_{\text{cr}}}{m}\right)^3 D_g + \left[1 - \left(\frac{m_{\text{cr}}}{m}\right)^3\right] D_{\text{cr}} \quad (18)$$

definitions given on page 46.

For a uniformly loaded span

$$\delta = \frac{l^2}{D_{\text{eff}}} \frac{b}{b_e} (0.104m - 0.021m') \quad (15)$$

where $m = (M'_1 + M'_2)/2b_e$

and M'_1, M'_2 = negative moments at the supports

The influence of long-term loading can be allowed for by replacing E_c in the calculation of D_g and D_{cr} by

$$E_{\text{eff}} = \left(\frac{1}{1 + \nu}\right) E_c,$$

where ν is the creep coefficient—see Table 4 (page 48).

Deflections because of shrinkage can be estimated using Appendix A of CP110⁽⁵⁾.

The proposed method of calculating short-term deflections is quite well supported by test evidence such as that presented in Section 4.5. There is a lack of well-controlled experimental data for long-term deflections of flat slabs, but the extension of methods verified for other types of structures does not seem to present any special problems.

8. Proposals for future research

1. The most serious single lack of information on flat slabs concerns the design of shear reinforcement to increase punching resistance. The recommendations of various codes are divergent, and none are well supported by tests.
2. The proposal made here for a means of reducing the risk of progressive collapse is tentative and needs experimental checking.
3. The treatment of slabs with column capitals and drop panels (and more particularly the suggestions for the design of waffle slabs made in Section 6) are incomplete, and are again lacking in experimental verification.
4. A somewhat longer-term objective should be the development of an overall approach to slab design, embracing, not only flat slabs and their variants, but also slabs supported by flexible beams and, in the limit, slabs with rigid boundary supports.

The information required in relation to points (1) to (3) could be obtained from test programmes which could be completed relatively quickly. Point (4) could not necessarily be best treated as any one particular research project, but could probably be dealt with more satisfactorily by a relatively long-term discussion in a forum such as a Study Group or CEB Commission.

References

1. REGAN, P.E.
Design of reinforced concrete slabs
CIRIA Project Record 220, October 1978
2. NICHOLLS, J.R.
Statical limitations upon steel requirements in reinforced concrete flat slab floors
Trans. Am. Soc. Civ. Engrs. 1912 **77** (Paper 1309) 1670 to 1736
3. WESTERGAARD, H.M. and SLATER, W.A.
Moments and stresses in slabs
J. Am. Concr. Inst. 1921 **17** 415 to 538
4. BRITISH STANDARDS INSTITUTION
The structural use of reinforced concrete in buildings
CP114 : 1969 (Part 2, metric units)

5. BRITISH STANDARDS INSTITUTION
The structural use of concrete
CP110 : 1972 Part 1, Design materials and workmanship
6. AMERICAN CONCRETE INSTITUTE
Building code requirements for concrete
ACI 318-77 (Detroit), 1977
7. COMITE EUROPEEN DU BETON
CEB-FIB model code for concrete structures
Bulletin d'Information N125E, (Paris), 1978
8. PFAFFINGER, D and THURLIMANN, B.
Tables for flat slabs
Verlags-AG, Akademischen Technischen Vereine (Zurich), 1967
9. BROTHIE, J.F.
General method for analysis of flat slabs and plates
J. Am. Concr. Inst. July 1957 **29** (No. 1) 31 to 50
10. BROTHIE, J.F.
General elastic analysis of flat slabs and plates
J. Am. Concr. Inst. August 1959 **31** (No. 9) 127 to 152
11. BROTHIE, J.F.
Elastic-plastic analysis of transversely loaded plates
Trans. Am. Soc. Civ. Engrs. 1961 **126** (Paper 3196) 928 to 961
12. BROTHIE, J.F. and RUSSEL, J.J.
Flat plate structures 1; Elastic-plastic analysis
J. Am. Concr. Inst. August 1964 **61** (No. 8) 959 to 977
13. KINNUNEN, S.
Bakgrund till dimensionering med hänsyn till böjande moment vid platta på ett flertal pelare (Background to flexural design of slabs on multiple columns)
Meddelande 102, Institutionen för Byggnadsstatik, Kungliga Tekniska Högskolan (Stockholm), 1973
14. COMITE EUROPEEN DU BETON
Dalles et planchers dalles (Slabs and flat slabs)
Bulletin D'Information 35 (Paris), March 1962
15. COMITE EUROPEEN DU BETON
Dalles, structures planes (Slabs, plane structures)
Bulletin d'Information 67 (Paris), April 1968
16. HILLERBORG, A.
Strip method of design
Cement and Concrete Association (London), 1975
17. KEMP, K.O. and FERNANDO, J.S.
Reinforced concrete slab design—a generalized strip method including concentrated loads and supports
Paper presented at Conference on reinforced concrete slabs, University of Dundee, 1979
18. STATENS BETONG KOMMITTE
Förslag till bestämmelser för dimensionering av betongplåttor på pelare (Proposed regulations for the design of concrete slabs on columns)
Stockholm, 1964

19. KINNUNEN, S. and NYLANDER, H.
Punching of concrete slabs without shear reinforcement
Handlingar 159, Kungliga Tekniska Högskolan (Stockholm), 1960
20. KINNUNEN, S.
Punching of slabs with two-way reinforcement
Handlingar 198, Kungliga Tekniska Högskolan (Stockholm), 1963
21. BRAESTRUP, M.W. *et al.*
Axisymmetric punching of plain and reinforced concrete
Afdelingen for Baerende Konstruktioner
Rapport R75, Danmarks Teckniske Højskole, 1976
22. HESS, U. *et al.*
Gennemlokning af jernbetonplader (Punching of reinforced concrete slabs)
Afdelingen for Baerende Konstruktioner
Rapport R90, Danmarks Teckniske Højskole, 1978
23. LONG, A.E. and BOND, D.
Punching failure of reinforced concrete slabs
Proc. Instn. Civ. Engrs. May 1967 **37** 109 to 135
24. LONG, A.E.
Punching failure of slabs—transfer of moment and shear
Proc. Am. Soc. Civ. Engrs.—J. Struct. Div. April 1973 **99** (ST4) 665 to 685
25. MASTERSON, D.M. and LONG, A.E.
The punching strength of slabs, a flexural approach using finite elements
in Shear in Reinforced Concrete
Special Publication SP 42, Am. Concr. Inst. (Detroit), 1974, 747 to 768
26. LONG, A.E.
A two-phase approach to the prediction of the punching shear stress of slabs
J. Am. Concr. Inst. February 1975 **72**(2) 37 to 45
27. INGVARSSON, H.
Underlag för begränsning av deformationer hos pelar-understödda platt fält
(Background to limitations of deflection in slabs supported on columns)
Meddelande 101, Institutionen för Byggnadsstatik, Kungliga Tekniska Hogskolan
(Stockholm), 1973
28. JOFRIET, J.C.
Short term deflections of concrete flat plates
Proc. Am. Soc. Civ. Engrs.—J. Struct. Div. January 1973 **99** (ST1) 167 to 182
29. NILSON, A.H. and WALTERS, D.B.
Deflection of two-way floor systems by the equivalent frame method
J. Am. Concr. Inst. May 1975 **72**(5) 210 to 218
30. RANGAN, B.V.
Prediction of long-term deflections of flat plates and slabs
J. Am. Concr. Inst. April 1976 **73**(4) 223 to 226
31. KRIPANARAYANAN, K.M. and BRANSTON, D.E.
Short-term deflections of flat plates, flat slabs and two-way slabs
J. Am. Concr. Inst. December 1976 **73**(12) 686 to 690
32. VANDERBILT, M.D., SOZEN, M.A. and SIESS, C.P.
Deflections of multiple-panel reinforced concrete flat slabs
Proc. Am. Soc. Civ. Engrs.—J. Struct. Div. August 1965 **91**(ST4) Part 1, 77 to 101

33. INGVARSSON, H. and SUNDQUIST, H.
Elasticitetsteoretisk behandling av plåttor upplagda på kant-eller hörnpelare
(Treatment of slabs supported on edge or corner columns by elastic theory)
Meddelande 116, Institutionen för Byggnadsstatik, Kungliga Tekniska Högskolan
(Stockholm), 1975
34. CORLEY, W.G. and JIRSA, J.O.
Equivalent frame analysis for slab design
J. Am. Concr. Inst. November 1970 **67**(11) 875 to 884
35. ANDERSSON, J.L.
Inspänningsmoment i kant pelare vid plattor utan kant balkar (Restraining
moments at edge columns of slabs without edge beams)
Nordisk Betong 1, 1965, 61 to 78
36. TANKUT, A.T.
The behaviour of reinforced concrete flat plate structures subjected to various
combinations of vertical and horizontal loads
PhD Thesis, Imperial College, University of London, November 1969
37. COMITE EUROPEEN DU BETON
Annexe aux recommandations internationales pour le calcul et l'exécution des
ouvrages en beton (Annex to the international recommendations for the
calculation and execution of works in concrete
Vol. 3 Dalles et structures planes (Slabs and plane structures) CEB (Paris), 1972
38. ANDERSSON, J.L.
Genomstansning av plattor understödda av pelare vid fri kant (Punching of slabs
supported by columns at free edges)
Nordisk Betong 2, 1966, 179 to 200
39. KINNUNEN, S.
Försök med betongplattor understödda av pelare vid fri kant (Tests on concrete
slabs supported by columns at free edges)
Rapport R2 Statens Institut för Byggnadsforskning (Stockholm), 1971
40. ANDERSSON, J.L.
Punching of concrete slabs with shear reinforcement
Handlingar 212, Kungliga Tekniska Högskolan (Stockholm), 1963
41. SUNDQUIST, H.
Betongplåttor på pelare vid dynamisk engångslast—1. resultat av statiska försök
(Concrete slabs on columns under dynamic loading—1. results of static tests)
Meddelande 124, Institutionen för Byggnadsstatik, Kungliga Tekniska Högskolan
(Stockholm), 1977
42. ELSTNER, R.C. and HOGNESTAD, E.
Shearing strength of reinforced concrete slabs
J. Am. Concr. Inst. October 1957 **54**(4) 265 to 298
43. MOWRER, R.D. and VANDERBILT, M.D.
Shear strength of lightweight aggregate reinforced concrete flat slabs
J. Am. Concr. Inst. November 1967 **64**(11) 722 to 729
44. IVY, C.B.
The diagonal tension resistance of structural lightweight concrete slabs
PhD Thesis, Texas A. and M. University, January 1966
45. HOGNESTAD, E., ELSTNER, R.C. and HANSON, J.A.
Shear strength of reinforced concrete structural lightweight aggregate concrete
slabs
J. Am. Concr. Inst. June 1964 **61**(6) 643 to 655

46. HANSON, J.M.
Influence of embedded service ducts on strength of flat plate structures
Portland Cement Association Research and Development Bulletin (Skokie, Illinois), 1970, 1 to 16
47. FORSELL, C. and HOLMBERG, A.
Stämpellast på plåttor av betong (Concentrated loads on concrete slabs)
Betong (Stockholm), February 1946 **31**(2) 95 to 123
48. VANDERBILT, M.D.
Shear strength of continuous plates
Proc. Am. Soc. Civ. Engrs—J. Struct. Div. May 1972 **98**(ST5) 961 to 973
49. RICHART, F.E. and KLUGE, R.W.
Tests of reinforced concrete slabs subject to concentrated loads
Bulletin 314, University of Illinois, Eng. Exp. Station, June 1939
50. CHAN, K.T. and LAU, S.K.L.
Pull out strength of concrete (unpublished report)
Polytechnic of Central London, 1979
51. HAWKINS, N.M., FALLSEN, H.B. and HINOJOSA, R.C.
Influence of column regularity on the behaviour of flat plate structures
in Cracking, deflection and ultimate load of concrete slab systems
Special Publication SP30, Am. Conc. Inst. (Detroit), 1971, 127 to 146
52. KINNUNEN, S. NYLANDER, H. and TOLF, P.
Undersökningar rörande genomstansning vid Institutionen för Byggnadsstatik
KTH (Investigations of punching at Building Statics Institute KTH)
Nordisk Betong 3, 1978, 25 to 27
53. BASE, G.D.
Some tests on punching shear strength of reinforced concrete slabs
Technical Report TRA 321, Cement and Concrete Association (London), July 1959
54. MOE, J.
Shearing strength of reinforced concrete slabs and footings under concentrated loads
Bulletin D47, Research and Development Laboratories, Portland Cement Association (Skokie, Illinois), 1961
55. MAHMOOD, K.F.
Bridges slabs supported on columns
MPhil. Thesis, Polytechnic of Central London, 1978
56. STAMENKOVIC, A. and CHAPMAN, J.C.
Local strength of flat slabs at column heads
CIRIA Report 39, August 1972
57. TAYLOR, R. and HAYES, B.
Some tests on the effect of edge restraint on punching shear in reinforced concrete slabs
Mag. Concr. Res. March 1965 **17**(50) 39 to 44
58. LONG, A.E. and MASTERSON, D.M.
Improved experimental procedure for determining the punching strength of reinforced concrete flat slab structures
in Shear in reinforced concrete
Special publication SP42, Am. Conc. Inst. (Detroit) 1974, 921 to 935

59. COMMISSIE VOOR UITVOERING VAN RESEARCH
Pons bij midden-, rand- en hoekkolommen (Punching at inner, edge and corner columns)
CUR Report (Netherlands), December 1976
60. NARASIMHAN, N.
Shear reinforcement in reinforced concrete column heads
PhD Thesis, Imperial College, University of London, 1971
61. ROSENTHAL, I.
Experimental investigation of flat plate floors
J. Am. Concr. Inst. August 1959 **56**(2) 153 to 166
62. AMERICAN CONCRETE INSTITUTE
Building code requirements for concrete
ACI 318-63 (Detroit), 1963
63. MAST, P.E.
Stresses in flat plates near columns
J. Am. Concr. Inst. October 1970 **67**(10) 761 to 768
64. ANIS, N.N.
Shear strength of reinforced concrete flat slabs without shear reinforcement
PhD Thesis, Imperial College, University of London, February 1970
65. GHALI, A., ELMASRI, M.Z. and DILGER, W.
Punching of flat plates under static and dynamic horizontal force
J. Am. Concr. Inst. October 1976 **73**(10) 566 to 572
66. HANSON, N.W. and HANSON, J.M.
Shear and moment transfer between concrete slabs and columns
J. Portland Cement Association, Res. and Dev. Labs. (Skokie, Illinois), January 1968, 2 to 16
67. ISLAM, S. and PARK, R.
Tests on slab-column connections with shear and unbalanced flexure
Proc. Am. Soc. Civ. Engrs.—J. Struct. Div. March 1976 **102**(ST3) 549 to 568
68. IWATA, K.
Shear and moment transfer from six-inch thick concrete flat slab to columns
MS Thesis, University of Washington (Seattle), 1971
69. NYLANDER, H. and SUNDQUIST, H.
Genomstansning av pelarunderstödd plattor av betong med ospänd armering
(Punching of column-supported slab bridges of ordinary reinforced concrete)
Meddelande 104, Institutionen för Byggnadsstatik, Kungliga Tekniska Högskolan (Stockholm), 1972
70. LONG, A.E., KIRK, D.M. and CLELAND, D.J.
Moment transfer and the ultimate capacity of slab-column structures
Structural Engineer, April 1978 **56A**(4) 95 to 102
71. HAWKINS, N.W. and CORLEY, W.G.
Moment transfer to columns in slabs with shearhead reinforcement
in Shear in reinforced concrete
Special Publication SP42, Am. Conc. Inst. (Detroit) 1974, 877 to 879
72. TAYLOR, H.P.J. and CLARKE, J.L.
Some detailing problems in concrete frame structures
Structural Engineer January 1976 **54**(1) 19 to 32

73. INGVARSSON, H.
Experimentellt studium av betong plattor understödda av hörn pelare
(Experimental study of concrete slabs supported by corner columns)
Meddelande 111, Institutionen för Byggnadstatik, Kungliga Tekniska Högskolan
(Stockholm) 1974
74. ZAGHLOOL, R.F. and de PAIVA, H.A.R.
Test of flat plate corner column-slab connections
Proc. Am. Soc. Civ. Engrs.—J. Struct. Div. March 1973 **99**(ST3) 551 to 572
75. ZAGHLOOL, R.F., de PAIVA, H.A.R. and GLOCKNER, P.G.
Tests of reinforced concrete flat plate floors
Proc. Am. Soc. Civ. Engrs.—J. Struct. Div. March 1970 **96**(ST3) 487 to 507
76. RASMUSSEN, B.H.
Betonindstøbte tvaerbelastede boltes og dornes bæreevne (Strength of transversely loaded bolts and dowels cast in concrete)
Bygningssatiske Meddelelser (Copenhagen), November 1963 **34**(2)
77. EISENBIEGLER, G. and LIEB, H.
Moments in and deformations of flat slabs with drop panels under uniform loading (in German)
Beton und Stahlbetonbau 9, 1979, 219 to 225
78. BIEGLER, S.E. and BROMS, C.E.
Dimensioneringsmall för kupolbjälklag (Design of ribbed slabs)
Rapport R85, V, Statens Råd för Byggnadsforskning, (Stockholm), 1978
79. BROMS, C.E.
Pelardäck i form av kupolbjälklag. Förslag till beräknings metod (Two-way ribbed flat slabs. Proposals for a computation method)
Nordisk Betong 1, 1974, 21 to 26
80. CONCRETE SOCIETY
Flat slabs in post-tensioned concrete with particular regard to the use of unbonded tendons—design recommendations
Report 17, The Concrete Society (London), 1979
81. ACI-ASCE COMMITTEE 423
Tentative recommendations for prestressed concrete flat plates
J. Am. Concr. Inst. February 1974 **71**(2) 61 to 71

Acknowledgements

Much of the experimental work at the Polytechnic of Central London was carried out by Dr K.A.A. Zakaria (University of Mosul) and Dr P.R. Walker (Oxford Polytechnic) who were research students at the Polytechnic of Central London at the time.

This project was partly funded by a special contribution from the Building Research Establishment.